ABSTRACT

Title of dissertation: STUDIES IN NONEQUILIBRIUM QUANTUM THERMODYNAMICS

Andrew M. Smith, Doctor of Philosophy, 2019

Dissertation directed by: Professor Christopher Jarzynski
Department of Chemistry

The first part of this thesis focuses on verifying the quantum nonequilibrium work relation in the presence of decoherence. The nonequilibrium work relation is a generalization of the second law of thermodynamics that links nonequilibrium work measurements to equilibrium free energies via an equality. Despite being well established for classical systems, a quantum work relation is conceptually difficult to construct for systems that interact with their environment. We argue that for a quantum system which undergoes decoherence but not dissipation, these conceptual difficulties do not arise and the work relation can be proven similarly to the case of an isolated system. This result is accompanied by an experimental demonstration using trapped ions.

The second part of this thesis examines the relationship between quantum work and coherence by constructing analogous quantities in classical physics. It has recently been shown that quantum coherence can function as a resource for work extraction. Furthermore, it has been suggested that this property could be a truly quantum aspect of thermodynamics with no classical analog. We examine this assertion within the framework of classical Hamiltonian mechanics and canonical quantization. For classical states we define a so called non-uniformity measure and show that it is a

resource for work extraction similar to quantum coherence. Additionally, we show that work extracted from non-uniformity and coherence agree in the classical limit. This calls into question the idea that coherence qualitatively separates classical and quantum thermodynamics.

The final part of this thesis explores the connection between decoherence and adiabatic (quasistatic) driving. This topic is inspired by an experiment where it was seen that strong dephasing suppressed energy level transitions. Using a perturbative method we investigate this mechanism in the regime of small to moderate decoherence rate and ask if decoherence can help suppress energy transitions when compared with an adiabatic process without decoherence. We find that strategies that include decoherence are inferior to those where decoherence is absent.

STUDIES IN NONEQUILIBRIUM QUANTUM THERMODYNAMICS

by

Andrew M. Smith

Dissertation submitted to the Faculty of the Graduate School of the
University of Maryland, College Park in partial fulfillment
of the requirements for the degree of
Doctor of Philosophy
2019

Advisory Committee:
Professor Christopher Jarzynski, Chair/Advisor
Professor Norbert Linke
Professor Sebastian Deffner
Professor Theodore Einstein
Professor Victor Yakovenko

Table of Contents

Chapter 1: Background and Context

1.1 Going Beyond Macroscopic Thermodynamics

While this thesis focuses on quantum nonequilibrium aspects of thermodynamics, it is useful to review some of the limitations of classical macroscopic thermodynamics so that we can truly appreciate the successes of modern thermodynamic research. Thermodynamics, in its original phenomenological formulation [18], is an oddball among physical theories. Unlike Newton's Laws, Maxwell's equations, relativity, quantum mechanics, and other pillars of physics born out of curiosity for the natural world, thermodynamics was developed out of necessity by engineers working to optimize the function of steam engines. It is perhaps this difference in perspective that helped form macroscopic thermodynamics' unique structure when compared to other physical theories. Despite its name, macroscopic thermodynamics is *not a dynamical theory* in the usual sense of the word. The fundamental starting point for most areas of physics is an equation of motion which models the time dependence of a system's degrees of freedom. In macroscopic thermodynamics, there generally is no Lagrangian or Hamiltonian or even effective differential equation that governs the time dependence of variables such as volume, internal energy, heat, and work in a closed, self-consistent way. This stems from the fact that this form of thermodynamics concerns itself only with macroscopic variables that simply do not contain enough information to describe the fully non-equilibrium behavior typically encountered in

dynamics.

Instead macroscopic thermodynamics is a phenomenological theory that focuses on the relationships – often in the form of inequalities – between macroscopic variables and the energy transferred during transitions between *equilibrium states*. To better understand this statement, we now consider some of the basic tenants of thermodynamics in the case of an isothermal process. Consider a macroscopic system of interest immersed in an environment of constant inverse temperature β and driven by some externally controlled field (or piston, weight, etc.). The first law of thermodynamics is a statement of energy conservation over the course of a thermodynamic process and is given by

$$\Delta \mathcal{U}_{eq} = \mathcal{Q} + \mathcal{W} \tag{1.1}$$

where $\Delta \mathcal{U}_{eq}$ is the total internal energy change of the system between our equilibrium states, $\mathcal{Q}$ is the total heat exchanged with the thermal reservoir, and $\mathcal{W}$ is the work invested in the system by the external field. On a microscopic level, the heat $\mathcal{Q}$ is associated with the disordered energy transfer that occurs due to contact with the more or less random degrees of freedom of the environment. In contrast work $\mathcal{W}$ is associated with orderly energy transfer that occurs when an external field is used to control a system. In thermodynamics, it is often a goal to minimize the work dissipated (or alternatively maximize work extracted) in a process as the control degrees of freedom can act as a battery that stores this energy for future mechanical tasks. The second law of thermodynamics for isothermal processes bounds the work invested in a system according to

$$\mathcal{W} \geq \Delta \mathcal{F}_{eq} = \Delta(\mathcal{U}_{eq} - \beta^{-1}\mathcal{S}_{eq}) \tag{1.2}$$

where $\mathcal{F}_{eq}$ is the equilibrium Helmholtz free energy and $\mathcal{S}_{eq}$ is the equilibrium entropy. In the best case scenario, this means the work invested when driving a system from one equilibrium state to another equals the free energy difference between those equilibrium states. While statistical mechanics and information theory shed light on the nature of entropy as a measure of disorder, in macroscopic thermodynamics it is a phenomenological function determined in an isothermal process through calorimetry and the fact $\Delta\mathcal{S}_{eq} = \beta\mathcal{Q}$ for reversible quasi-static processes. In more general processes, the Clausius theorem can be used to determine entropy.

It must be emphasized that a number of physical assumptions are made within the framework of macroscopic thermodynamics. The first is that macroscopic thermodynamics is only concerned with transitions between *equilibrium states* – a fact that stems largely from how entropy is formulated in macroscopic thermodynamics. Here entropy is the primary function of interest as it characterizes all thermodynamic aspects of a particular system either directly or through Legendre transformations to other thermodynamic potentials [18]. Differences in entropy are found empirically from reversible processes which are necessarily quasi-static and evolve through a sequence of equilibrium states. It follows that in this framework entropy can only be defined in equilibrium.

Additionally there are limitations to studying *macroscopic systems*. In macroscopic thermodynamics variables such as work, heat, internal energy, and volume take definite values and do not fluctuate. With the aid of statistical physics, we understand that this fact is not fundamental. Rather the measurement of macroscopic variables is akin to averaging over huge amounts of microscopic degrees of freedom where the law of large numbers ensures that fluctuations are virtually non-existent. The macroscopic assumption also means that one can often ignore all surface effects, treat environmental interactions as weak, and focus on modeling a material's bulk as

an ensemble of weakly interacting parts. When these assumptions hold, the entropy is a homogeneous first-order function of extensive variables such as internal energy, volume, and particle number, and one obtains a plethora of additional thermodynamic information such as the cherished Maxwell relations which surprisingly link quantities such as compressibility, thermal expansion, and heat capacities of materials.

Modern approaches to thermodynamics aim to overcome these limitations and provide a formulation of thermodynamics that is valid in nonequilibrium situations and applies to arbitrarily small systems where thermal fluctuations are important. The topic of this thesis – quantum thermodynamics – is one of the most recent iterations in a long line of research aiming to achieve these goals. It follows on the heels of kinetic theory, open quantum systems, information theory, many-body physics, and stochastic thermodynamics, to name a few, and, unsurprisingly, is a highly multidisciplinary field. It is a natural progression of nanoscale thermodynamics that describes systems so small that the inherent randomness of quantum mechanics must be accounted for in addition to the randomness introduced by thermal effects.

To get a flavor for how quantum thermodynamics achieves its goals, the remainder of this chapter focuses on two generalizations of the macroscopic second law (1.2) which form the building blocks for this thesis. In section 1.2, we will investigate how work enters into the second law but will not attempt to move beyond equilibrium free energies. There we will find the surprising result that incorporating both thermal and quantum work fluctuations allows the second law to be rewritten as an equality. Along the way, we will be introduced to the important and not fully resolved issue of defining thermodynamic work in quantum systems. In section 1.3 we will take the alternative approach to generalizing the macroscopic second law (1.2) in which we still focus on average work but generalize the concept of free energy to include nonequilibrium states. We will see in this case how concepts from quantum information

theory such as von Neuman entropy and quantum relative entropy play a natural role in the thermodynamics of quantum systems.

1.2 Quantum Nonequilibrium Work Relation from Multiple Energy Measurements

In the last few decades, researchers have discovered that properly accounting for microscopic fluctuations of thermodynamic quantities allows one to rewrite many of the standard inequalities of thermodynamics as *equalities*. These results, known as fluctuation theorems, have become a cornerstone of classical non-equilibrium thermodynamics [115, 116] and their extension to the quantum regime has more recently become a priority in the field of quantum thermodynamics [24, 136]. At the classical level, fluctuation theorems have provided a method for calculating the values of equilibrium properties from non-equilibrium information in both simulations and experiments as well as given foundational insights into the second law of thermodynamics. It is the hope that properly formulated quantum fluctuation theorems will find similar applications in the quantum setting. In this section we will focus specifically on the non-equilibrium work relation [62, 63], which is perhaps the best known and most easily interpreted fluctuation theorem. We will first introduce the non-equilibirum work relation in the setting of classical Hamiltonian dynamics and then develop the two time energy measurement formulation of the quantum work relation which is important background for Chapter 2 of this thesis.

As its name implies, thermodynamic work is the fluctuating quantity at the center of the non-equilibrium work relation. To better understand the origin these fluctuations, let us consider a classical ideal gas that is initially in thermal equilibrium with a reservoir of inverse temperature β. At time $t = 0$ the gas is isolated from

its environment and then is compressed by a piston which follows a predefined time dependent protocol of duration τ. At time $t = \tau$ the gas is once again put in contact with the thermal reservoir and allowed to equilibrate. Note that the gas undergoes a well defined change in free energy $\Delta\mathcal{F}_{eq}$ since it is in equilibrium at both the beginning and end of the process. When the gas consists of a macroscopic number of particles (i.e. $N \sim 10^{23}$), the frequency of collisions between the piston and gas particles is enormous. The law of large numbers ensures that for virtually all initial micro-states drawn from equilibrium, the differences in pressure at the piston's surface and hence the differences in work $\mathcal{W}$ are essentially immeasurable from one experimental run to another.

In contrast, now consider the opposite extreme where there is only a single gas particle in the container. When sampled from equilibrium, the velocity of the particle follows the Maxwell-Boltzmann velocity distribution and varies significantly from one experimental realization to another. When this sampling results in a large velocity, it is expected that the particle will collide multiple times with the piston. With each collision, the particle gains or loses energy in the form of work while the motion of the piston is virtually unaffected. In general, the total work in such an experimental run is non-zero. Alternatively, there exist situations with measurable probability where the particle is sampled from equilibrium, has a very small velocity, and is located in a portion of the container that the piston does not intersect during its motion. Here it is plausible that the particle does not collide with the piston even once during the process and hence the net work vanishes. In each case the work performed in the final equilibration step is zero. From these examples it should now be clear that for systems with a small number of degrees of freedom, work is not a constant but rather fluctuates based a system's initial micro-state.

With this example in mind, we now set up a more general Hamiltonian framework

in which classical work fluctuations can be more precisely analyzed. Consider a system that over a time interval $t \in [0, \tau]$ is weakly coupled to a thermal reservoir and driven by an external time dependent control field. In our previous example, the gas is our system of interest and the piston represents the time dependent control. In any given realization of the driving process, the micro-state of the system and reservoir are represented by phase space points denoted respectively by $z = (x_1, x_2, \dots, p_1, p_2, \dots)$ and $\zeta = (\chi_1, \chi_2, \dots, \wp_1, \wp_2, \dots)$. The Hamiltonian of the joint system is given by

$$\mathcal{H}^{sys+res}(z, \zeta, t) = \mathcal{H}^{sys}(z, t) + \mathcal{H}^{res}(\zeta) + \mathcal{H}^{int}(z, \zeta) \tag{1.3}$$

where $\mathcal{H}^{sys}$ is the system Hamiltonian, $\mathcal{H}^{res}$ is the Hamiltonian of the thermal environment, and $\mathcal{H}^{int}$ is a weak interaction between the system and reservoir. Note that only the system is driven by the external field and therefore all time dependence of the composite system is carried by $\mathcal{H}^{sys}$. Like the gas example, we will assume that both the system and reservoir are initially in thermal equilibrium at inverse temperature β. In other words, the initial states of the composite system are sampled from the canonical phase space distribution

$$\pi(z, \zeta) = \frac{e^{-\beta[\mathcal{H}^{sys}(z,0)+\mathcal{H}^{res}(\zeta)]}}{Z^c} \tag{1.4}$$

where Z^c is the classical partition function of the joint system and the weak interaction has been neglected. Unlike the gas example given before, we will not assume that the system and reservoir are decoupled during the driving process.

At the microscopic level work $\mathcal{W}$ is defined as the net energy that flows into the system via the control field over the course of the process. Since this is the only mechanism by which the energy of the joint system can change, we conclude that for

any single realization of the driving process

$$\mathcal{W} = \mathcal{H}^{sys+res}(z(\tau), \zeta(\tau), \tau) - \mathcal{H}^{sys+res}(z(0), \zeta(0), 0) \tag{1.5}$$

$$= \int_0^\tau \frac{\partial \mathcal{H}^{sys}}{\partial t}(z(s), s) ds. \tag{1.6}$$

This suggests two separate schemes for measuring work in classical Hamiltonian systems. Line (1.5) suggests measuring the energy of the combined system and reservoir at both time $t = 0$ and $t = \tau$ and calculating the work by taking the difference of these energy values. While this procedure is conceptually sound, in practice it not feasible to make direct measurements of the reservoir. Alternatively, the integral formulation of work (1.6) is based on continuously measuring the power that is injected into the system by the control field. When a system's trajectory can accurately be tracked, this is generally the preferred method of calculating work as no measurements of the environment are required. Note that while classical Hamiltonian mechanics focuses on the integrated power formulation of work (1.6), the total energy change formulation (1.5) will be of importance in the quantum mechanical systems.

One might expect that fluctuations in the work (1.6) resulting from initial equilibrium sampling would be more or less random around the mean work value and contain little thermodynamic information. To the contrary, these fluctuations satisfy the rather surprising *equality*

$$\langle e^{-\beta \mathcal{W}} \rangle = e^{-\beta \Delta \mathcal{F}_{eq}^{sys}} \tag{1.7}$$

known as the non-equilibrium work relation. Here the average on left hand side of equation (1.7) is understood to be over all realizations of the process with initial conditions sampled from the equilibrium distribution (1.4). This is equivalent to

building a distribution of work from many process realizations and performing the average with respect to the work distribution directly. Note that the initial and final equilibrium free energies on the right hand side of equation (1.7) correspond to the system Hamiltonians $\mathcal{H}^{sys}(z,0)$ and $\mathcal{H}^{sys}(z,\tau)$. The reservoir plays no role in the free energy difference as its Hamiltonian does not change over the course of the process.

While the work relation as set up in this section can be proven straightforwardly using the properties of classical Hamiltonian mechanics [65], we now choose to focus on the applications and interpretation of equation (1.7). A derivation of the quantum non-equilibrium work relation will be given later in this section. One of the most important insights from the non-equilibirum work relation is the fact that work measurements from a highly non-equilibrium process can be used to obtain valuable equilibrium free energies. From a computational point of view, the work relation reveals a new way to calculate equilibrium free energy differences from simulations [34]. Where traditional methods such a thermodynamic integration [69] and thermodynamic perturbation theory [143] effectively depend on either very slow or fast driving protocols, the work relation makes no assumption on process speed and hence adds a parameter over which algorithms can be optimized. At the experimental level, the work relation allows free energy differences to be inferred by building work distributions from many experimental trials [15, 29, 42, 54, 66, 80, 112, 117]. This non-equilibrium approach is especially applicable in experiments in which technical limitations prohibit quasi-static methods of measuring free energy. On a foundational level, the non-equilibrium work relation can be viewed as a generalization of the the second law of thermodynamics for isothermal processes (1.2). This connection is most easily seen through the application of Jensen's inequality $\langle e^x \rangle \geq e^{\langle x \rangle}$ to the

work relation (1.7) from which it immediately follows

$$\langle \mathcal{W} \rangle \geq \Delta \mathcal{F}_{eq}. \tag{1.8}$$

Moreover, the fluctuation theorem can be used to further show that work values that violate the second law in the sense $\mathcal{W} < \Delta \mathcal{F}_{eq}$ are exponentially rare, making violations of more than a few $k_b T$ all but non-existent [64].

With this we conclude our review of the classical non-equilibrium work relation and move to the quantum case. Following the classical setup, consider a composite system consisting of a system of interest weakly coupled to a thermal reservoir that undergoes a driving process of duration τ. The Hamiltonian of the joint system is given by

$$\hat{H}(t) = \hat{H}^{sys}(t) \otimes \hat{I}^{res} + \hat{I}^{sys} \otimes \hat{H}^{res} + \hat{H}^{int}. \tag{1.9}$$

where

$$\hat{H}^{sys} = \sum_n \epsilon^{sys}(t) |n^{sys}(t)\rangle\langle n^{sys}(t)| \tag{1.10}$$

$$\hat{H}^{res} = \sum_n \epsilon^{res} |n^{res}\rangle\langle n^{res}|. \tag{1.11}$$

As before we will assume that the driving field acts only on the system of interest and that the joint system begins in the thermal equilibrium state

$$\hat{\pi} = \frac{e^{-\beta[\hat{H}^{sys}(0) \otimes \hat{I}^{res} + \hat{I}^{sys} \otimes \hat{H}^{res}]}}{Z^q(0)} \tag{1.12}$$

where $Z^q(0)$ is the quantum partition function at $t = 0$.

In order to develop a quantum work relation, we must first define quantum analogs of the various physical quantities in equation (1.7). The equilibrium free

energy difference of the system comes straightforwardly from the the standard formula $\mathcal{F}_{eq} = -\beta^{-1} \ln Z^q$. In contrast, finding a satisfactory definition of the quantum work distribution is a significantly more challenging task. For simplicity, we now discuss this issue in the context of an isolated system. Based on the classical integrated power formulation of work (1.6), one might propose that the operator

$$\hat{\mathcal{W}} = \int_0^\tau \frac{d\tilde{H}^{sys}}{dt}(s)ds = \tilde{H}^{sys}(\tau) - \hat{H}^{sys}(0) \tag{1.13}$$

could act as a sort of work observable for a quantum system. Here we use $\tilde{H}^{sys}$ to denote the system's Hamiltonian in the Heisenberg picture. This definition seems reasonable in the context of isolated systems since at the level of expectation values the average work is equal to the average change in system energy. This is exactly what the first law of thermodynamics predicts in the absence of heat. Unfortunately, it can be shown [6, 140] that a work distribution based on measurements of the observable (1.13) does not satisfy the work relation (1.7). From a thermodynamic perspective, one might have guessed an observable formulation of work is incorrect. In thermodynamics work is represented by an inexact differential, meaning it is a process dependent quantity that cannot be represented by a state function. These observations lead to the general consensus in the quantum thermodynamics community that even for the case of an isolated system quantum, work cannot be formulated as an observable [128].

An alternative perspective on quantum work can be motivated from the total energy difference formulation of classical work presented on line (1.5). Here work is calculated by taking the difference of the joint system and environment energy at times $t = 0$ and $t = \tau$. In the quantum case this suggests a protocol, originally developed in [74, 95, 130], in which work is defined by two projective energy measurements.

We will now explore this idea. Assume that for $t < 0$ a quantum system and its surrounding environment are in the thermal equilibrium state (1.12). At time $t = 0$, a projective measurement is made of the joint system energy $\hat{H}^{sys}(0) \otimes \hat{I}^{res} + \hat{I}^{sys} \otimes \hat{H}^{res}$ resulting in energy $\epsilon_i^{sys}(0) + \epsilon^{res}$ with probability $p(ij)$. Note that the weak interaction has been ignored. The system, now in the post measurement state $|i^{sys}(0), j^{res}\rangle$, then evolves in the interval $t \in [0, \tau]$ according to the unitary $\hat{U}$ generated by the full Hamiltonian (1.9). Finally at $t = \tau$ another projective energy measurement is made which results in energy $\epsilon_r^{sys}(\tau) + \epsilon_s^{res}$ with probability $p(rs|ij)$. The work associated with a single realization of the process is then given simply by the difference $\mathcal{W} = [\epsilon_r^{sys}(\tau) + \epsilon_s^{res}] - [\epsilon_i^{sys}(0) + \epsilon_j^{res}]$. The work distribution obtained from many realizations of this procedure is given by

$$\begin{aligned} \rho(\mathcal{W}) &= \sum_{ijrs} p(ij)p(rs|ij)\delta[\mathcal{W} - (\epsilon_r^{sys}(\tau) + \epsilon_s^{res} - \epsilon_i^{sys}(0) - \epsilon_j^{res})] \\ &= \sum_{ijrs} \frac{e^{-\beta(\epsilon_i^{sys}(0) - \epsilon_j^{res})}}{Z^q} |\langle r^{sys}(\tau), s^{res}|\hat{U}|i^{sys}(0), j^{res}\rangle|^2 \\ &\quad \times \delta[\mathcal{W} - (\epsilon_r^{sys}(\tau) + \epsilon_s^{res} - \epsilon_i^{sys}(0) - \epsilon_j^{res})]. \end{aligned} \tag{1.14}$$

Note that the number of values of work outcomes in this scheme exceeds the dimension of the system and thus agrees with the idea that work cannot be formulated as a system observable.

Armed with the work distribution (1.14), we now conclude this section with a derivation of the quantum nonequilibrium work relation for a system weakly coupled

to its environment. Observe

$$\begin{aligned}\langle e^{-\beta \mathcal{W}} \rangle &= \int \rho(\mathcal{W}) e^{-\beta \mathcal{W}} d\mathcal{W} \qquad (1.15)\\ &= \sum_{ijrs} e^{-\beta(\epsilon_r^{sys}(\tau)+\epsilon_s^{res}-\epsilon_i^{sys}(0)-\epsilon_j^{res})} \frac{e^{-\beta(\epsilon_i^{sys}(0)-\epsilon_j^{res})}}{Z^q(0)} |\langle r^{sys}(\tau), s^{res}|\hat{U}|i^{sys}(0), j^{res}\rangle|^2 \\ &= \sum_{ijrs} \frac{e^{-\beta(\epsilon_r^{sys}(\tau)-\epsilon_s^{res})}}{Z^q(0)} \langle r^{sys}(\tau), s^{res}|\hat{U}|i^{sys}(0), j^{res}\rangle \langle i^{sys}(0), j^{res}|\hat{U}^\dagger|r^{sys}(\tau), s^{res}\rangle \\ &= \frac{Z^q(\tau)}{Z^q(0)} \\ &= e^{-\beta \Delta \mathcal{F}_{eq}}.\end{aligned}$$

1.3 Nonequilibrium Generalizations of The Second Law

In the last section, we explored how the nonequilibrium work relation generalizes the second law of thermodynamics by taking into account work fluctuations. Importantly we saw that like the macroscopic formulation of the second law, the work relation connects work to changes in *equilibrium* free energy. In this section we examine another generalization of the second law, which we will refer to as the nonequilibrium second law, that instead focuses on transitions between *nonequilibrium* states. This well known result [49, 55, 126] will be used extensively in Chapter 3 of this thesis. Conceptually the nonequilibrium second law is somewhat less difficult to understand than the nonequilibirum work relation. Consequently, we will briefly describe the result and then focus on proving its validity using two different frameworks.

Consider a quantum system in contact with a thermal reservoir that undergoes a driving process of duration τ. The system's total Hamiltonian, including the effects of the driving, is given by $\hat{H}^{sys}(t)$ while the inverse reservoir temperature is given by β. The main idea of the nonequilibrium second law is to replace the equilibrium

free energy $\mathcal{F}_{eq} = \beta^{-1} \ln Z^q$ with a suitable definition that can also be applied to nonequilibrium states. Note that in macroscopic thermodynamics, the Helmholtz free energy can be written as $\mathcal{F}_{eq} = \mathcal{U}_{eq} - \beta^{-1}\mathcal{S}_{eq}$ where $\mathcal{U}_{eq}$ and $\mathcal{S}_{eq}$ are respectively internal energy and entropy. Using this fact and our intuition from statistical mechanics, we define a nonequilibrium free energy for any system density operator $\hat{\rho}$ according to

$$\mathcal{F} = \mathcal{U} - \mathcal{S}/\beta \tag{1.16}$$

$$\mathcal{U} = \mathrm{Tr}[\hat{H}^{sys}\hat{\rho}] \tag{1.17}$$

$$\mathcal{S} = -\mathrm{Tr}[\hat{\rho}\ln\hat{\rho}] \tag{1.18}$$

where, importantly, thermodynamic entropy has been associated with von Neumann entropy [124]. Additionally we can link thermodynamic work and heat to the dynamical quantities

$$\langle \mathcal{W} \rangle = \int_0^\tau \mathrm{Tr}\left[\frac{d\hat{H}^{sys}}{dt}\hat{\rho}\right] ds \tag{1.19}$$

$$\langle \mathcal{Q} \rangle = \int_0^\tau \mathrm{Tr}\left[\hat{H}^{sys}\frac{d\hat{\rho}}{ds}\right] ds. \tag{1.20}$$

which can easily be shown to satisfy the first law $\Delta\mathcal{U} = \langle \mathcal{W} \rangle + \langle \mathcal{Q} \rangle$. These definitions follow from the idea that work is energy transferred to the system via the external driving while heat is energy that flows into the system from the reservoir. As a check, note that in the absence of external driving the Hamiltonain is constant and the average work (1.19) vanishes. Alternatively, for an isolated system that evolves solely according to $\hat{H}^{sys}(t)$ it can be shown that the average heat (1.20) is zero. More rigorously, it is possible to motivate definitions (1.19) and (1.20) by carefully accounting for energy transfer in a Hamiltonian model that explicitly includes the system and thermal reservoir.

Now consider a process in which an external field invests work $\langle \mathcal{W} \rangle$ while our system is driven from an initial state $\hat{\rho}(0)$ to a final state $\hat{\rho}(\tau)$. The nonequilibrium second law states that

$$\langle \mathcal{W} \rangle \geq \Delta \mathcal{F} \tag{1.21}$$

where $\Delta \mathcal{F}$ denotes the nonequilibrium free energy difference between states $\hat{\rho}(\tau)$ and $\hat{\rho}(0)$. This result is valid for a wide variety of classical and quantum dynamics including isolated systems, master equations that effectively model the environment, and Hamiltonian models that explicitly treat both the system and reservoir [48, 55, 126].

In the remainder of this section we sketch proofs of this result in two different contexts. First using theorems from information theory, we will show that the nonequilibirum second law holds for the case in which the reservoir is modeled by a Lindblad master equation. The second proof relies on the notion of passive states and models the environment through repeated interactions with idential thermal auxilary systems. Note that the argument of functions will often be denoted by a subscript in sections 1.3.1 and 1.3.2. The subscript may be omitted for expressions where the argument is clear from context.

1.3.1 Nonequilibrium Second Law for a Quantum Master Equation

Consider a driven quantum system with Hamiltonian $\hat{H}_t$ in contact with a thermal reservoir at inverse temperature β. The system's evolution can be modeled by a Lindblad master equation

$$\frac{d\hat{\rho}}{dt} = -\frac{i}{\hbar}[\hat{H}_t, \hat{\rho}] + \mathcal{D}_t \hat{\rho} \equiv \mathcal{L}_t \hat{\rho} \tag{1.22}$$

where the influence of the thermal bath is captured by a dissipator $\mathcal{D}_t$. Lindblad master equations are linear in form, preserve the properties of the density operator, and are the most common way to model a quantum system coupled to an environment with many degrees of freedom [102]. For this derivation we must use the fact that for a thermal environment, the dissipator preserves the instantaneous equilibrium state. In other words we will insist that $\mathcal{D}_t\hat{\pi}_t = 0$ where

$$\hat{\pi}_t = \frac{e^{-\beta\hat{H}_t}}{\mathrm{Tr}[e^{-\beta\hat{H}_t}]}. \tag{1.23}$$

Note that no stronger assumptions on the master equation such as detailed balance (i. e. no currents in equilibrium) will be necessary to prove the nonequilibrium second law. Because (1.22) is of Lindblad form, it follows that $\mathcal{L}_t$ generates a completely positive trace preserving (super-)operator

$$\Lambda_t = \mathcal{T}\exp[\int_0^t \mathcal{L}_s ds]. \tag{1.24}$$

which governs the evolution of the system according to $\hat{\rho}_t = \Lambda_t\hat{\rho}_0$. In the case where the dissipator vanishes, we recover the the well known expression for Hamiltonian dynamics $\Lambda_t\hat{\rho}_0 = \hat{U}_t\hat{\rho}_0\hat{U}_t^\dagger$ where $\hat{U}_t$ is the unitary generated by the Hamiltonain $\hat{H}_t$.

With our basic setup outlined, we now present a useful mathematical property of completely positive trace preserving operators and quantum relative entropy that allows for the derivation of the nonequilibrium second law. Consider density operators $\hat{\rho}$ and $\hat{\sigma}$. The quantum relative entropy [98] of state $\hat{\rho}$ with respect to state $\hat{\sigma}$ is defined according to

$$D(\hat{\rho},\hat{\sigma}) = \mathrm{Tr}[\hat{\rho}(\ln\hat{\rho} - \ln\hat{\sigma})]. \tag{1.25}$$

Heuristically it is useful to think of the relative entropy as an abstract distance

between density operators since it has the properties $D(\hat{\rho}, \hat{\sigma}) > 0$ for $\hat{\rho} \neq \hat{\sigma}$ and $D(\hat{\rho}, \hat{\rho}) = 0$. That being said, in calculations it is important to recognize relative entropy is not a true metric. It is not symmetric in the operators $\hat{\rho}$ and $\hat{\sigma}$ and additionally fails to satisfy the triangle inequality. For the purposes of deriving the nonequilibrium second law, the most important property of relative entropy is its monotonicity under the action of a completely positive trace preserving operator [79]. More precisely, for a completely positive trace preserving operator Λ and any two states $\hat{\rho}$ and $\hat{\sigma}$, we have the inequality

$$D(\Lambda\hat{\rho}, \Lambda\hat{\sigma}) \leq D(\hat{\rho}, \hat{\sigma}). \tag{1.26}$$

Recalling that the dynamics of our setup are governed by the completely positive trace preserving operator (1.24), this means that the relative entropy between any two states is a monotonically decreasing function of time. For the interested reader, result (1.26) follows from the properties of completely positive maps and the application of Uhlmann's theorem [132].

With this result the nonequilibrium second law can be proven as follows.

$$
\begin{aligned}
\Delta\mathcal{F} - \mathcal{W} &= \Delta\mathcal{U} - \Delta\mathcal{S}/\beta - \mathcal{W} \\
&= \mathcal{Q} - \Delta\mathcal{S}/\beta \\
&= \int_0^t \mathrm{Tr}\left[\hat{H}_s \frac{d\hat{\rho}_s}{ds} + \frac{1}{\beta}\frac{d\hat{\rho}_s}{ds}(\ln\hat{\rho}_s + 1)\right] ds \\
&= \frac{1}{\beta}\int_0^t \mathrm{Tr}\left[\frac{d\hat{\rho}_s}{ds}(\ln\hat{\rho}_s + \beta\hat{H}_s)\right] ds \\
&= \frac{1}{\beta}\int_0^t \mathrm{Tr}\left[\frac{d\hat{\rho}_s}{ds}(\ln\hat{\rho}_s + \hat{\pi}_s)\right] ds \\
&= \frac{1}{\beta}\int_0^t \frac{d}{ds} D(\hat{\rho}_s, \hat{\pi}_u)\Big|_{u=s} ds \\
&= \frac{1}{\beta}\int_0^t \lim_{\delta\to 0}\frac{1}{\delta}\left[D(\hat{\rho}_{s+\delta}, \hat{\pi}_s) - D(\hat{\rho}_s, \hat{\pi}_s)\right] ds \\
&= \frac{1}{\beta}\int_0^t \lim_{\delta\to 0}\frac{1}{\delta}\left[D(e^{\mathcal{L}_s\delta}\hat{\rho}_s, \hat{\pi}_s) + \mathcal{O}(\delta^2) - D(\hat{\rho}_s, \hat{\pi}_s)\right] ds \\
&= \frac{1}{\beta}\int_0^t \lim_{\delta\to 0}\frac{1}{\delta}\underbrace{\left[D(e^{\mathcal{L}_s\delta}\hat{\rho}_s, e^{\mathcal{L}_s\delta}\hat{\pi}_s) - D(\hat{\rho}_s, \hat{\pi}_s)\right]}_{\leq 0} ds \\
\implies \mathcal{W} &\geq \Delta\mathcal{F}
\end{aligned}
\tag{1.27}
$$

Here monotanicity of the relative entropy has been applied in the last line of the derivation. There we recognized that $e^{\mathcal{L}_s\delta}$ is a completely positive operator since $\mathcal{L}_t$ is of Lindblad form at all times.

1.3.2 Nonequilibrium Second Law from Copied Auxiliaries

We now consider a second situation, developed by the author, in which the nonequilibirum second law can be derived. Consider a composite system made up of a system of interest and N identical auxiliary systems which play the role of a thermal environment. Jointly the system and auxiliaries are driven according to Hamiltonian

dynamics in process of duration τ described by a unitary $\hat{U}$. At times $t = 0$ and $t = \tau$, the system's components are uncoupled and the full Hamiltonian is given by

$$\hat{H}_0 = \hat{H}_0^{sys} + \sum_n \hat{h}^{(n)} \tag{1.28}$$

$$\hat{H}_\tau = \hat{H}_\tau^{sys} + \sum_n \hat{h}^{(n)} \tag{1.29}$$

where $\hat{H}^{sys}$ and $\hat{h}^n$ are the Hamiltonians of the system of interest and n^{th} auxiliary system respectively. Note that 1) during the process the full Hamiltonian is arbitrary and the components may become coupled and 2) the auxiliary Hamiltonian returns to its initial value at the end of the process. The system components are initially uncorrelated with the system of interest being described by a density operator $\hat{\rho}_0^{sys}$ and each auxiliary starting in the thermal state

$$\hat{\pi}^{(n)} = \frac{e^{-\beta\hat{h}^{(n)}}}{\mathrm{Tr}[e^{-\beta\hat{h}^{(n)}}]} \tag{1.30}$$

where β is inverse temperature. In this setup the relevant thermodynamic quantities are defined according to

$$\mathcal{U} = \mathrm{Tr}[\hat{H}^{sys}\hat{\rho}] \tag{1.31}$$

$$\mathcal{W} = \mathcal{U}_\tau - \mathcal{U}_0 \tag{1.32}$$

$$\mathcal{U}^{sys} = \mathrm{Tr}[\hat{H}^{sys}\hat{\rho}^{sys}] \tag{1.33}$$

$$\mathcal{S}^{sys} = -\mathrm{Tr}[\hat{\rho}^{sys}\ln\hat{\rho}^{sys}] \tag{1.34}$$

$$\mathcal{F}^{sys} = \mathcal{U}^{sys} - \mathcal{S}^{sys}/\beta \tag{1.35}$$

where we emphasize that $\mathcal{U}$ is the combined energy of the system and auxilaries. Since the auxiliary systems explicitly model the thermal environment, no energy change of the joint system is due to heat and we may equate work with the energy change of the full system.

The proof of the second law in this context follows from three relatively simple mathematical properties of Hamiltonian mechanics and canonical states. The first property is that 1) the von Neumann entropy $\mathcal{S}$ of a density operator $\hat{\rho}$ is invariant under Hamiltonian dynamics. This follows immediately from the fact unitary dynamics preserve the eigenvalues of $\hat{\rho}$.

The second important piece of mathematics is analogous to the well known fact that the lowest energy state for a given entropy is always of canonical form. Specifically, 2) consider a composite system made up of two noninteracting subsystems A and B with Hamiltonians given respectively by $\hat{H}^A$ and $\hat{H}^B$. Assume furthermore that the dimension of A's Hilbert space is less than that of B's. For a given von Neumann entropy $\mathcal{S}$ of the composite system and reduced state $\hat{\rho}^A$ of system A, the joint state $\hat{\rho}$ that minimizes average energy $\mathcal{U}$ is $\hat{\rho}^A \otimes \hat{\pi}^B$ where $\hat{\pi}^B$ is of canonical form. A proof of this result is given at the end of this section.

The third result that we need for the derivation of the nonequilibrium second law states that 3) the quantity

$$\tilde{\mathcal{W}}(N) = \min_{\hat{\rho}}{}^{*}\mathrm{Tr}[\hat{H}_\tau \hat{\rho} - \hat{H}_0 \hat{\rho}_0] \tag{1.36}$$

is a non-increasing function of N where N is the number of auxilary systems, the

asterisk signifies that the minimization is restricted to only states $\hat{\rho}$ that satisfy

$$\mathcal{S}(\hat{\rho}) = \mathcal{S}(\hat{\rho}_0) \tag{1.37}$$

$$\mathrm{Tr}^{aux}[\hat{\rho}] = \hat{\rho}_\tau^{sys}, \tag{1.38}$$

and the initial state is of the form $\hat{\rho}_0 = \hat{\rho}^{sys} \otimes_i^N \hat{\pi}_\beta$. This can be seen from the following argument. From property 2) we know that $\tilde{\mathcal{W}}(N) = \mathrm{Tr}[\hat{H}_\tau \hat{\rho}^{sys} \otimes_i^N \hat{\pi}_{\tilde{\beta}} - \hat{H}_0 \hat{\rho}_0]$ for some $\tilde{\beta}$ different from the initial inverse temperature β. Note that in the minimization that defines $\tilde{\mathcal{W}}(N+1)$, one possible choice of $\hat{\rho}$ consistent with conditions (1.37) and (1.38) is $\hat{\sigma} = \hat{\rho}^{sys} \otimes_i^N \hat{\pi}_{\tilde{\beta}} \otimes \hat{\pi}_\beta$. It follows immediately from the fact $\mathrm{Tr}[\hat{H}_\tau \sigma - \hat{H}_0 \hat{\rho}_0 \otimes \hat{\pi}_\beta] = \tilde{\mathcal{W}}(N)$ that $\tilde{\mathcal{W}}(N) \geq \tilde{\mathcal{W}}(N+1)$. Roughly this means that a larger bath is a more useful resource for work extraction than a smaller bath.

For the setup defined in this section, the second law can be proven as follows. Consider the case of N auxiliary systems and a process where the final state of the

system of interest is given by $\hat{\rho}_\tau^{sys}$. Observe,

$$\begin{aligned}
\mathcal{W} &= \mathrm{Tr}[\hat{H}_\tau \hat{\rho}_\tau - \hat{H}_0 \hat{\rho}_0] && (1.39)\\
&= \mathrm{Tr}[\hat{H}_\tau \hat{U} \hat{\rho}_0 \hat{U}^\dagger - \hat{H}_0 \hat{\rho}_0] \\
&\geq \min_{\hat{\rho}}{}^{*} \mathrm{Tr}[\hat{H}_\tau \hat{\rho} - \hat{H}_0 \hat{\rho}_0] && (1.40)\\
&= \tilde{\mathcal{W}}(N) \\
&\geq \lim_{N\to\infty} \tilde{\mathcal{W}}(N) && (1.41)\\
&= \lim_{N\to\infty} \mathrm{Tr}[\hat{H}_\tau \hat{\rho}_\tau^{sys} \overset{N}{\underset{i=1}{\otimes}} \hat{\pi}_{\tilde{\beta}} - \hat{H}_0 \hat{\rho}_0^{sys} \overset{N}{\underset{i=1}{\otimes}} \hat{\pi}_\beta] \\
&= \lim_{N\to\infty} \mathcal{U}_\tau^{sys} + N\mathcal{U}_{\tilde{\beta}}^{aux} - \mathcal{U}_0^{sys} - N\mathcal{U}_\beta^{aux} \\
&= \Delta\mathcal{U}^{sys} + \lim_{N\to\infty} N \left(\mathcal{U}_{\tilde{\beta}}^{aux}|_{1/N\to 0} + \frac{d\mathcal{U}_{\tilde{\beta}}^{aux}}{dS_{\tilde{\beta}}^{aux}} \left.\frac{dS_{\tilde{\beta}}^{aux}}{d(1/N)}\right|_{1/N\to 0} \frac{1}{N} + \mathcal{O}(\frac{1}{N^2}) - \mathcal{U}_\beta^{aux} \right) && (1.42)\\
&= \Delta\mathcal{U}^{sys} + \lim_{N\to\infty} N \left(\mathcal{U}_\beta^{aux} + \frac{\mathcal{S}_0^{sys} - \mathcal{S}_\tau^{sys}}{\beta} \frac{1}{N} + \mathcal{O}(\frac{1}{N^2}) - \mathcal{U}_\beta^{aux} \right) \\
&= \Delta\mathcal{F}^{sys}.
\end{aligned}$$

Note that the line (1.40) of the proof uses fact 1), line (1.41) uses fact 3), and the expansion in line (1.42) uses the standard formula $d\mathcal{U}/d\mathcal{S} = 1/\beta$ and conservation of entropy of the total joint system.

We now conclude this section with a sketch of the proof of mathematical fact 2). The goal of the following is to find a state $\hat{\rho}$ that minimizes the average energy

$$\mathcal{U} = \mathrm{Tr}[(\hat{H}^A + \hat{H}^B)\hat{\rho}] \tag{1.43}$$

when restricted to states that satisfy the constraints

$$f = -\mathrm{Tr}[\hat{\rho} \ln \hat{\rho}] - \mathcal{S} = 0 \tag{1.44}$$

$$g_{ij} = \mathrm{Tr}^B[\hat{\rho}]_{ij} - \hat{\rho}^A_{ij} = 0. \tag{1.45}$$

It is convenient to express the density operator of the joint system by

$$\hat{\rho} = \sum_{mn\mu\nu} \rho_{mn\mu\nu} |m\rangle\langle n| \otimes |\mu\rangle\langle\nu| \tag{1.46}$$

where the basis sets for the subsystems, denoted respectively by $|n\rangle$ and $|\nu\rangle$, are defined according to

$$\hat{\rho}^A = \sum_n p^A_n |n\rangle\langle n| \tag{1.47}$$

$$\hat{H}^B = \sum_\nu \epsilon^B_\nu |\nu\rangle\langle\nu|. \tag{1.48}$$

The method of Lagrange multipliers asserts that a state $\hat{\rho}$ that satisfies the constraints (1.44) and (1.45) is an extremum of the above problem whenever there exists constants λ_0 and λ_{ij} such that

$$\frac{\partial \mathcal{U}}{\partial \rho_{mn\mu\nu}} = \lambda_0 \frac{\partial f}{\partial \rho_{mn\mu\nu}} + \sum_{ij} \lambda_{ij} \frac{\partial g_{ij}}{\partial \rho_{mn\mu\nu}}. \tag{1.49}$$

Note that g_{ij} is assumed to be written in the basis $|n\rangle$ defined by equation (1.47). Now consider the canonical state $\hat{\pi}^B$ with inverse temperature β defined by the entropy balance equation

$$\mathcal{S} = \mathcal{S}^A + \mathcal{S}^B \tag{1.50}$$

where $\mathcal{S}^A = \mathcal{S}(\hat{\rho}^A)$ and $\mathcal{S}^B = \mathcal{S}(\hat{\pi}^B)$. We assumed the dimension of A's Hilbert space is less than B's to ensure equation (1.50) has a solution. Trivially the state $\hat{\rho} = \hat{\rho}^A \otimes \hat{\pi}^B$ satisfies the constraints (1.44) and (1.45). We now show through direct substitution that $\hat{\rho}^A \otimes \hat{\pi}^B$ satisfies (1.49) when the Lagrange multipliers are chosen according to

$$\lambda_0 = \beta^{-1} \tag{1.51}$$

$$\lambda_{ij} = \langle j|\hat{H}^A|i\rangle + \beta^{-1}(\ln p_i^A - \ln Z + 1)\delta_{ij}. \tag{1.52}$$

When evaluated at $\hat{\rho}^A \otimes \hat{\pi}^B$, the derivatives of equation (1.49) have the form

$$\frac{\partial \mathcal{U}}{\partial \rho_{mn\mu\nu}} = (\langle n|\hat{H}^A|m\rangle + \epsilon_\mu^B \delta_{mn})\delta_{\mu\nu} \tag{1.53}$$

$$\frac{\partial f}{\partial \rho_{mn\mu\nu}} = -(\ln p_n^A - \beta\epsilon_\mu^B - \ln Z + 1)\delta_{mn}\delta_{\mu\nu} \tag{1.54}$$

$$\frac{\partial g_{ij}}{\partial \rho_{mn\mu\nu}} = \delta_{im}\delta_{jn}\delta_{\mu\nu}. \tag{1.55}$$

With some algebra it is straightforward to show that equation (1.49) is satisfied by expressions (1.51)-(1.55). Therefore $\hat{\rho}^A \otimes \hat{\pi}^B$ is an extremum which we assume is also a global minimum.

Chapter 2: Dephasing and the Quantum Work Relation

Statements of the second law of thermodynamics are generally expressed as inequalities. For instance the work performed on a system during an isothermal process must not exceed the net change in its free energy: $\mathcal{W} \geq \Delta\mathcal{F}$. When statistical fluctuations are appropriately included these inequalities can be reformulated as equalities, such as the nonequilibrium work relation [63]

$$\langle e^{-\beta\mathcal{W}} \rangle = e^{-\beta\Delta\mathcal{F}} \tag{2.1}$$

where β is an inverse temperature and angular brackets denote an average over repetitions of the process. For classical systems, this prediction and related *fluctuation theorems* have been extensively studied both theoretically [65] and experimentally [15, 29, 42, 54, 66, 80, 112, 117], and have been applied to the numerical estimation of free energy differences [28, 104].

The last decade has seen growing interest in extending these results to quantum systems [53]. This pursuit is made challenging both by the fact that classical work is defined in terms of trajectories – a notion that is typically absent in the quantum setting – and by the lack of a quantum "work operator" [128]. To avoid these difficulties, many studies have focused on closed quantum systems, which evolve unitarily. In the absence of a heat bath there is no heat transfer to or from the system and the

first law of thermodynamics reads,

$$\mathcal{W} = \Delta\mathcal{U} \equiv E_f - E_i. \tag{2.2}$$

Here the classical work depends only on a system's initial and final configuration and can be determined from two measurements. This idea is easily lifted to the quantum regime through the *two-point measurement* (TPM) protocol [74, 95, 130], according to which the work performed during a single experimental run is the difference between energy values E_i and E_f resulting from initial and final projective measurements.

If a system is prepared in equilibrium at inverse temperature β with initial Hamiltonian $\hat{H}(0) = \sum \epsilon_n |n\rangle\langle n|$, then evolves unitarily as the Hamiltonian is varied from $\hat{H}(0)$ at $t = 0$ to $\hat{H}(\tau) = \sum \bar{\epsilon}_m |\bar{m}\rangle\langle\bar{m}|$ at $t = \tau$, the TPM work distribution is given by

$$p(W) = \sum_{nm} p_n \, p_{\bar{m}|n} \, \delta[W - (\bar{\epsilon}_m - \epsilon_n)]. \tag{2.3}$$

Here $p_n = Z_0^{-1} e^{-\beta\epsilon_n}$ is the probability to obtain the value $E_i = \epsilon_n$ during the initial energy measurement, $p_{\bar{m}|n}$ is the conditional probability to obtain the final energy value $E_f = \bar{\epsilon}_m$, given the initial value ϵ_n, and Z_0 is the partition function for the initial equilibrium state. To date, both proposed [41, 61, 90, 110] and implemented [8, 11, 91, 97] experimental tests of the quantum work relation (2.1) have focused on evaluating equation (2.3) for a closed system.

Subtle conceptual issues arise if the system's initial state contains coherences in the energy basis, since such states are disturbed by the initial measurement [68, 122]. Even in this situation equation (2.1) remains valid under the TPM scheme, provided the diagonal elements of the initial density matrix are given by Boltzmann factors [129]. These issues will not affect our analysis, as we will always assume our

system begins in equilibrium, and is thus described by a diagonal (in the energy basis) density matrix.

A number of authors have proposed definitions of work and derived fluctuation theorems for quantum systems in contact with general thermal environments [21, 30, 32, 48, 109, 127, 140]. Our more focused aim in this chapter is to consider a quantum system in contact with a thermal environment that produces decoherence but no dissipation. From a theoretical viewpoint, we argue that the TPM protocol provides a natural definition of quantum work in this situation, and we give an elementary, physically motivated derivation of equation (2.1) that agrees with more general results obtained by previous authors [3, 67, 89, 106, 107]. We then describe an experimental implementation constructed from trapped ions that makes use of noise to achieve the effects of a bath which causes decoherence but no dissipation. From the data we verify the validity of the quantum work relation, providing the first experimental confirmation of equation (2.1) for a system undergoing decoherence.

2.1 Theoretical Development

When a quantum system is coupled to a thermal environment, there arise two distinct departures from unitary dynamics: dissipation, that is the exchange of energy, and decoherence, the leakage of the system's quantum coherences into the environment [142]. *We will consider situations in which dissipation is negligible over experimentally relevant time scales, but decoherence is substantial.* Under such conditions the environment is a *decohering* (or *dephasing*) environment: it suppresses coherences but does not exchange energy.

Consider a system in contact with a decohering environment. At $t = 0$, following a projective energy measurement, the system begins in an energy eigenstate $|n\rangle$,

then it evolves as its Hamiltonian is varied with time. At $t = \tau$ its energy is again measured, yielding $\bar{\epsilon}_m$. By assumption, no energy is exchanged with the environment, therefore we claim that it is natural to identify work to be the difference between the initial and final energies, $\mathcal{W} = \bar{\epsilon}_m - \epsilon_n$, just as for a closed quantum system (see equation (2.2)). If we accept this as a plausible definition of work in the presence of a decohering environment, then does equation (2.1) remain valid in this situation? This question can be answered affirmatively within the general framework of quantum channels [89, 106, 107]. We now take a phenomenological approach to arrive at the same answer.

We begin by modeling the dynamics of the system. In the energy representation, a decohering environment does not affect the diagonal elements (populations) of the system's density matrix $\hat{\rho}(t)$, but may cause off-diagonal matrix elements (coherences) to decay. We capture these features with the equation

$$\frac{d\hat{\rho}}{dt} = -\frac{i}{\hbar}[\hat{H}(t), \hat{\rho}] - \sum_{i \neq j} \gamma_{ij} \rho_{ij} |i\rangle\langle j| \;\equiv\; \mathcal{L}\hat{\rho} \quad , \tag{2.4}$$

which describes both unitary evolution under $\hat{H}(t)$ and the decohering effects of the environment. Here $\gamma_{ij} \geq 0$ are phenomenological decay rates for the coherences $\rho_{ij} \equiv \langle i|\hat{\rho}|j\rangle$, in the instantaneous eigenbasis of $\hat{H}(t)$.

Although we have motivated equation (2.4) heuristically, it can also be obtained from the perspective of *quantum detailed balance master equations* (QDBME) [4]. These equations are a special type of Lindblad master equation and are of physical relevance as they rigorously describe a quantum system coupled to an infinite, thermal quantum reservoir under appropriate assumptions of weak interaction and separation of time scales [51, 73, 124].

For an N-level quantum system with no degenerate energy gaps, the QDBME

governing the evolution of the density operator can be written in the form

$$\begin{aligned} \frac{d\hat{\rho}}{dt} &= -\frac{i}{\hbar}[\hat{H},\hat{\rho}] + \sum_{ij} J_{ij}|i\rangle\langle i| + \sum_{i\neq j}\Gamma_{ij}|i\rangle\langle j| \\ J_{ij} &\equiv R_{ij}\rho_{jj} - R_{ji}\rho_{ii} \\ \Gamma_{ij} &\equiv (R_{ii} + R_{jj} - \gamma_{ij})\rho_{ij} < 0 \\ \gamma_{ij} &\equiv \sum_k d_k (O_{ki} - O_{kj})^2 \geq 0 \end{aligned} \tag{2.5}$$

where the R_{ij}'s form a stochastic rate matrix [135] satisfying detailed balance, the O_{ij}'s form a real orthogonal matrix, and $d_k > 0$ for all k. For the readers convenience, we show in subsection 2.1.1 how this result can be derived from the more general but less intuitive detailed balance condition presented by Alicki in [4]. The three terms on the right side of equation (2.5) respectively describe unitary evolution, dissipation, and decoherence. The dissipative term evolves the diagonal elements of $\hat{\rho}$ (populations) according to a classical Markov process described by the rate matrix R, whereas the decohering term causes the decay of off-diagonal elements (coherences). To model a decohering environment we set all $R_{ij} = 0$, thereby suppressing thermally induced transitions between energy eigenstates. This leads immediately to equation (2.4).

As a final note on equation (2.4), we point out that it can also be derived from a microscopic model where the environment is explicitly modeled. This setup is advantageous since all fluctuations in both heat and work can be carefully accounted for using the TMP protocol on the joint system. Specifically it is possible to argue that for a strictly dephasing master equation both the mean heat and fluctuations in heat vanish. In subsection 2.1.2, we present a simple repeated interaction bath model that exemplifies this point and strengthens the conceptual arguments given

previously.

Note that evolution under equation (2.4) preserves the identity, $\mathcal{L}\hat{I} = 0$, hence this evolution is *unital*, and equation (2.1) follows as an immediate consequence of a general result derived by Rastegin [106]. To keep our presentation self-contained, we now derive equation (2.1) assuming only a linear master equation that preserves the identity.

Let $\Lambda_\tau : \hat{\rho}_0 \to \hat{\rho}_\tau$ denote the quantum evolution that maps an initial density matrix to a final density matrix, under the dynamics of equation (2.4). After initial equilibration, an energy measurement at time $t = 0$ yields an energy eigenvalue ϵ_n with probability $p_n = Z_0^{-1} e^{-\beta\epsilon_n}$, and "collapses" the system into a pure state $\hat{\rho}_0 = |n\rangle\langle n|$. This state then evolves under equation (2.4) to $\hat{\rho}_\tau = \Lambda_\tau(\hat{\rho}_0)$ and a final energy measurement at $t = \tau$ yields a value $\bar{\epsilon}_m$ with probability $p_{\bar{m}|n} = \langle \bar{m}|\hat{\rho}_\tau|\bar{m}\rangle$. Summing over all possible measurement outcomes, and using the linearity and identity preservation of Λ_τ, we have [106]

$$\begin{aligned} \langle e^{-\beta\mathcal{W}} \rangle &= \sum_{nm} p_n \, p_{\bar{m}|n} \, e^{-\beta(\bar{\epsilon}_m - \epsilon_n)} \\ &= \sum_{nm} \frac{e^{-\beta\epsilon_n}}{Z_0} \langle \bar{m}|\Lambda_\tau(|n\rangle\langle n|)|\bar{m}\rangle e^{-\beta(\bar{\epsilon}_m - \epsilon_n)} \\ &= \frac{1}{Z_0} \sum_m e^{-\beta\bar{\epsilon}_m} \langle \bar{m}|\Lambda_\tau(\hat{I})|\bar{m}\rangle \\ &= \frac{Z_\tau}{Z_0} = e^{-\beta\Delta\mathcal{F}} \quad . \end{aligned} \tag{2.6}$$

2.1.1 Detailed Balance Quantum Master Equations

Consider a quantum detailed balance master equation with a Hamiltonian $\hat{H} = \sum \epsilon_i |i\rangle\langle i|$ and an equilibrium state $\hat{\pi}$ satisfying the standard thermal relation

$$\hat{\pi} = \frac{e^{-\beta \hat{H}}}{Tr[e^{-\beta \hat{H}}]}. \tag{2.7}$$

Additionally assume that the gaps $\epsilon_i - \epsilon_j$ in the spectrum of $\hat{H}$ are non-degenerate. Under these conditions, Alicki showed [4] that the master equation may be written in the form

$$\frac{d\hat{\rho}}{dt} = -\frac{i}{\hbar}[\hat{H}, \hat{\rho}] + \sum_{i,j=1}^{N} D_{ij}\Big\{[\hat{X}_{ij}, \hat{\rho}\hat{X}_{ij}^{\dagger}] + [\hat{X}_{ij}\hat{\rho}, \hat{X}_{ij}^{\dagger}]\Big\} \tag{2.8}$$

where N is the dimension of the system's Hilbert space and the real numbers D_{ij} and operators $\hat{X}_{ij}$ satisfy the conditions

$$D_{ij}e^{-\beta\epsilon_j} = D_{ji}e^{-\beta\epsilon_i} \;\; ; \;\; D_{ij} \geq 0 \tag{2.9}$$

$$[\hat{H}, \hat{X_{ij}}] = (\epsilon_i - \epsilon_j)\hat{X}_{ij} \tag{2.10}$$

$$Tr[\hat{X}_{ij}^{\dagger}\hat{X}_{kl}] = \delta_{ik}\delta_{jl} \tag{2.11}$$

$$\hat{X}_{ij} = \hat{X}_{ji}^{\dagger}. \tag{2.12}$$

In what follows, we will use the non-degenerate gaps of $\hat{H}$ along with conditions (2.9)-(2.12) to gain insight into the constants D_{ij} and operators $\hat{X}_{ij}$. This in turn will allow for equation (2.8) to be written in a form where the processes of relaxation and decoherence are manifest.

Constants D_{ij} – The constants D_{ij} can largely be interpreted within the framework of a classical continuous time Markov process [135]. Assuming discrete states indexed by i, such processes describe the evolution of a probability distribution p_i according to

$$\frac{dp_i}{dt} = \sum_j r_{ij} p_j \tag{2.13}$$

where r_{ij} is a transition rate matrix with the properties

$$r_{ij} \begin{cases} \geq 0; & (i \neq j) \\ \\ = -\sum_{k \neq i} r_{ki} & (i = j). \end{cases} \tag{2.14}$$

Furthermore the matrix r_{ij} is said to satisfy detailed balance with respect to an equilibrium probability distribution π_i when

$$r_{ij}\pi_j - r_{ji}\pi_i = 0. \tag{2.15}$$

Given these definitions, one immediately recognizes from condition (2.9) that the off diagonal elements of D_{ij} coincide with the elements of a transition rate matrix satisfying the detailed balance condition (2.15) with $\pi_i \propto \exp(-\beta\epsilon_i)$. In what follows,

we will find that the energy populations $\rho_{ii} = \langle i|\hat{\rho}|i\rangle$ relax thermally according to

$$\begin{aligned} \frac{d\rho_{ii}}{dt} &= \sum_{j\neq i}(2D_{ij})\rho_{jj} + (-2\sum_{j\neq i} D_{ji})\rho_{ii} \\ &= \sum_{j\neq i} r_{ij}\rho_{jj} + r_{ii}\rho_{ii}. \end{aligned} \tag{2.16}$$

Hence for $i \neq j$ we will interpret D_{ij} as half the thermally induced transition rate from energy state j to state i. Note that r_{ii} is defined according to equation (2.14) and $D_{ii} \neq r_{ii}/2$. Condition (2.9) only constrains the constants D_{ii} to be positive. These numbers will later be interpreted in terms of decoherence rates. Anticipating these connections, the elements of D_{ij} will be redefined according to

$$D_{ij} = \begin{cases} r_{ij}/2 & (i \neq j) \\ \\ d_i & (i = j). \end{cases} \tag{2.17}$$

Operators $\hat{X}_{ij}$ – Before finding the explicit form of the operators $\hat{X}_{ij}$, it is instructive to recast conditions (2.10) and (2.11) in the language of linear algebra. Specifically note that condition (2.10) dictates that $\hat{X}_{ij}$ is an eigen-operator of the super-operator $[\hat{H}, \cdot]$ with eigenvalue $\epsilon_i - \epsilon_j$ while condition (2.11) asserts that the operators $\hat{X}_{ij}$ form an orthonormal set with respect to the matrix inner product $\langle \hat{A}, \hat{B}\rangle = Tr[\hat{A}^\dagger \hat{B}]$.

First consider the operators $\hat{X}_{ij}$ for which $i \neq j$. In this case, each eigenvalue $\epsilon_i - \epsilon_j$ of equation (2.10) is non-degenerate (due to the gap structure of $\hat{H}$) and hence the corresponding eigen-operator $\hat{X}_{ij}$ is confined to a one dimensional eigenspace. By inspection this eigenspace is determined to be $\{\alpha|i\rangle\langle j| : \alpha \in \mathbb{C}\}$. The normalization

condition (2.11) further gives the constraint that $|\alpha|^2 = 1$. Without loss of generality, it is now possible to set

$$\hat{X}_{ij} = |i\rangle\langle j| \quad (i \neq j) \tag{2.18}$$

due to the fact that the master equation (2.8) is independent of the phase of α since $\hat{X}_{ij}$ and $\hat{X}_{ij}^{\dagger}$ appear in conjugate pairs.

For the case where $i = j$, the eigenvalue in equation (2.10) vanishes and corresponds to the N dimensional eigenspace $\{\sum_k O_{ik}|k\rangle\langle k| : O_{ik} \in \mathbb{C}\}$. Application of conditions (2.11) and (2.12) gives

$$O_{ik} \in \mathbb{R} \ ; \ \sum_k O_{ik}O_{jk} = \delta_{ij} \tag{2.19}$$

which is exactly the condition that the matrix O_{ik} belong to the set of real orthogonal matrices $O(N)$. In conclusion

$$\hat{X}_{ii} = \sum_k O_{ik}|k\rangle\langle k| \ ; \ O_{ik} \in O(N). \tag{2.20}$$

The form of the detailed balance master equation in the main body of this manuscript can now be deduced. Following substitution of equations (2.17), (2.18), and (2.20) into the master equation (2.8) and some manipulation, the result is given by

$$\frac{d\hat{\rho}}{dt} = -\frac{i}{\hbar}[\hat{H}, \hat{\rho}] + \sum_{ij} J_{ij}|i\rangle\langle i| + \sum_{i \neq j} \Gamma_{ij}|i\rangle\langle j| \tag{2.21}$$

$$J_{ij} \equiv r_{ij}\rho_{jj} - r_{ji}\rho_{ii}$$

$$\Gamma_{ij} \equiv [(r_{ii} + r_{jj})/2 - \gamma_{ij}]\rho_{ij} \leq 0$$

$$\gamma_{ij} \equiv \sum_k d_k(O_{ki} - O_{kj})^2 \geq 0.$$

As stated earlier, the virtue of writing the master equation in the above form is that the processes of relaxation and decoherence are clearly displayed – they are the second and third terms on the right hand side of equation (2.21) respectively. The relaxation is seen to shuffle the diagonal elements of the density operator according to a Markov process while the decoherence term causes exponential decay of off-diagonal elements.

2.1.2 The Decohering Master Equation from a Hamiltonian Model

In our main theoretical development, we argued that it is plausible no heating occurs during a decohering process and hence it is reasonable to determine work values using the two-point measurement protocol. Here we strengthen this argument by presenting a specific microscopic model where our intuition can be verified according to the definitions of heat and work presented by Campisi *et al* [19].

Specifically, we consider a simple repeated interaction model where the bath is represented by a stream of identical auxiliary systems which we will refer to as *units*. Each unit begins in a thermal state $\hat{\pi}$ and interacts with the system of interest for a time δt. Over every interaction interval, the total Hamiltonian (system plus units) is fixed but the system's Hamiltonian and the interaction may change suddenly between intervals. We will denote the total Hamiltonian during the nth interval by

$$\hat{H}_n = \hat{H}_n^{sys} \otimes \hat{I}^{aux} + \hat{I}^{sys} \otimes \hat{H}^{aux} + \lambda \hat{V}_n \tag{2.22}$$

where $\hat{H}_n^{sys}$ is the system's Hamiltonian, $\hat{H}^{aux}$ is the Hamiltonian of the non-interacting units which each have individual Hamiltonians $\hat{h}^{aux}$, λ is the interaction strength, and $\hat{V}_n$ is an interaction that acts only on the system and nth unit. Furthermore to assure the process only produces dephasing in the system of interest, we assume that the

interaction is of the form

$$\hat{V}_n = \hat{A}_n \otimes \hat{B} \tag{2.23}$$

where $\hat{A}_n$ acts on the system and commutes with $\hat{H}_n^{sys}$ while $\hat{B}$ acts on the nth unit and commutes with $\hat{h}^{aux}$. In the following, we outline two important properties of this model: 1) the existence of a regime where the system's dynamics are described by a decohering master equation and 2) the absence of heat transfer between the system and units.

In order to show 1), we take

$$\hat{H}_n^{sys} = \hat{H}^{sys}(n\delta t) \tag{2.24}$$

$$\hat{A}_n = \hat{A}(n\delta t) \tag{2.25}$$

where $\hat{H}^{sys}(t)$ and $\hat{A}(t)$ are operators that vary continuously with time and make the standard assumption [102] that $Tr[\hat{\pi}\hat{B}] = 0$. Taking the limit $\delta t \to 0$ while simultaneously letting the interaction strength grow according to $\lambda = k\delta t^{-1/2}$ where k is a positive real constant, it can be shown [125] that

$$\begin{aligned} \frac{d\rho^{sys}}{dt} = & - \frac{i}{\hbar}[\hat{H}^{sys}(t), \rho^{sys}] \\ & - C\left[\hat{A}(t)\rho^{sys}\hat{A}(t) - \frac{1}{2}\{\hat{A}^2(t), \rho^{sys}\}\right] \end{aligned} \tag{2.26}$$

$$C = \frac{2k\mathrm{Tr}[\hat{B}^2\hat{\pi}]}{\hbar^2}$$

Since $\hat{H}(t)$ and $\hat{A}(t)$ commute at all times, they share a common eigenbasis $\{|i(t)\rangle\}$. Rewriting the dissipator (second term on the RHS of equation (2.27)) in this basis,

the master equation becomes

$$\frac{d\rho^{sys}}{dt} = -\frac{i}{\hbar}[\hat{H}^{sys}(t), \rho^{sys}] \\ -\sum_{i\neq j} \gamma_{ij} |i(t)\rangle\langle i(t)|\rho^{sys}|j(t)\rangle\langle j(t)| \tag{2.27}$$

$$\gamma_{ij} = \frac{\mathrm{Tr}[\hat{B}^2\hat{\pi}]}{\hbar^2}(a_i - a_j)^2$$

where a_i are the eigenvalues of $\hat{A}$.

We now show property 2) holds according to the definitions of heat and work proposed in [19]. In this setup, work is determined (for initially thermal states) by applying the two point measurement protocol to the joint system and environment. Assuming that the system is decoupled from the units at the beginning and end of the process, the work performed during a single realization is given by $W = \epsilon_m^{sys} + \epsilon_k^{aux} - \epsilon_n^{sys} - \epsilon_l^{aux}$ where $\epsilon_m^{sys} + \epsilon_k^{aux}$ and $\epsilon_n^{sys} + \epsilon_l^{aux}$ respectively are the initial and final energy measurements. Since the total Hamiltonian of the system and units commutes with $\hat{H}^{aux}$ at all times, it follows that $\epsilon_k^{aux} = \epsilon_l^{aux}$ which implies that the work is fully determined by local measurements on the system of interest as claimed in the main text of this manuscript.

2.2 Experimental Verification

To test equation (2.1) experimentally, we employ a two state system engineered from a $^{171}Yb^{+}$ ion's total angular momentum degree of freedom, using the energy levels $|F = 0, m_F = 0\rangle \equiv |\downarrow\rangle$ and $|F = 1, m_F = -1\rangle \equiv |\uparrow\rangle$ belonging to the ground-state manifold of $^2S_{1/2}$ [141]. See [99] for an overview of techniques related to this system. By applying microwave pulses resonant to our states' energy difference

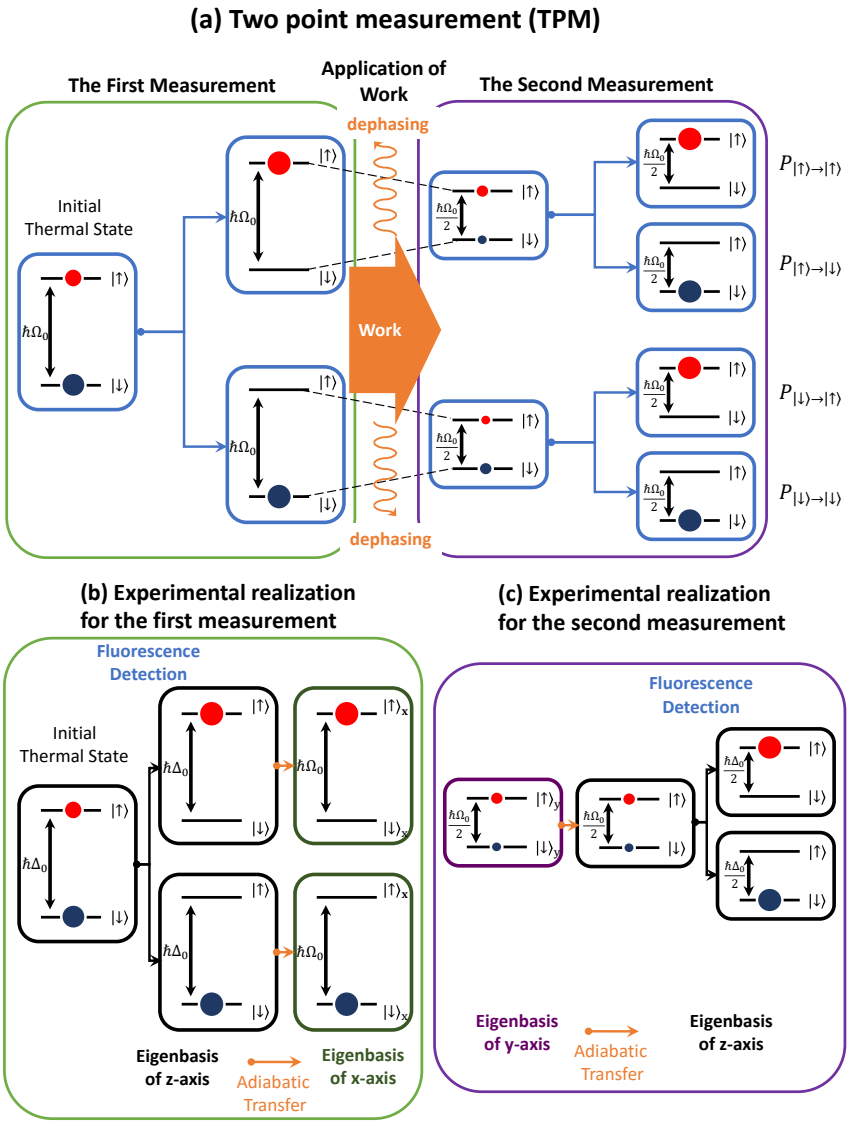

Figure 2.1: (a) and (b)(c) respectively show conceptual and actual experimental schematics of the TMP protocol in our setup. (b) indicates that in the true experiment thermal state preparation and initial energy measurement occur in the $\hat{\sigma}_z$ eigenbasis before being transfered to the basis of $\hat{\sigma}_x$ with the aid of an adiabatic shortcut. (c) indicates how the system is again rotated–this time from the $\hat{\sigma}_y$ to $\hat{\sigma}_z$ basis–proceeding the second fluorescence measurement. Note that the level splitting in the $\hat{\sigma}_z$ basis is set by Δ_0 which is the frequency difference between the laser beat-note and ω_0.

$\omega_0 \equiv \omega_{\mathrm{HF}} - \omega_{\mathrm{Z}}$, where $\omega_{\mathrm{HF}} = (2\pi)\,12.642821\mathrm{GHz}$ and $\omega_{\mathrm{Z}} = (2\pi)\,13.586\mathrm{MHz}$, the

system can be driven according to the Hamiltonian

$$\hat{H}(t) = \frac{\hbar\Omega(t)}{2}\left[\hat{\sigma}_{\mathrm{x}}\cos\phi(t) + \hat{\sigma}_{\mathrm{y}}\sin\phi(t)\right]. \tag{2.28}$$

Here $\hat{\sigma}_{x,y}$ are the standard Pauli matrices in the $\{|\uparrow\rangle, |\downarrow\rangle\}$ basis while Ω and ϕ are parameters controlled through the amplitude and phase of the microwave pulses. In our experiment, we use the driving protocols

$$\Omega(t) = \Omega_0\left(1 - \frac{t}{2\tau}\right) \;\; ; \;\; \phi(t) = \frac{\pi t}{2\tau} \tag{2.29}$$

where τ is the duration of the process. Together equations (2.28) and (2.29) represent the Hamiltonian portion of our system's dynamics. The decohering term of equation (2.4) is realized by the addition of noise in the microwave pulse sequence. In our setup this adds a stochastic term $\Omega_0\xi(t)$ to the protocol $\Omega(t)$ where $\xi(t)$ is gaussian white noise characterized by zero mean $\xi(t) = 0$ and variance $\Delta\xi(t)\xi(t+\tau) = \alpha^2\delta(\tau)$. Averaging over all realizations of the noise $\xi(t)$ produces an equation of motion identical to equation (2.4) with $\gamma_{ij} = \gamma = \frac{1}{2}\alpha^2\Omega_0^2$ [26, 78, 85, 121] (see also Appendix 2.5.1).

Given this setup, the procedure for measuring the work applied during a single experimental trial involves four steps: (*i*) thermal state preparation, (*ii*) initial energy measurement, (*iii*) application of the driving protocol, and (*iv*) final energy measurement, as shown in figure 2.1(a).

Our Hamiltonian has the form $\hat{H}(t) = \mathbf{B}(t)\cdot\hat{\boldsymbol{\sigma}}$, where the field $\mathbf{B}(t)$ undergoes rotation by 90° in the xy-plane (see equation (2.28)). For technical reasons the initial thermalization and both measurements are performed in the $\hat{\sigma}_z$ basis. Therefore after the initial thermalization and measurement we rotate the system from the z-axis into the xy-plane, then we implement the driving as per equation (2.28), and finally

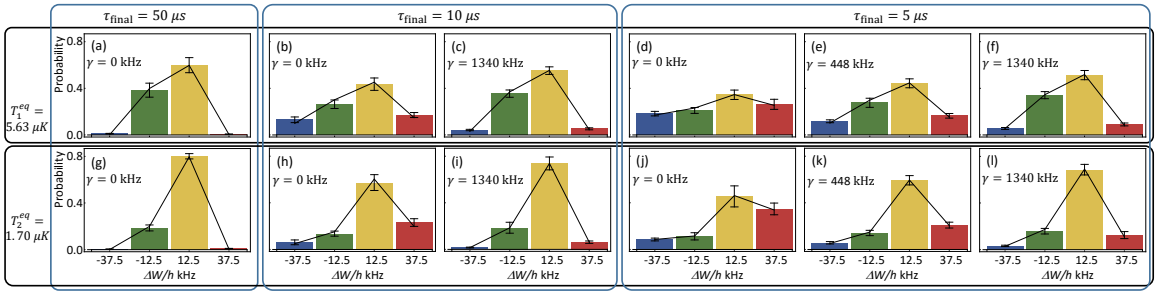

Figure 2.2: The work distributions (a)-(f) correspond to an initial temperature of $T_1 = 5.63\ \mu$K while (g)-(l) have $T_2 = 1.70\ \mu$K. The driving times $\tau = 50\mu s$, $\tau = 10\mu s$, and $\tau = 5\mu s$ represent near adiabatic (a)(g), moderate(a)(c)(h)(i), and fast (d)(e)(f)(j)(k)(i) driving regimes. The dephasing rate γ took values of 0, 448, and 1340 kHz for the cases of no (a)(b)(d)(g)(h)(j), intermediate (e)(k), and large (c)(f)(i)(l) dephasing respectively.

we rotate the system back to the z-axis to perform the final measurement. These rotations do not affect the work distribution. The rotations are achieved with *adiabatic shortcuts* [7, 13, 35], which produce transformations equivalent to adiabatically switching the system's Hamiltonian, but in a finite time (see Appendix 2.5.4). Figure 2.1 (b)(c) show detailed schematics of the measurement protocols, including these shortcuts.

(i) Thermal state preparation - We create the initial thermal state using the following procedure. First we prepare the pure state $|\psi\rangle = c_\uparrow|\uparrow\rangle + c_\downarrow|\downarrow\rangle$ using a standard optical pumping sequence followed by the application of resonant microwaves over a proper duration. After waiting more than 10 times the coherence time (see Appendix 2.5.2), the state becomes a mixed-state described by the density operator $\hat{\rho}_{\text{ini}} = |c_\uparrow|^2|\uparrow\rangle\langle\uparrow| + |c_\downarrow|^2|\downarrow\rangle\langle\downarrow|$, which is identical to thermal equilibrium state $\exp(-\hat{H}(0)/k_{\text{B}}T)$ with an effective temperature

$$T = \frac{\hbar\Omega_0}{k_{\text{B}}\ln(|c_\downarrow|^2/|c_\uparrow|^2)}. \tag{2.30}$$

For our experiment, $\Omega_0 = 2\pi \times 50$ kHz while $|c_\downarrow|^2$ took values of 0.605 ± 0.041 and 0.804 ± 0.034, corresponding to effective initial state temperatures of $T_1 = 5.63$ μK and $T_2 = 1.70$ μK, respectively.

(ii) Initial energy measurement - Following initial state preparation, the energy of the system is measured using a standard state-sensitive fluorescence detection sequence. In this procedure, fluorescence or the absence of fluorescence during the detection sequence indicate a measurement of the $|\uparrow\rangle$ or $|\downarrow\rangle$ state respectively. When the ground state $|\downarrow\rangle$ (dark state) is measured, we continue to the next step of the experiment. If the excited state $|\uparrow\rangle$ (bright state) is detected, we re-prepare the $|\uparrow\rangle$ state before continuing (see Appendix 2.5.3). As noted above, the actual measurements are performed with respect to the Hamiltonian $\hbar\Omega_0\hat{\sigma}_z/2$ which is then switched to $\hbar\Omega_0\hat{\sigma}_x/2$ using an adiabatic shortcut (see Appendix 2.5.4). It should also be pointed out that the results of our experiment would not be altered if step (i) were omitted and instead the states $|\uparrow\rangle$ and $|\downarrow\rangle$ were prepared with the known thermal probabilities. Step (i) is preformed so that our demonstration most closely mimics the the standard setup of the work relation in which a system is driven from thermal equilibrium.

(iii) Application of driving with dephasing - At this point noisy microwave pulses are applied to the system resulting in evolution according to the Hamiltonian (2.28) with the protocols (2.29) and decoherence. For our trials, τ took values $50\mu s$, $10\mu s$, and $5\mu s$ representing near adiabatic, intermediate, and fast driving speeds. The decoherence rate γ in equation (2.4) was set to 0, 448, or 1340 kHz which correspond to the cases of no, intermediate, or large dephasing strength respectively.

(iv) The final energy measurement - Prior to the final energy measurement, another adiabatic shortcut is used to switch the system's Hamiltonian–this time from $\hbar\Omega_0\hat{\sigma}_y/4$ to $\hbar\Omega_0\hat{\sigma}_z/4$. Following this transfer, the energy of the system is once again

measured using a state-sensitive fluorescence detection sequence. By calculating the difference between the initial and final energy measurements, a work value for the experimental trial is obtained.

Figure 2.2 shows the work distributions resulting from experiments conducted with twelve different combinations of effective temperature T, driving time τ, and decoherence rate γ. From the data, it is clear that decoherence non-trivially affects the work distribution for a given process – for instance compare (d) - (f) in figure 2.2. A more careful inspection reveals that the qualitative behavior of the work distribution is governed by a competition between driving speed and decoherence. For near-adiabatic driving, the work distribution is peaked at values $\mathcal{W} = \bar{\epsilon}_i - \epsilon_i$ corresponding to the measurement of two energies with the same quantum number. Increasing driving speed (decreasing τ) tends to induce transitions among energy states with different quantum numbers, thereby broadening the work distribution. This effect is exemplified in figure 2.2 by distributions (a), (b), and (d). In contrast, decoherence in the eigenbasis of $\hat{H}(t)$ suppresses these transitions bringing the work distribution closer to its adiabatic form. This can be seen by comparing the near adiabatic distribution (a) with the fast driving cases (d),(e), and (f) which have varying degrees of decoherence. Interpreting this decoherence as environmental measurement of the system's energy, one can see that the system is forced to follow the adiabatic trajectory due to wave function collapse. When the collapse rate γ becomes large, the system becomes trapped in an eigenstate of the instantaneous Hamiltonian – a scenario analogous to the quantum Zeno effect.

With these distributions, the work relation can be tested for each choice of the experimental parameters T, τ, and γ by direct comparison of the left and right hand sides of equation (2.1). Note that the quantity $\langle e^{-\beta\mathcal{W}} \rangle$ is calculated using the work distribution while $e^{-\beta\Delta\mathcal{F}}$ follows straightforwardly from knowledge of the energy levels

of $\hat{H}(0)$ and $\hat{H}(\tau)$. The results of these calculations, shown in figure 2.3, agree to within the error of the experiment and hence validate the work relation.

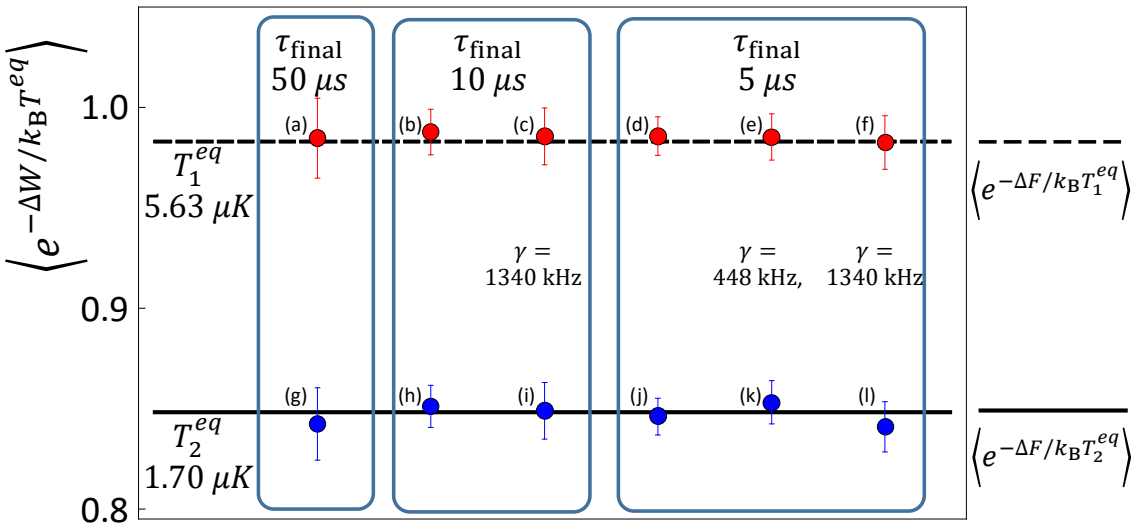

Figure 2.3: Comparison of the exponential average of work for distributions (a)-(l) in figure 2.2 to the exponential of the free energy difference calculated from the initial and final energy levels of $\hat{H}(t)$.

2.3 Multiple Interpretations

While our theoretical development focuses on environment-induced decoherence, the dephasing master equation (2.4) can be interpreted in various ways. For instance, (a) the same master equation describes – at the ensemble level – a system that evolves unitarily but is interrupted at random by projective measurements. More precisely, if our experimenter makes measurements in the instantaneous eigenbasis of $\hat{H}(t)$ at times dictated by a Poisson process with rate γ, then the density operator resulting from averaging over all measurement realizations obeys equation (2.4), with $\gamma_{ij} = \gamma$. Yet another interpretation of the dephasing master equation arises when

(b) one averages over noise that is introduced by adding an appropriately designed, randomly fluctuating term to the bare system Hamiltonian $\hat{H}(t)$ [85, 121]. The validity of equation (2.1) in case (a) has been noted explicitly by Campisi, Talkner and Hänggi [22, 23], and in case (b) by Campisi, Pekola and Fazio [20]. More generally, both interpretations, (a) and (b), support a fluctuation theorem because the system evolves according to a unital channel during each realization, and the average of any number of unital maps is again unital, hence Rastegin's general analysis [106] applies.

Thus the non-unitary dephasing term appearing in equation (2.4) can arise either due to weak coupling to a bath, as described earlier, or due to externally imposed randomness, as described in the previous paragraph. In this paper we focus on the former interpretation because it most closely resembles the canonical setup for fluctuation theorems, namely a small system coupled to a bath in thermal equilibrium. As outlined in the experimental section of this manuscript, we simulate the effects of a decohering bath by the addition of noise to produce dephasing. Of course, our experiments can equally well serve as a direct verification of the above-mentioned prediction of Ref. [20].

2.4 Discussion and Conclusions

Throughout this manuscript we have considered systems that experience only decoherence, but significant theoretical progress has been made in understanding quantum fluctuation theorems in situations where dissipation is also important. We outline some of these advances as they give context for our results and provide direction for future experimental work.

Perhaps the most conceptually appealing framework that addresses general thermal environments is based on considering the system and environment jointly as a

closed composite system [19, 21, 32, 127]. Here the TPM scheme can be employed as the work is simply the change in energy of the joint system. (In the weak coupling limit, work can also be defined as $\Delta\mathcal{U} - \mathcal{Q}$ where the energy change $\Delta\mathcal{U}$ and the heat $\mathcal{Q}$ are obtained by applying the TPM protocol separately to the system and environment.) Despite defining a work distribution that satisfies equation (2.1), this approach suffers from the need to measure bath degrees of freedom, which is difficult to realize in practice.

Other studies of the work relation overcome this issue by defining work at the system level without referencing an environment. In this vein there are several equivalent formalisms for treating quantum detailed balance master equations [27, 47, 81–84, 118] of which we focus on the quantum jump trajectory method [56, 59, 60, 76, 82, 83, 89]. Originally developed in the field of quantum optics [31], this approach treats a system's density operator as an average over pure states evolving according to stochastic trajectories. The construction of these trajectories is called an *unraveling* and is generally not unique. When this unraveling is chosen properly, a consistent trajectory-based thermodynamics can be defined in a manner similar to classical stochastic thermodynamics, and the work relation remains valid [56, 59, 60, 76, 82, 83, 89]. When applied to the decohering master equation (2.4), the quantum trajectory approach agrees with the theoretical development section of this paper.

Various approaches might be taken in future experimental tests of quantum fluctuation theorems. For instance, rather than producing decoherence through the addition of noise, the results of this manuscript could be complemented with an experiment using a true decohering bath engineered from an interaction commuting (at all times) with the bare Hamiltonians of the system and environment. For systems with dissipation, the quantum work relation could be tested for general thermal environments using the TPM protocol and a continuous environmental measurement

technique [102, 103, 138, 139] such as single photon detection in a cavity QED experiment. Alternatively using only the TPM protocol on a dissipative system, one could test the energy change fluctuation theorem which is a modified version of equation (2.1) devised by Pekola and co-workers [101]. For non-unital dynamics, Goold *et al* [50] have obtained fluctuationlike relations for *heat*, in the context of the quantum Landauer Principle. It remains an open, interesting question whether the quite general approach of Ref. [50] can be used to obtain an experimentally testable version of the nonequilibrium work relation (2.1) when both decoherence and dissipation are present. Alternative frameworks for defining heat and work present yet another direction for potential experimental tests of quantum fluctuation theorems. For example, in Elouard *et al* [44–46], energy changes are expressed in terms of three contributions – work, classical heat, and quantum heat. In the interpretation developed in Ref. [44], work is defined differently than in the present manuscript, and the energy changes measured in our experiment include contributions from quantum heat. Using a definition of work similar to that of Ref. [44], Deffner *et al* [33] have derived a modified version of equation (2.1) that accounts for the thermodynamic cost of projective measurements.

In summary, we have studied the quantum work relation for a system in contact with a decohering bath. We obtained equation (2.1) within a simple, phenomenological model that complements the more general approaches of unital quantum channels and quantum trajectories. Using a system constructed from trapped ions subjected to noisy dynamics, we conducted an experiment that demonstrated the work relation's validity for a dephasing process and represents the first test of equation (2.1) beyond the regime of closed quantum systems. These results demonstrate the applicability of fluctuation theorems to open quantum systems, at least for the special case of a decohering heat bath, and may spur additional tests of the work relation for systems

with dissipation.

While this manuscript was under review, we learned that Naghiloo *et al* [96], also under review, describes experimental work verifying equation (2.1) for an open quantum system in which feedback control is used to compensate for the heat exchanged with the environment.

2.5 Appendices

2.5.1 Stochastic Noise and Decoherence Rate

In our experiment, decoherence is induced by the introduction of noise. The system is driven by the total Hamiltonian

$$\hat{H}(t) = \frac{\hbar[\Omega(t) + \Omega_0\xi(t)]}{2}\hat{\sigma}_{\vec{n}}(t) \tag{2.31}$$

where $\hat{\sigma}_{\vec{n}}(t) = \hat{\sigma}_x \cos\phi(t) + \hat{\sigma}_y \sin\phi(t)$ and $\xi(t)$ is Gaussian white noise characterized by $\langle\xi(t)\rangle = 0$ and $\langle\xi(t)\xi(t+\tau)\rangle = \alpha^2\delta(\tau)$. $\hat{H}(t)$ can be decomposed into a control part $\hat{H}_c(t) = \hbar\Omega(t)\hat{\sigma}_{\vec{n}}(t)/2$ and stochastic part $\hat{H}_s(t) = \hbar\Omega_0\xi(t)\hat{\sigma}_{\vec{n}}(t)/2$.

Taking the ensemble average over all noise realizations, the evolution of the system is described by the Lindblad master equation[9, 85, 135]

$$\frac{d\hat{\rho}}{dt} = -\frac{i}{\hbar}[\hat{H}_c(t), \hat{\rho}] - \gamma(\rho_{\downarrow\uparrow}|\downarrow\rangle\langle\uparrow| + \rho_{\uparrow\downarrow}|\uparrow\rangle\langle\downarrow|) \tag{2.32}$$

where $|\uparrow\rangle, |\downarrow\rangle$ are the instantaneous eigenvectors of $\hat{H}_c(t)$ and γ is the decoherence rate which satisfies

$$\gamma = \frac{(\alpha\Omega_0)^2}{2}. \tag{2.33}$$

In practice we applied discrete noise with a sampling rate of R_s instead of ideal

continuous-Gaussian white noise. When $R_s^{-1}/2$ is much less than the duration of the operation, the digital noise can be approximated as Gaussian white noise, with auto-correlation function $\langle \xi(t)\xi(t+\tau)\rangle = \sigma^2 R_s^{-1}\delta(\tau)$. Therefore equation (2.33) should be revised as

$$\gamma = \frac{(\sigma\Omega_0)^2}{2R_s} \tag{2.34}$$

In our experiment, the systems decoheres for durations of $5\mu s, 10\mu s$ and $50\mu s$ and the noise sampling rate is set to 1 MHz. Hence the decoherence rate is given by $\gamma_{\text{exp}} = (\sigma\Omega_0)^2/2\,\text{MHz}$ when Ω_0 is measured in MHz.

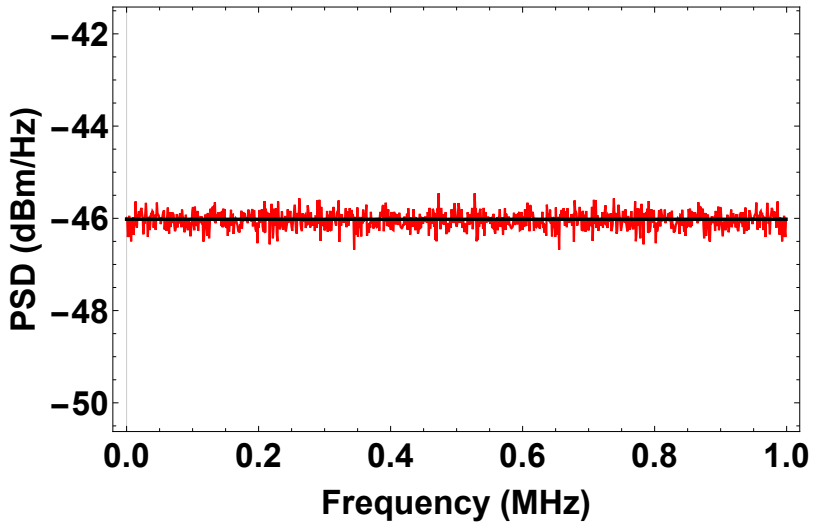

Figure 2.4: Power spectral density of discrete Gaussian white noise with standard deviation $\sigma = 5$ and sampling rate 1 MHz.

2.5.2 Thermal State Preparation

We use the magnetic field sensitive states $|^2S_{1/2}, F = 1, m_F = -1\rangle \equiv |\uparrow\rangle$ and $|^2S_{1/2}, F = 0, m_F = 0\rangle \equiv |\downarrow\rangle$ to create an effective two state system with a typical coherence time of 0.14 ms. After preparing a superposition state with the de-

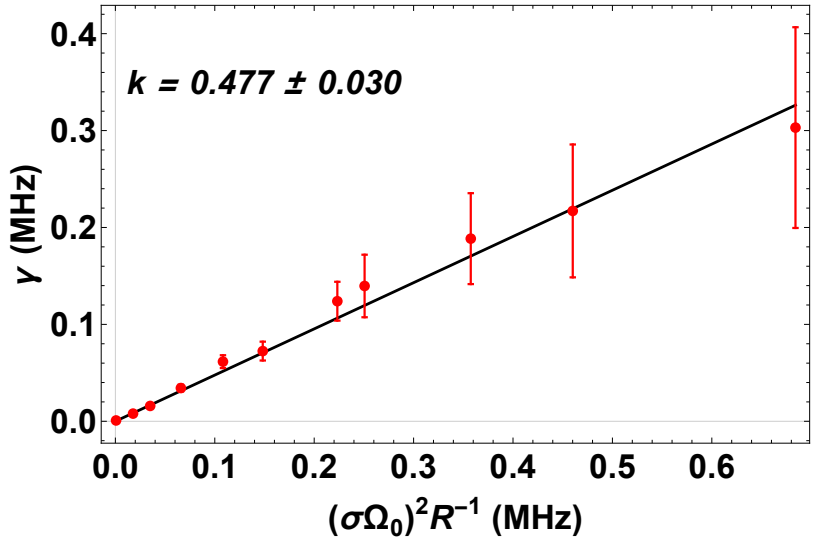

Figure 2.5: Experiment results of decoherence rate γ relation with $(\sigma\Omega_0)^2 R_s^{-1}$. Here sampling rate is set as 1 MHz.

sired populations, we wait 1.5 ms for the system to decohere. We confirm that the state is effectively thermal using state-tomography [141]. As shown in figure 2.7, the off-diagonal components of the density matrix are negligible for both effective temperatures used in our setup.

2.5.3 Energy Measurements

The first and the second energy measurements are performed in the $\hat{\sigma}_z$ basis using standard fluorescence detection as shown in figure 2.6. Depending on whether the system is in the excited state $|\uparrow\rangle$ or ground state $|\downarrow\rangle$, fluorescence or no fluorescence respectively occurs during the detection sequence. When the ground state $|\downarrow\rangle$ (dark state) is measured, the system remains unchanged during the detection sequence and we simply continue to the next step of the experiment. If the excited state $|\uparrow\rangle$ (bright state) is detected, the system is left in a mixture of the three levels of $F = 1$ in $^2S_{1/2}$ manifold. Therefore, we re-prepare the $|\uparrow\rangle$ state using standard optical pumping and

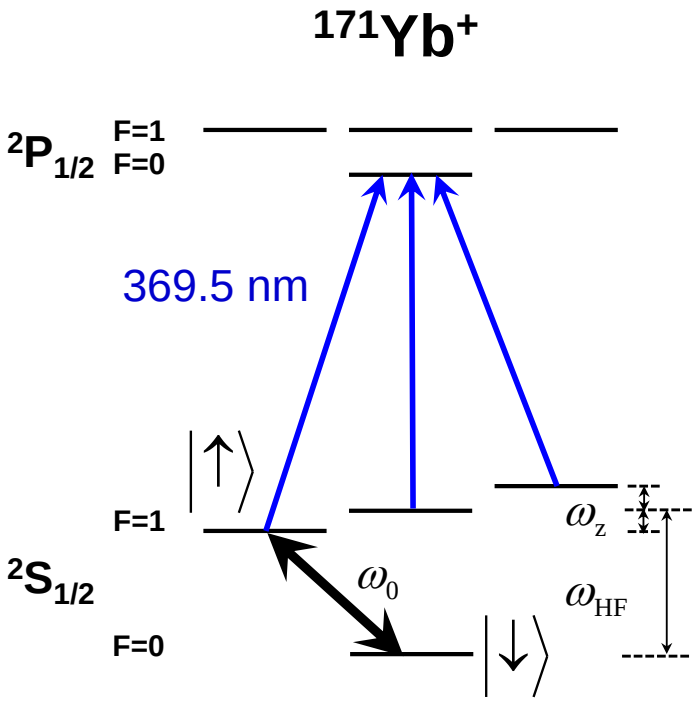

Figure 2.6: Energy levels of our $^{171}Yb^{+}$ ion system. The two level system used in our experiment is composed from the states $\uparrow$ and $\downarrow$. Transitions between these states are driven using resonant microwaves.

a π-pulse of microwaves before continuing the experiment. A fluorescence detection sequence is also used for the final measurement which constitutes the end of an experimental run.

2.5.4 Adiabatic Rotation

For our setup, the initial and the final energy measurements are performed in the $\hat{\sigma}_z$ basis. Between the measurement sequences and the driving protocol, the state of the system must be transferred between the z-axis and x-y plane of the Bloch sphere. To accomplish this task, we use adiabatic shortcuts – a protocol that has the same effect as an adiabatic switching of the Hamiltonian but occurs in finite time [7, 13, 35]. Specifically we apply an additional counterdiabatic term to our Hamiltonian during

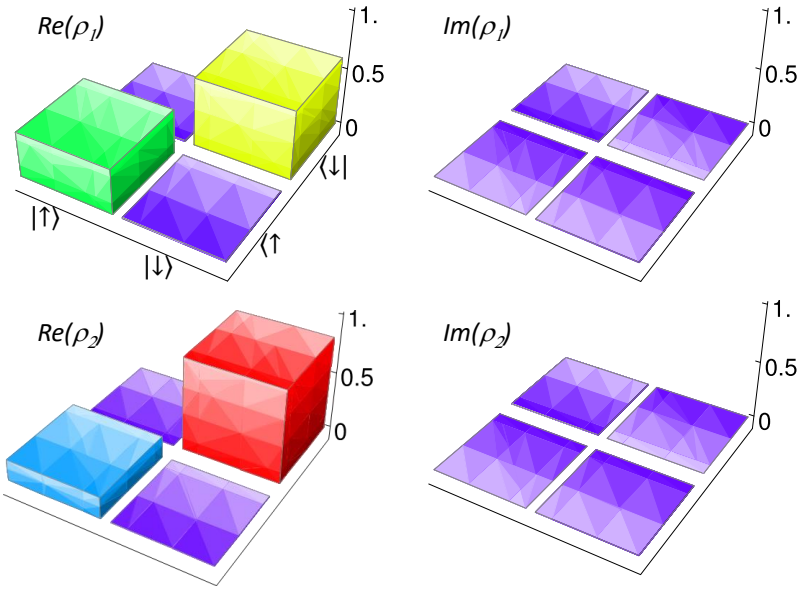

Figure 2.7: Density matrices after preparing effective thermal states, which are equivalent to (a) $T_1^{eq} = 5.63\ \mu$K and (b) $T_2^{eq} = 1.70\ \mu$K.

the switching process to achieve the shortcut.

After thermal state preparation and the first energy measurement, our system collapses into the $|\uparrow\rangle$ or $|\downarrow\rangle$ state. In principle, we have to adiabatically rotate the $|\uparrow\rangle$ or $|\downarrow\rangle$ state to the corresponding state in the x-y plane of the Bloch sphere. In our experiment, the coherence time of a superposition of the $|\uparrow\rangle$ and $|\downarrow\rangle$ states is short and hence would introduce an error in the rotation if it were carried out in a truly adiabatic fashion. Therefore, we apply an adiabatic shortcut to reduce the time for the rotation. In this scheme, we change the Hamiltonian of the system according to

$$\hat{H}_1(t) = \frac{\Delta_0}{2}\hat{\sigma}_z \cos(\omega_1 t) + \frac{\Omega_0}{2}(\hat{\sigma}_x \sin(\omega_1 t) + \hat{\sigma}_y) \tag{2.35}$$

where $\omega_1 = \Omega_0 = \Delta_0 = (2\pi)50$ kHz and t varies from $t = 0$ to $t = \pi/2\omega_1 = 5\ \mu$s. The term proportional to $\hat{\sigma}_y$ is the counterdiabatic which suppresses the excitations. Note that true adiabatic rotation requires at least hundreds of μs, which is much longer

than transfer time using the adiabatic shortcut.

After the driving sequence, we rotate the system's state back to the z-axis of the Bloch sphere using the Hamiltonian

$$\hat{H}_2(t) = \frac{\Omega_0}{4}(\hat{\sigma}_\mathrm{y}\cos(\omega_2 t) + \hat{\sigma}_\mathrm{x}) + \frac{\Delta_0}{4}\hat{\sigma}_\mathrm{z}\sin(\omega_2 t) \tag{2.36}$$

where $\omega_2 = \Omega_0/2 = \Delta_0/2 = (2\pi)25$ kHz and t varies from $t = 0$ to $t = \pi/2\omega_2 = 10$ μs. This time the courterdiabatic term is proportional to $\hat{\sigma}_\mathrm{x}$.

Chapter 3: Insights on Quantum Work and Coherence from Classical Physics

The ubiquitous role of coherence in quantum systems makes it a natural point of study in the field of quantum thermodynamics. In recent years, there has been a significant interest in understanding whether coherence can act as a resource in thermodynamic settings. For example the utility of coherence has been investigated in the context of work extraction [68, 119, 123], quantum heat machine operation [70, 94, 111, 114, 133], and quantum resource theories [1, 17, 58, 72, 87, 134].

Beyond determining the thermodynamic differences between coherent and incoherent quantum states, the quantum character of coherence has also made it a focus of research aiming to separate the quantum and classical aspects of thermodynamics. Of particular interest have been situations in which coherence leads to quantum thermodynamic results that are qualitatively different or superior to that of their classical counterparts. However this line of reasoning is complicated by the fact that there are multiple definitions employed for describing quantum-classical correspondences depending on the context and physical problem at hand.

In this chapter, we attempt to better understand the role of coherence in thermodynamics by examining quantum and classical work extraction for cyclic processes. Specifically, we consider the maximum average work that can be extracted from a system that is subject to a thermal environment and driving fields under the constraint

that these external influences vanish before and after the process. Such a process is cyclic in the sense that the dynamics are fully described both initially and finally by the system's base Hamiltonian. It has been shown [68] that for quantum systems, more work can be extracted from states with coherence in the energy basis than from their incoherent counterparts. Since incoherent states lack quantum features such as superposition of energy levels, they are often called classical and this work extraction result is sometimes viewed as a signature of a quantum thermodynamic advantage.

We test this assertion by comparing quantum and classical systems within the framework of canonical quantization. Here quantum density operators are analogous to phase space probability distributions while the quantum and classical Hamiltonians are linked by the standard procedure of replacing position and momentum coordinates with their respective quantum operators. A defining feature of quantum states with energy basis coherence is that they are non-stationary with respect to the system Hamiltonian. Using this property, we are naturally led to connect non-stationary classical states to quantum density operators with coherences in the energy basis. In this picture, incoherent quantum states correspond to mixtures of classical microcanonical distributions while quantum states with coherence can be related to classical states where probability is non-uniformly distributed between nearby energy shells. Analogous to the quantum case, we show that these classical non-uniformities lead to additional work extraction when compared to the corresponding microcanonical mixture. Furthermore we develop, a framework of so-called energy-equivalent sets in which we can directly compare the work extracted from quantum coherence and classical non-uniformity in the classical limit $\hbar \to 0$. In this regime we find that the work extracted from quantum coherence does not vanish and furthermore agrees with results pertaining to classical non-uniformity. This suggests that in the context of cyclic work extraction and canonical quantization, coherence may not provide a

qualitative difference between quantum and classical thermodynamics.

The structure of this chapter is as follows. In section 3.1 we lay out the optimal work extraction problem and review the results of Kammerlander and Anders. [68] showing work can be extracted from coherence. We then go on in section 3.2 to introduce non-uniformity as a classical analogue to coherence and show it is a resource for classical work extraction. In section 3.3 we define energy-equivalent sets and use this concept to more directly compare work extraction from quantum coherence and classical non-uniformity. Finally section 3.4 outlines how this research relates to other notions of quantum and classical in thermodynamics and comments on possible future extensions of this research.

3.1 The Work Extraction Problem and Quantum Coherence

Consider a system with self-Hamiltonian $\hat{H}_0$ that is initially isolated and described by a density operator $\hat{\rho}_0$. Throughout this chapter, we will assume that $\hat{H}_0$ is non-degenerate and has eigenvectors $|n\rangle$ and eigenvalues ϵ_n arranged such that the energies increase monotonically with n. The non-degenerate spectrum assumption ensures that there is a well-defined energy basis in which coherence can be considered. At time $t = 0$, the system is subjected to a time dependent external driving field and coupled to a thermal environment with inverse temperature β. In the driving interval $t \in (0, \tau)$, we use $\hat{H}(t)$ to denote the full system Hamiltonain which includes the base system Hamiltonian $\hat{H}_0$ and all time dependent effects of the driving. After a duration τ, the external field is turned off and the reservoir is removed leaving the system isolated with Hamiltonian $\hat{H}_0$ and density operator $\hat{\rho}_\tau$. The process is cyclic in the sense that the system's dynamics are fully described by $\hat{H}_0$ at $t = 0$ and $t = \tau$. Note that the following discussion is relatively insensitive to the exact dynamics used

to model the system's evolution in the interaction interval. We will only demand 1) that in the absence of driving the system relaxes to the thermal equilibrium state and 2) that the dynamics supports a generalized second law linking suitably defined notions of free energy and work.

Specifically, we assume that the dynamics satisfy a generalized non-equilibrium second law of the form

$$\mathcal{W}^q \leq -\Delta\mathcal{F}^q \tag{3.1}$$

where work *extracted*, nonequilibrium free energy, internal energy, and entropy are respectively defined by

$$\mathcal{W}^q = -\int_0^\tau \mathrm{Tr}[\frac{d\hat{H}}{dt}\hat{\rho}]dt \tag{3.2}$$

$$\mathcal{F}^q = \mathcal{U}^q - \mathcal{S}^q/\beta \tag{3.3}$$

$$\mathcal{U}^q = \mathrm{Tr}[\hat{H}\hat{\rho}] \tag{3.4}$$

$$\mathcal{S}^q = -\mathrm{Tr}[\hat{\rho}\ln\hat{\rho}]. \tag{3.5}$$

The superscript "q" refers to quantum and distinguishes this case from the classical setup that will be introduced later. It must be stressed that definitions (3.3)-(3.5) generalize the standard equilibrium notions [18] of free energy, internal energy, and entropy to all non-equilibrium states of a quantum system. The generalized non-equilibrium formulation of the second law (3.1) bounds work extraction for fully non-equilibrium processes and is in no way restricted to transitions between equilibrium states. Such a result is possible for a wide range of dynamics including detailed balance master equations, isolated Hamiltonian systems, and even strongly coupled systems where the system and bath are explicitly modeled [49]. Observe that we follow engineering convention and work extraction is positive. While quantity (3.2)

should be interpreted as average work extracted from an ensemble, fluctuations will not be considered in this chapter and hence (3.2) will simply be referred to as work extracted.

We use the definition (3.2) of work for several reasons. It is one of the oldest and most established notions of thermodynamic work in quantum systems [5, 105]. Additionally it agrees with the notion of average work derived from the quantum work (quasi-) distribution in [122], which satisfies a fluctuation theorem. Finally this definition closely resembles those used in classical stochastic thermodynamics [39, 115] and, as we see in later sections, agrees with results from classical Hamiltonian physics.

It must be acknowledged, however, that there are alternative definitions of average work commonly used in quantum thermodynamics. For instance, defining a work distribution according to the popular two-time energy measurement protocol [74, 95, 130] leads to a mean value that disagrees with (3.2) whenever $\hat{\rho}_0$ has initial energy coherences. Additionally some definitions of work coming from quantum resource theory [87] have a so-called work-locking property which prevents the extraction of work from coherence. These resource theory definitions, which explicitly model the heat bath and demand that work is transferred deterministically, also disagree with (3.2).

With cyclic processes and work defined, we now review the results of [68] related to the optimization of work extraction for a process that removes coherence. In other words, for the remainder of this section we will consider isothermal processes during which the system begins in a state $\hat{\rho}_0$ that contains coherences (i.e. non-zero off-diagonal elements in the eigenbasis of $\hat{H}_0$) and ends in the diagonal state

$$\hat{\sigma} = \sum |n\rangle\langle n|\hat{\rho}_0|n\rangle\langle n|. \tag{3.6}$$

Note that $\hat{\sigma}$ has energy populations identical to $\hat{\rho}_0$ but unlike the initial state has no off-diagonal elements. By examining this situation, we can determine the extent to which coherence (in the energy basis) represents a thermodynamic resource. The maximum work extraction $\widetilde{\mathcal{W}}^q$ is defined by the largest possible value of (3.2) for a fixed system Hamiltonian $\hat{H}_0$, inverse reservoir temperature β, and initial state $\hat{\rho}_0$. The process duration τ is unconstrained and the maximization is performed over all cyclic protocols $\hat{H}(t)$ that lead to the final decohered system state $\hat{\sigma}$. In this scenario, the non-equilibrium second law (3.1) bounds the maximum work according to $\widetilde{\mathcal{W}}^q \leq \mathcal{F}_0^q - \mathcal{F}_\sigma^q$. This inequality can in turn be saturated by the driving protocol

$$\hat{H}(t) = \begin{cases} \hat{H}_0 & t \leq 0 \\ -\ln[(1-t/\tau)\hat{\rho}_0 + t/\tau\hat{\sigma}]/\beta & 0 < t < \tau \\ \hat{H}_0 & \tau \leq t \end{cases} \tag{3.7}$$

assuming that τ is sufficiently large so that the process is essentially quasi-static from $t = 0^+$ to $t = \tau^-$. Notice that processes of this type are also used in [49] to saturate the non-equilibrium second law for both quantum systems and discrete state stochastic systems. Intuitively, this protocol consists of a sudden change of the Hamiltonian at $t = 0$ that brings the instantaneous equilibrium state into coincidence with $\hat{\rho}_0$ (since $\hat{H}(0^+) = -\beta \ln \hat{\rho}_0$), followed by a quasistatic step where the system evolves through a sequence of equilibrium states, before a final step in which the cyclic process is completed by turning off the external field. Our assumption that the full dynamics drives the system towards the instantaneous thermal equilibrium ensures that in the quasistatic limit the system tracks the instantaneous equilibrium state. For a two state system undergoing protocol (3.7), an example of a density operator's evolution on the Bloch sphere is shown in figure 3.1. For the benefit of the reader, a derivation

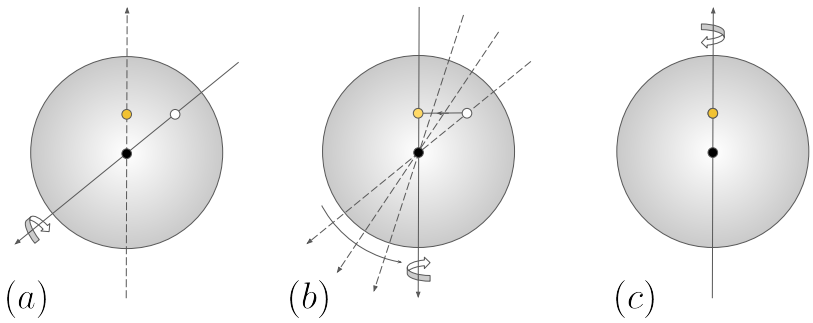

Figure 3.1: Bloch sphere representation of the maximum work extraction protocol for coherence removal. The white and yellow dots respectively represent an arbitrary initial density operator $\hat{\rho}_0$ and the corresponding energy decohered state $\hat{\sigma}$. The axis of Hamiltonian rotation is represented by an arrow crossing the sphere's center with vertical orientation corresponding to $\hat{H}_0$. (a) Hamiltonian suddenly changes at $t = 0$ (b) quasistatic transition over the interval $0 < t < \tau$ (c) Hamiltonian is suddenly to $\hat{H}_0$ at $t = \tau$.

of the work extracted in protocol (3.7) is presented in appendix 3.5.2 from which it follows that

$$\begin{aligned}
\widetilde{\mathcal{W}}^q(\hat{H}_0, \hat{\rho}_0) &= \mathcal{F}_0^q - \mathcal{F}_\sigma^q \\
&= (\cancelto{0}{\mathcal{U}_0^q - \mathcal{U}_\sigma^q}) - \frac{1}{\beta}(\mathcal{S}_0^q - \mathcal{S}_\sigma^q) \\
&= \frac{1}{\beta} D(\hat{\rho}_0 | \hat{\sigma}) \\
&\equiv \frac{1}{\beta} C(\hat{\rho}_0) \\
&\geq 0.
\end{aligned} \tag{3.8}$$

Intermediate details of calculation (3.8) are presented in appendix 3.5.1. In the above, $D(\hat{\rho}_0|\hat{\sigma})$ is the quantum relative entropy [98, 137] of state $\hat{\rho}_0$ with respect to $\hat{\sigma}$ which

is defined according to

$$D(\hat{\rho}_0|\hat{\sigma}) = \mathrm{Tr}[\hat{\rho}_0(\ln\hat{\rho}_0 - \ln\hat{\sigma})]. \tag{3.9}$$

Despite failing to fulfill all the properties of a distance measure, the relative entropy satisfies the relations $D(\hat{\rho}_1|\hat{\rho}_2) > 0$ for $\hat{\rho}_1 \neq \hat{\rho}_2$ and $D(\hat{\rho}|\hat{\rho}) = 0$. Crucially this ensures that optimal work extraction is always positive for a coherence removal process. The quantity $C(\hat{\rho}_0)$ is a well known measure of a quantum state's total (energy basis) coherences called the *relative entropy of coherence* [12]. When states are represented in the eigenbasis of $\hat{H}_0$, $C(\hat{\rho}_0)$ vanishes for diagonal density operators and increases monotonically with a state's off-diagonal elements as quantified by the l_1-norm measure of coherence $C_{l_1} = \sum_{nm} |\langle n|\hat{\rho}_0|m\rangle|$.

With equation (3.8) we conclude our review of previous research by Kammerlander and Anders. [68] linking coherence to work extraction. In other words, this result simply states the optimal work extraction from coherence removal is always positive and moreover given by the thermal energy $k_B T$ times the total coherence as measured by $C(\hat{\rho}_0)$. In the quantum thermodynamics literature, it is common to refer to incoherent states as classical (or quasi-classical) and view coherence as an indicator of truly quantum phenomenon. In this light, result (3.8) is sometimes presented as a signature of quantum systems' thermodynamic advantage over their classical counterparts. In the next section we probe this assertion by considering the quantum classical correspondence from the perspective of canonical quantization.

3.2 Classical Systems and Work Extraction from Non-uniformity

While coherence is often associated with quantum features such as superposition and entanglement, quantum states with energy basis coherence are fully characterized by a property they share with many classical states– namely non-stationary dynamics. As can be seen from the von Neumannn equation

$$\frac{d\hat{\rho}}{dt} = -\frac{\mathrm{i}}{\hbar}[\hat{H}_0, \hat{\rho}], \tag{3.10}$$

incoherent states that commute with $\hat{H}_0$ remain fixed in time whereas only those states with coherences in the energy basis evolve non-trivially when subject to the system's base dynamics. Contrary to much of the language surrounding quantum coherence, this suggests that quantum states with energy coherence are analogous to classical states which are non-stationary. In this section we aim to develop this idea by both building an intuition for classical non-stationary states and investigating the relation of these states to the classical work extraction problem.

Consider a classical system with N degrees of freedom and phase space coordinates $z = (x_1, ..., x_N, p_1, ..., p_N)$. The state of the system is described by a probability density $\rho(z)$ over phase space and the system's dynamics are generated by the Hamiltonian $\mathcal{H}_0(z)$. Since our previous arguments assumed that the quantum Hamiltonian was non-degenerate, we will analogously demand that the classical Hamiltonian is ergodic. Roughly this means that every system trajectory traverses the entirety of its energy shell given sufficient time and excludes Hamiltonians with non-trivial symmetries or disconnected energy shells.

Stationary and non-stationary states can be characterized in the classical context

with the help of Liouville's equation

$$\frac{\partial \rho}{\partial t} = \{\mathcal{H}(z), \rho\} = \sum_i \frac{\partial \mathcal{H}}{\partial x_i}\frac{\partial \rho}{\partial p_i} - \frac{\partial \mathcal{H}}{\partial p_i}\frac{\partial \rho}{\partial x_i}. \tag{3.11}$$

Clearly classical states lack time dependence whenever the Poisson bracket $\{\mathcal{H}(z), \rho\}$ vanishes. For ergodic systems, this condition is satisfied exactly by densities of the form $\rho(z) = f(\mathcal{H}(z))/K$. Here $f(\cdot)$ is any function of a single real variable where the normalization factor $K = \int f(\mathcal{H})dz$ exists. It is straightforward to show that such states can be written in the form

$$\rho(z) = \int \eta_\rho(E)\omega_E(z)dE \tag{3.12}$$

where $\eta_\rho(E) = \int \rho(z)\delta(\mathcal{H}(z) - E)dz$ is the state's marginal energy distribution and $\omega_E(z) = \delta(\mathcal{H}(z) - E)/\Omega(E)$ is the microcanonical distribution corresponding to energy E. Furthermore writing $\omega_E(z)$ in the limiting form

$$\omega_E(z) = \lim_{\Delta E \to 0} \frac{I_{[E,E+\Delta E]}(\mathcal{H}(z))}{\int I_{[E,E+\Delta E]}(\mathcal{H}(z))dz} \tag{3.13}$$

where $I_{[E,E+\Delta E]}(\cdot)$ is the indicator function over the interval $[E, E + \Delta E]$, it is immediately apparent that the probability density of a microcanonical state is uniform between infinitesimally spaced energy shells. Combining these facts, we deduce that the stationary states in this setup are mixtures of microcanonical energy distributions and can be distinguished by their uniform probability densities on level surfaces of the Hamiltonian. In contrast, non-stationary states are signified by non-uniformly spread probabilities between infinitesimally spaced energy shells in phase space. Examples of uniform and non-uniform states are graphically depicted in figure 3.2.

With quantitative and qualitative notions of non-stationary classical states in

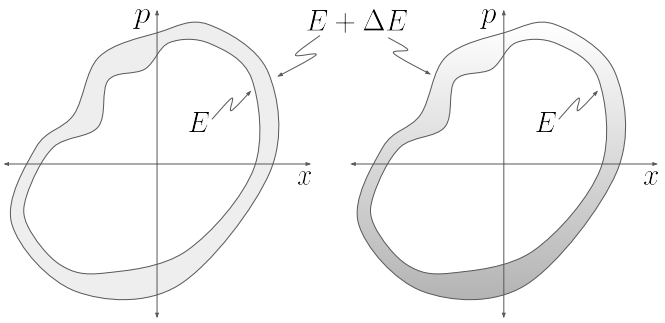

Figure 3.2: Illustration of uniform (left) and non-uniform (right) distributions between infinitesimally separated energy shells.

hand, we now move to the issues of developing a classical analog for the quantum coherence removal process and understanding such a process's relationship with classical work extraction. Recall from the quantum setup that an energy decohering process is one in which a non-stationary state $\hat{\rho}$ becomes a stationary state $\hat{\sigma}$ without altering the state's energy populations. In analogy, for any classical state $\rho(z)$ with energy distribution $\eta_\rho(E)$, we may associate a unique uniform state $\sigma(z)$ via the correspondence

$$\sigma(z) = \int \eta_\rho(E)\omega_E(z)dE \tag{3.14}$$

and define a non-uniformity removal process as one in which the state $\rho(z)$ transitions to $\sigma(z)$. Much like the quantum state $\hat{\sigma}$, the classical state $\sigma(z)$ is stationary and has an energy distribution identical to the original state $\rho(z)$.

For a variety of dynamics modeling an isothermal process, it can be shown [55, 126] that classical systems obey the generalized non-equilibrium second law

$$\mathcal{W}^c \leq -\Delta\mathcal{F}^c \tag{3.15}$$

where the classical thermodynamic quantities are given by

$$\mathcal{W}^c = -\int_0^\tau \left(\int \frac{\partial \mathcal{H}}{\partial t} \rho(z) dz \right) dt \tag{3.16}$$

$$\mathcal{F}^c = \mathcal{U}^c - \mathcal{S}^c/\beta \tag{3.17}$$

$$\mathcal{U}^c = \int \mathcal{H}(z)\rho(z) dz \tag{3.18}$$

$$\mathcal{S}^c = -\int \rho(z) \ln[h^N \rho(z)] dz \tag{3.19}$$

and h is a constant with dimensions of action that ensures the argument of the logarithm is dimensionless. We will choose h to coincide with Planck's constant as this will facilitate comparisons of quantum and classical work extraction later in this chapter. Note that unlike the quantum von Neumann entropy which is always non-negative, the classical Shannon entropy (3.19) can become arbitrarily negative for probability distributions that are highly concentrated in phase space. As before, this second law can be saturated [55, 126] with the classical protocol

$$\mathcal{H}(z,t) = \begin{cases} \mathcal{H}_0(z) & t \leq 0 \\ -\ln[(1-t/\tau)\rho_0(z) + t/\tau \sigma(z)]/\beta & 0 < t < \tau \\ \mathcal{H}_0(z) & \tau \leq t \end{cases} \tag{3.20}$$

which is shown in appendix 3.5.2 and has roughly the same interpretation as the quantum case. At time $t = 0$ the Hamiltonian is suddenly changed from $\mathcal{H}_0(z)$ to a new Hamiltonian tailored such that $\rho_0(z)$ is the new thermal equilibrium state. This has the effect of stabilizing the initial state. In the interval $(0, \tau)$, the quasistatic switching of the Hamiltonian drives the system through a sequence of equilibrium states which begins at $\rho_0(z)$ and terminates at $\sigma(z)$. At $t = \tau$ the cyclic process is

completed by suddenly returning the Hamiltonian to $\mathcal{H}_0$. It follows that the maximum work extraction for a non-uniformity removal process is given by

$$\begin{aligned}\widetilde{\mathcal{W}}^c(\mathcal{H}_0(z),\rho_0(z)) &= \mathcal{F}_0^c - \mathcal{F}_\sigma^c \\ &= (\cancel{\mathcal{U}_0 - \mathcal{U}_\sigma})^0 - \frac{1}{\beta}(\mathcal{S}_0 - \mathcal{S}_\sigma) \\ &= \frac{1}{\beta} D(\rho_0(z)|\sigma(z)) \\ &\geq 0.\end{aligned} \tag{3.21}$$

The details of calculation (3.21) are similar to the quantum case, which can be found in appendix 3.5.1. Inspired by the quantum relative entropy of coherence, we define a classical relative entropy of non-uniformity according to

$$D(\rho(z)|\sigma(z)) = \int \rho(z) \ln \frac{\rho(z)}{\sigma(z)} dz \tag{3.22}$$

and assume that it quantifies the non-uniformity of classical states in the same way the that relative entropy of coherence measures coherence in quantum systems.

In this section we have shown that the effects of coherence in quantum work extraction are at least qualitatively similar to a suitably defined classical setup. States with quantum coherence are defined by their non-stationary behavior which is manifest in classical systems through the notion of non-uniformity. Removal of non-uniformity is analogous to removal of coherence and moreover, like the quantum case, the optimal work that can be extracted during such a process is given by the thermal energy $k_b T$ multiplied by a relative entropy. Building on this qualitative comparison, the next section puts forward a framework in which these results can be compared on a more quantitative level.

3.3 A Quantitative Comparison of Work Extraction from Coherence and Non-uniformity

For both classical and quantum systems, the optimal work extracted when the system's initial non-stationary features are removed is a function of the system's base Hamiltonian and initial state. In this section, we present a correspondence between the quantum operators $\hat{H}_0$ and $\hat{\rho}$ and classical phase space functions $\mathcal{H}(z)$ and $\rho(z)$ so that quantum and classical values of work can be more quantitatively compared. To facilitate the Hamiltonian correspondence, we will assume for the remainder of this chapter that our system has N degrees of freedom and a Hamiltonian of the kinetic plus potential type. In this context, the process of canonical quantization gives a straightforward recipe for determining $\hat{H}_0$ from $\mathcal{H}(z)$. Here the quantum Hamiltonian is derived from its classical counterpart by elevating position and momentum coordinates in phase space to quantum operators satisfying the canonical commutation relation. Due to the lack of cross position momentum terms in kinetic plus potential type Hamiltonians, there is no ambiguity in this process.

While canonical quantization provides a bridge between quantum and classical dynamics, finding a reasonable one-to-one correspondence between classical and quantum states is somewhat less straightforward. Common approaches which map density operators into phase space [25, 57] suffer from undesirable properties. For instance, neither the Wigner nor Husimi function representation of the quantum thermal state correspond to the classical thermal phase space distribution. Additionally, the Wigner function in general fails to be positive while the Husimi function is dependent on a choice of coherent states.

To circumvent such issues, our study focuses on comparing *energy-equivalent sets*

of classical and quantum states rather than individual states. We define a quantum energy-equivalent set to consist of all states that share a particular energy distribution with respect to the system's Hamiltonian. An example is the quantum thermal energy-equivalent set given by

$$\Pi^q = \{\hat{\rho} \,|\langle n|\hat{\pi}|n\rangle = \langle n|\hat{\rho}|n\rangle\} \tag{3.23}$$

$$\hat{\pi} = \frac{1}{Z^q} e^{-\beta \hat{H}_0} \tag{3.24}$$

where $\hat{\pi}$ is the thermal equilibrium state, Z^q is the quantum partition function, and as before $|n\rangle$ are the eigenstates of the Hamiltonian. Note that in addition to including the equilibrium state $\hat{\pi}$, the set Π^q also includes exotic far from equilibrium states that have significant energy basis coherence such as the pure state

$$|\pi\rangle = \sum_n \sqrt{\frac{e^{-\beta \epsilon_n}}{Z^q}} |n\rangle. \tag{3.25}$$

For examples of the state (3.25) in quantum optics see [10, 40]. Similarly to the quantum case, we define a classical energy-equivalent set to consist of all phase space distributions with a particular marginal energy distribution $\eta(E)$ and positive Shannon entropy measured according to definition (3.19). The entropy condition, roughly speaking, allows for a fair comparison of quantum and classical energy-equivalent sets and will be further justified later in this section. Here an example is given by the classical thermal energy-equivalent set

$$\Pi^c = \{\rho(z) \,|\eta_\rho(E) = \eta_\pi(E), S^c(\rho(z)) \geq 0\} \tag{3.26}$$

$$\pi(z) = \frac{1}{Z^c} e^{-\beta \mathcal{H}_0(z)} \tag{3.27}$$

where $\pi(z)$ is the classical canonical distribution and $\eta_\rho(E)$ and $\eta_\pi(E)$ are the marginal energy distributions corresponding respectively to $\rho(z)$ and $\pi(z)$. Just as Π^q contains members with energy basis coherences, the classical set Π^c contains members with substantial non-uniformity between nearby energy shells. For instance, in the case of a harmonic oscillator, the set Π^c includes the phase space density

$$\rho(E,T) = \underbrace{\left(\beta e^{-\beta E}\right)}_{\eta_\pi(E)} \underbrace{\left(\omega \frac{e^{\delta\cos(\omega T)}}{I_0(\delta)}\right)}_{\zeta(T)} \tag{3.28}$$

where E and T are the canonical energy and tempus (angle-like) coordinates [71] defined according to $q = \sqrt{2E/m\omega^2}\cos(\omega T)$ and $p = \sqrt{2mE}\sin(\omega T)$, δ is positive parameter, and I_0 is the modified Bessel function of order zero. The distribution $\zeta(T)$ is the well known von Mises distribution, which is a rough analog to a Gaussian distribution for an angular coordinate. In our example the mean of $\zeta(T)$ is zero and its variance is controlled by the parameter δ. In other words, the distribution is concentrated on the positive x-axis of phase space.

With quantum and classical energy-equivalent sets defined, we now turn our attention to formulating a correspondence between these sets. Consider a positive function of a single real variable $f(\cdot)$ with the property that the normalization factors $K^q = \mathrm{Tr}[f(\hat{H})]$ and $K^c = \int f(\mathcal{H}(z))dz$ are finite. With the aid of $f(\cdot)$ we construct the quantum reference state $\hat{\sigma}_f = f(\hat{H})/K^q$ and classical reference state $\sigma_f(z) = f(\mathcal{H}(z))/K^c$ and propose that it is reasonable to compare the energy-equivalent sets

$$\Sigma_f^q = \{\hat{\rho} \,|\langle n|\hat{\sigma}_f|n\rangle = \langle n|\hat{\rho}|n\rangle\} \tag{3.29}$$

$$\Sigma_f^c = \{\rho(z) \,|\eta_\rho(E) = \eta_{\sigma_f}(E), S^c(\rho(z)) \geq 0\}. \tag{3.30}$$

Note that if we take $f(\cdot) = e^{-\beta(\cdot)}$, then the reference states take the form $\hat{\sigma}_f = \hat{\pi}$ and $\sigma_f(z) = \pi(z)$ and we obtain a correspondence between the thermal energy-equivalent sets Π^q and Π^c. With this example in mind we can gain some intuition on the physical meaning of the function $f(\cdot)$. Just like the Boltzmann factor $e^{-\beta(\cdot)}$ allows one to ascertain the relative frequencies of a system's microstates in thermal equilibrium, the function $f(\cdot)$ determines the relative frequencies of a system's microstates when drawn from the reference state $\hat{\sigma}_f$ or $\sigma_f(z)$.

In the context of the isothermal work extraction problem, linking the sets Σ_f^q and Σ_f^c has a few desirable properties. Firstly these sets are fully defined by the Hamiltonains $\hat{H}_0$ and $\mathcal{H}(z)$ and hence the correspondence between Σ_f^q and Σ_f^c follows straightforwardly from canonical quantization of the Hamiltonian. Additionally in this thermodynamic setting, it is natural to construct a correspondence between quantum and classical states that maps the classical thermal state to its quantum counterpart. In this vein, the choice $f(\cdot) = e^{-\beta(\cdot)}$ produces the sets Π^q to Π^c which respectively contain the classical and quantum thermal states.

At this point, we are in the position where optimal work extraction can be quantitatively compared for quantum and classical systems. To do so, we maximize the optimal quantum (3.8) and classical (3.21) work extraction, respectively, over the sets Σ_f^q and Σ_f^c. We denote the optimal quantum work over the set Σ_f^q by $\widetilde{\mathcal{W}}^q(\hat{H}_0, \Sigma_f^q)$ and the optimal classical work over the set Σ_f^c by $\widetilde{\mathcal{W}}^c(\mathcal{H}_0(z), \Sigma_f^c)$. Despite not being able to link the members of Σ_f^q and Σ_f^c in a one-to-one way, this allows us to simply ask if states with quantum coherence are more or less useful for work extraction than classical states with non-uniformity. In the following, it is useful to note that the von Neumannn entropy of a quantum state is always non-negative and is exactly zero for pure quantum states. Furthermore the quantum energy-equivalent set Σ_f^q always contains pure states, an example of which is $|\psi\rangle = \sum_n \sqrt{\langle n|\hat{\sigma}_f|n\rangle}|n\rangle$. In the classical

case our setup demands that the Shannon entropy is non-negative. Like the quantum case, this bound can always be saturated by a member of the classical set Σ_f^c that is sufficiently concentrated in phase space. Observe that,

$$\begin{aligned}
\widetilde{\mathcal{W}}^q(\hat{H}_0, \Sigma_f^q) &= \max_{\hat{\rho}\in\Sigma_f^q} \widetilde{\mathcal{W}}^q(\hat{H}_0, \hat{\rho}) \qquad (3.31)\\
&= \max_{\hat{\rho}\in\Sigma_f^q} [(\cancelto{0}{\mathcal{U}_\rho^q - \mathcal{U}_\sigma^q}) - (S_\rho^q - S_\sigma^q)/\beta]\\
&= (S_\sigma^q - \cancelto{0}{\min_{\hat{\rho}\in\Sigma_f^q} S_\rho^q})/\beta\\
&= S_\sigma^q/\beta\\
\widetilde{\mathcal{W}}^c(\mathcal{H}_0(z), \Sigma_f^c) &= \max_{\rho(z)\in\Sigma_f^c} \widetilde{\mathcal{W}}^c(\mathcal{H}_0(z), \rho(z)) \qquad (3.32)\\
&= \max_{\rho(z)\in\Sigma_f^c} [(\cancelto{0}{\mathcal{U}_\rho^c - \mathcal{U}_\sigma^c}) - (S_\rho^c - S_\sigma^c)/\beta]\\
&= (S_\sigma^c - \cancelto{0}{\min_{\rho(z)\in\Sigma_f^c} S_\rho})/\beta\\
&= S_\sigma^c/\beta.
\end{aligned}$$

This shows that for both the quantum set Σ_f^q and classical set Σ_f^c, the maximum work extracted is given by the reference state entropy multiplied by thermal energy $k_B T$.

It is now clear as to why we demanded that the classical entropy be non-negative. Had we not made this restriction, Σ_f^c would include states with arbitrarily negative values of the Shannon entropy and hence $\widetilde{\mathcal{W}}^c(\mathcal{H}_0(z), \Sigma_f^c)$ would have diverged. Beyond mathematical convenience, the condition $S^c \geq 0$ can be physically motivated as it prohibits probability distributions concentrated in volumes of phase space smaller than the quantum limit h^N. To see this consider a classical distribution that is uniform on a phase space region with $2N$-dimensional volume V and zero elsewhere. The classical entropy of this state is given by $S^c = -\log(h^N/V)$ which is non-negative

exactly when $V \geq h^N$. Roughly this ensures that the classical states in Σ_f^c satisfies the uncertainty principle and resemble the quantum states in the set Σ_f^q at finite h but allows all classical probability distributions in the limit of vanishing h.

Of particular interest is comparing quantum and classical work extraction in the limit $h \to 0$. In general both the quantum and classical entropies diverge in this regime so instead of considering the classical and quantum work extraction individually, we look at the difference

$$\begin{aligned} \Delta &= \widetilde{W}^q(\hat{H}_0, \Pi^q) - \widetilde{W}^c(\mathcal{H}_0(z), \Pi^c) \\ &= (S_\sigma^q - S_\sigma^c)/\beta. \end{aligned} \tag{3.33}$$

We now show using standard arguments from semi-classical physics that in the classical limit S_σ^q and S_σ^c agree and hence the difference in work Δ vanishes. In the semi-classical limit it is well known that the quantum density of states g(E) can be approximated by the number of h^N volume cells that fit into the classical phase space volume between E and $E + dE$. Using this reasoning, one can make the association $g(E) \approx \Omega(E)/h^N$ where $\Omega(E)$ is the classical micro-canonical partition function. It follows immediately that

$$K^q = \mathrm{Tr}[f(\hat{H}_0)] = \sum_n f(E_n)g(E_n) \approx \int f(E)\frac{\Omega(E)}{h^N}dE = \frac{K^c}{h^N}. \tag{3.34}$$

where K^q and K^c are the normalization factors associated with the reference states

$\hat{\sigma}_f$ and $\sigma_f(z)$. Now considering the quantum-classical work difference Δ, we find

$$\begin{aligned}\lim_{h\to 0}\Delta &= \frac{1}{\beta}\lim_{h\to 0}\{-Tr[\hat{\sigma}\ln\hat{\sigma}] + \int \sigma(z)\ln[h^N\sigma(z)]dz\} \\ &= \frac{1}{\beta}\lim_{h\to 0}\{-\sum_n g(E_n)\frac{f(E_n)}{K^q}\ln[\frac{f(E_n)}{K^q}] + \int \Omega(E)\frac{f(E)}{K^c}\ln[h^N\frac{f(E)}{K^c}]dz\} \\ &= \frac{1}{\beta}\lim_{h\to 0}\{-\int \frac{\Omega(E)}{h^N}\frac{f(E)}{K^c/h^N}\ln[\frac{f(E)}{K^c/h^N}]dE + \int \Omega(E)\frac{f(E)}{K^c}\ln[h^N\frac{f(E)}{K^c}]dz\} \\ &= 0.\end{aligned} \tag{3.35}$$

For thermal energy-equivalent states this can also be established by writing

$$\Delta_\pi = (\frac{1}{\beta} + \frac{\partial}{\partial\beta})\log\frac{Z^c}{Z^q} \tag{3.36}$$

and applying the well known result [75] that the quantum partition function Z^q for kinetic plus potential type Hamiltonians can be expanded in a power series of h where the first term is exactly the classical partition function Z^c. From this we can conclude that in the classical limit, the work extracted from the coherence of a quantum state $\hat{\rho} \in \Sigma_f^q$ does not exceed the work that could be extracted from the non-uniformity of a classical state $\sigma(z) \in \Sigma_f^c$. This strengthens the argument from previous sections of this chapter that the work extracted from coherence is qualitatively similar to work extracted from non-uniformity. Furthermore it calls into question the idea that quantum coherence could be a resource that somehow divides the realms of quantum and classical thermodynamics.

3.4 Discussion and Conclusions

In this chapter we reviewed how work can be extracted from quantum coherence and investigated the classical analog of this process. Through the concept of non-

stationary dynamics, we linked quantum states with coherence to classical states with non-uniform probability densities between nearby energy shells. We showed that like coherence in the quantum case, non-uniformity in classical phase space densities is a resource that always allows for more work extraction than from the corresponding uniform state. Furthermore for quantum and classical energy-equivalent sets, we showed that the maximum work extracted from coherence coincides with the maximum work extracted from non-uniformity in the limit of vanishing h.

Beyond making a link between work, quantum coherence, and classical non-uniformity, this research aims to clarify issues related to quantum-classical correspondence in quantum thermodynamics. Many studies in quantum thermodynamics are written from the perspective of quantum information theory. This is with good reason as the function of nanoscale components making up quantum computers will certainly be limited by thermal effects. It is within the realm of quantum thermodynamics to understand these effects and quantify the energetic costs of managing them. That being said, quantum information often focuses on a quantum-classical correspondence centered around comparing classical and quantum computers. Particularly in quantum thermodynamics, it is common to link a density operator $\hat{\rho}$ to a corresponding diagonal state $\sum |n\rangle\langle n|\hat{\rho}|n\rangle\langle n|$ and refer to this diagonal state as "classical." One reason for this procedure is that the operation of a discrete state classical stochastic computer governed by permutations and a rate equation can be mimicked by a quantum computer evolving through a sequence of diagonal states. In this correspondence a classical stochastic computer can essentially be thought of as an incoherent quantum computer. From a thermodynamics perspective, this means quantum coherence is a resource for work extraction with no analog in classical stochastic systems. Following the language of Levy and Gelbwaser in chapter 4 of [14], we believe that this type of correspondence should be referred to as a quantum-stochastic correspon-

dence to avoid confusion with the more traditional quantum-classical correspondence presented in this chapter.

In the future it would be useful to more completely investigate the link between work, coherence, and non-uniformity in the small h limit. One possibility could be to look at work extraction from Gaussian phase space functions. In this situation, states could be linked on a one-to-one basis as a Gaussian Wigner function can also be directly interpreted as a classical phase space density. In the small $\hbar$ limit these states also do not suffer from the divergences in work extraction produced by the maximization over the sets Σ_f^q and Σ_f^c presented in this text. Additionally, no entropy condition would need to be introduced as the quantum and classical state would always be concentrated in exactly the same phase space volume. It is also important to note that while we found agreement in work extraction between quantum coherence and classical non-uniformity for energy-equivalent sets, there could be other reasonable connections between quantum density operators and classical phase space distributions where disagreement remains even in the small h limit. Such situations could allow for a quantum advantage similar to the results found using the quantum-stochastic correspondence.

3.5 Appendices

3.5.1 Connecting Entropy and Relative Entropy

Consider quantum and classical systems with respective Hamiltonians $\hat{H}_0$ and $\mathcal{H}(z)$. For both quantum and classical systems, the non-equilibrium free energy of any state can be expresses in terms relative entropy. Specifically for quantum and

classical states $\hat{\rho}_0$ and $\rho(z)_0$, we have

$$\mathcal{F}_\rho^q = -D[\hat{\rho}_0|\hat{\pi}]/\beta \tag{3.37}$$

$$\mathcal{F}_\rho^c = -D[\rho(z)_0|\pi(z)]/\beta. \tag{3.38}$$

In general differences of free energy, such as those that bound work extraction in the non-equilibrium second laws (3.1) and (3.15), cannot be expressed in terms of a single relative entropy. In this appendix we show that free energy differences between states with identical energy distributions can be written as a single relative entropy. This fact is especially important as it ensures that in an optimal process the energy extracted from a state's non-stationary features is always positive. This is a key feature that allows for quantum coherence and classical non-uniformity to be interpreted as thermodynamic resources.

In the quantum case, we define the energy decohered state corresponding to $\hat{\rho}_0$ according to $\hat{\sigma} = \sum |n\rangle\langle n|\hat{\rho}_0|n\rangle\langle n|$. The free energy difference between states $\hat{\rho}_0$ and $\hat{\sigma}$ can be calculated as follows.

$$\begin{aligned}
\mathcal{F}_0^q - \mathcal{F}_\sigma^q &= (\mathcal{S}_\sigma^q - \mathcal{S}_0^q)/\beta \\
&= \mathrm{Tr}[\hat{\rho}\ln\hat{\rho}] - \mathrm{Tr}[\hat{\sigma}\ln\hat{\sigma}] \\
&= \mathrm{Tr}[\hat{\rho}\ln\hat{\rho}] - \sum_n \langle n|\hat{\rho}|n\rangle \ln(\langle n|\hat{\sigma}|n\rangle) \\
&= \mathrm{Tr}[\hat{\rho}\ln\hat{\rho}] - \sum_n \langle n|(\hat{\rho}\ln\hat{\sigma})|n\rangle \\
&= \mathrm{Tr}[\hat{\rho}\ln\hat{\rho}] - \mathrm{Tr}[\hat{\rho}\ln\hat{\sigma}] \\
&= D(\hat{\rho}|\hat{\sigma}) \\
&\geq 0
\end{aligned} \tag{3.39}$$

Alternatively for a classical system, the stationary state corresponding to $\rho_0(z)$ is given by $\sigma(z) = \eta(\mathcal{H}(z))/\Omega(\mathcal{H}(z))$ where $\eta(E)$ is the marginal energy distribution of $\rho(z)$ and $\Omega(E)$ is the microcanonical partition function. The classical free energy difference of $\rho(z)$ and $\sigma(z)$ is given by

$$\begin{aligned}
\mathcal{F}_0^c - \mathcal{F}_\sigma^c &= (\mathcal{S}_\sigma^c - \mathcal{S}_0^c)/\beta \qquad (3.40)\\
&= \int \rho(z) \ln[h^N \rho(z)] dz - \int \sigma(z) \ln[h^N \sigma(z)] dz \\
&= \int \rho(z) \ln[h^N \rho(z)] dz - \int \frac{\eta(\mathcal{H}(z))}{\Omega(\mathcal{H}(z))} \ln[h^N \frac{\eta(\mathcal{H}(z))}{\Omega(\mathcal{H}(z))}] \int \delta[E - \mathcal{H}(z))] dE dz \\
&= \int \rho(z) \ln[h^N \rho(z)] dz - \int \eta(E) \ln[h^N \frac{\eta(E)}{\Omega(E)}] dE \\
&= \int \rho(z) \ln[h^N \rho(z)] dz - \int (\int \rho(z) \delta[\mathcal{H}(z) - E] dz) \ln[h^N \frac{\eta(E)}{\Omega(E)}] dE \\
&= \int \rho(z) \ln[h^N \rho(z)] dz - \int \rho(z) \ln[h^N \sigma(z)] dz \\
&= D(\rho(z)|\sigma(z)) \\
&\geq 0
\end{aligned}$$

3.5.2 Optimal Isothermal Work Extraction

In this appendix section we show that the quantum protocol (3.7) and classical protocol (3.20) saturate the generalized non-equilibrium form of the second law. Note that for both the quantum and classical case, our key assumption is that in the absence of driving the system relaxes to the thermal equilibrium state. This ensures that in the limit of quasistatic driving the system trajectory simply tracks the instantaneous equilibrium state.

Before considering protocols (3.7) and (3.20), it is useful to review the formulas

$$\mathrm{Tr}[\frac{d\hat{H}}{d\lambda}\hat{\pi}(\lambda)] = \frac{d}{d\lambda}[-\beta^{-1}\ln Z^q(\lambda)] \tag{3.41}$$

$$\int \frac{\partial\mathcal{H}}{d\lambda}\pi(z,\lambda)dz = \frac{d}{d\lambda}[-\beta^{-1}\ln Z^q(\lambda)] \tag{3.42}$$

which are well known from the thermodynamic integration technique of free energy calculation. Here λ is a parameter that characterizes a sequence of Hamiltonians and π represents the instantaneous equilibrium state. In other words this result states that the equilibrium average of the λ derivative of the Hamiltonian is equal to λ derivative of the equilibrium free energy.

Consider a quantum system initial described by density operator $\hat{\rho}_0$ and driven according to protocol (3.7). The initial step of this protocol consists of a instantaneous change of the Hamiltonian from $\hat{H}(0_-) = \hat{H}_0$ to $\hat{H}(0_+) = -\beta^{-1}\ln\hat{\rho}_0$. The associated work is performed is given by

$$\begin{aligned}
\mathcal{W}^q_{0_-\to 0_+} &= -\int_{0_-}^{0_+} \mathrm{Tr}[\frac{d\hat{H}}{dt}\hat{\rho}]dt \\
&= \mathrm{Tr}[(\hat{H}(0_-) - \hat{H}(0_+))\hat{\rho}_0] \\
&= \mathrm{Tr}[(\hat{H}_0 + \beta^{-1}\ln\hat{\rho}_0)\hat{\rho}_0] \\
&= \mathcal{U}^q_0 - \beta^{-1}\mathcal{S}^q_0 \\
&= \mathcal{F}^q_0.
\end{aligned} \tag{3.43}$$

In the quasistatic step of the protocol, we make use of the fact that the system follows a sequence of equilibrium states and apply equation (3.41) where λ can in this case

be identified with time. The resulting work is given by

$$\begin{aligned}
\mathcal{W}^q_{0_+\to\tau_-} &= -\int_{0_+}^{\tau_-} \mathrm{Tr}[\frac{d\hat{H}}{dt}\hat{\rho}]dt \\
&= -\int_{0_+}^{\tau_-} \mathrm{Tr}[\frac{d\hat{H}}{dt}\hat{\pi}]dt \\
&= -\int_{0_+}^{\tau_-} \frac{d}{dt}[-\beta^{-1}\ln Z^q(t)]dt \\
&= \beta^{-1}(\mathrm{Tr}[e^{-\beta\hat{H}(0_+)}] - \mathrm{Tr}[e^{-\beta\hat{H}(\tau_-)}]) \\
&= \beta^{-1}(\mathrm{Tr}[\hat{\rho}] - \mathrm{Tr}[\hat{\sigma}]) \\
&= 0
\end{aligned} \tag{3.44}$$

A calculation similar to (3.43) leads to the work extraction $\mathcal{W}^q_{\tau_-\to\tau_+} = -\mathcal{F}^q_\sigma$ during the final instantaneous change of the Hamiltonian at $t = \tau$. Thus the total work over the entire process is $\mathcal{W}^q = \mathcal{F}^q_0 - \mathcal{F}^q_\sigma$ as claimed section 3.1. With the aid of equation (3.42), an analogous calculation for the classical system shows that protocol (3.20) also saturates the generalized non-equilibirum second law.

Chapter 4: An Attempt to Suppress Transitions in Adiabatic Processes via Deoherence

Adiabatic driving is a powerful method of state preparation in quantum systems. In this chapter we will follow the nomenclature of quantum mechanics and use the term adiabatic to mean quasi-static. Let us examine the prototypical problem of ground state preparation as an example. Consider a Hamiltonian $\hat{H}$ and assume that it is desirable to prepare our system in its ground state $|g\rangle$ but unfortunately it is not feasible to do so directly. To overcome this challenge we instead consider an alternative Hamiltonian $\hat{H}_0$ with the ground state $|g_0\rangle$ that is easily prepared. By initializing our system in the state $|g_0\rangle$ and driving according to the Hamiltonian $\hat{H}(\varepsilon t)$ where $\hat{H}(0) = \hat{H}_0$ and $\hat{H}(1) = \hat{H}$, the quantum adiabatic theorem ensures that at $t = 1/\varepsilon$ our system is overwhelmingly likely to be found in the desired final ground state $|g\rangle$ given that ε is sufficiently small (slow driving) and the ground state is not degenerate at any point in our driving protocol (positive spectral gap). One application of current relevance which exactly fits this paradigm is adiabatic quantum computation [2]. In this situation, the Hamiltonian $\hat{H}$ is engineered such that its ground state $|g\rangle$ encodes the solution to an optimization problem. While the state $|g\rangle$ cannot be produced directly, the ground state of a much simpler Hamiltonian can be used in conjunction with the procedure outlined above to produce $|g\rangle$ nonetheless.

The downside of producing quantum states using this procedure is that it often

takes a long time. In the case of adiabatic quantum computing, successful computation mandates [43] that the process duration $T = 1/\varepsilon$ must be of order $1/\delta^2$ where δ is the minimum spectral gap of $\hat{H}(\varepsilon t)$ in the interval $t \in [0, 1/\varepsilon]$. For sufficiently complex Hamiltonians where δ is often very small, long process duration can make gathering statistics inconvenient or in the worst case spoil the entire setup when weak environmental effects culminate to significantly perturb the system. Due to these issues, improving the rate at which quantum states are transported along their adiabatic trajectories is an active area of research. In recent years, for instance, there has been significant interest is so called *shortcuts to adiabaticity* [131]. In the transitionless tracking variant of this approach [13, 36–38], a counterdiabatic Hamiltonian $\hat{V}(t)$ is specially constructed such that states driven according to $\hat{H}(\varepsilon t)+\hat{V}(\varepsilon t)$ *exactly* follow their adiabatic trajectories for any protocol duration $T = 1/\varepsilon$.

In this chapter we take a different approach and ask if transitions can be suppressed in an adiabatic processes through careful coupling to an environment. Somewhat against standard intuition, we specifically focus on the situation where a system undergoes decoherence in the instantaneous eigenbasis of its Hamiltonain $\hat{H}(\varepsilon t)$. This occurs for instance when the environmental coupling is tuned such that no energy is transfered between the system and environment. See section 2.1 or alternatively [120] for a more in depth look at this scenario.

Our intuition for examining decoherence in the context of adiabatic driving protocols is rooted in both experiment and theory. In Chapter 2 of this thesis, quantum work was measured in a trapped ion system for a variety of initial states, decoherence rates γ, and process durations $T = 1/\varepsilon$. It was found that for all process durations, large decoherence rates led to work distributions that closely agreed with the adiabatic work distribution corresponding to slow driving and no decoherence. For example see panels (a),(c) and (f) of figure 2.2. This suggests that in the presence

of strong decoherence, no energy transitions took place and the dynamics guided eigenstates of the initial Hamiltonian to the corresponding eigenstates of the final Hamiltonian. This can be understood from a theoretical viewpoint by interpreting decoherence in terms of an environment making effective energy measurements of the system. Each measurement causes the system's wave function to collapse into one of the energy eigenstates of the instantaneous Hamiltonian according to the reduction postulate of quantum mechanics. When the decoherence rate or equivalently the number of measurements per unit time becomes large, the quantum Zeno effect [93, 100] ensures that the probability of the system transitioning from one eigenstate to another becomes vanishingly small. One might hope that outside of the strong decohering regime, this mechanism still can be used to suppress energy transitions.

With this motivation in mind, we now precisely state the problem on which this chapter focuses. Consider a slowly driven system subject to decoherence whose evolution can be modeled by the master equation

$$\frac{d\hat{\rho}}{dt} = -\frac{i}{\hbar}[\hat{H}(\varepsilon t), \hat{\rho}] - \gamma \sum_{i \neq j} \hat{\Pi}_i(\varepsilon t)\hat{\rho}\hat{\Pi}_j(\varepsilon t) \equiv \mathcal{L}(\varepsilon t)\hat{\rho} \tag{4.1}$$

where $\hat{H}(\varepsilon t)$ is the system Hamiltonian, $\hat{\Pi}_i(\varepsilon t)$ is the projection operator onto the i^{th} eignestate of $\hat{H}(\varepsilon t)$, $\varepsilon > 0$ is a small parameter related to process duration via $T = 1/\varepsilon$, and $\gamma > 0$ is the decoherence rate. Note that the second term on the right hand side of equation (4.1) causes the off-diagonal elements of the density operator $\hat{\rho}$ to decay in the instantaneous eigenbasis of the Hamiltonian as would be expected for energy basis decoherence. Throughout this chapter we will assume that at all times in the process interval $t \in [0, 1/\varepsilon]$ the spectrum of $\hat{H}(\varepsilon t)$ is non-degenerate. We additionally assume that the system is initially prepared in the ground state $\hat{\rho}(0) = \hat{\Pi}_0(0) = |0(0)\rangle\langle 0(0)|$ of $\hat{H}(0)$ but point out that our analysis is easily generalized to

other initial eigenstates. Our aim is to determine if in the slow driving limit the success probability of the system ending in the ground state $P_0 = \mathrm{Tr}[\hat{\Pi}_0(T)\hat{\rho}(T)]$ can be increased for small to moderate values of $\gamma > 0$ when compared to traditional adiabatic setups where $\gamma = 0$. Focusing on the regime where γ is not too large and therefore the dynamics is not dominated by the decoherence ensures that we are considering the experimentally relevant situation where equation (4.1) describes a system that is weakly coupled to its environment.

To analyze this problem we take advantage of the small parameter ε and construct approximate solutions to equation (4.1) using the method of multi-scale perturbation theory. This approach is similar to the technique of adiabatic perturbation theory [108] which was developed for systems that can be described by a state vector evolving according to the Schrodinger equation. In the multi-scale framework we find that in agreement with our intuition, the zeroth order solution of (4.1) exactly tracks the system's ground state. By examining first order corrections to the system's evolution, we are then able to obtain leading order expressions for the success probability P_0 which we can compare to the standard situation without decoherence. The key result of this chapter is that in the regime of slow driving and small to moderate decoherence rate, the master equation (4.1) always produces more energy transitions than the corresponding system without decoherence. In other words, the standard intuition that decoherence should be avoided is correct– isolating a system is always a better strategy for suppressing transitons than coupling to an environment where equation (4.1) holds.

The structure of this chapter is as follows. In section 4.1, we develop the framework of multi-scale perturbation theory through a simple example. We then go on in section 4.2 to apply this method to analyze the master equation (4.1) up to first order in the driving rate ε. The results of the multi-scale analysis are validated numerically in

section 4.3. Finally in section 4.4, we interpret the results of the multi-scale analysis in the context of preventing energy transitions in a adiabatic process.

4.1 Introduction to Multi-Scale Perturbation Theory

Perturbation theory is a collection of mathematical techniques which take advantage of a small parameter ε to transform a difficult problem into a (many times infinite) hierarchy of simplified equations. The analysis of these simplified equations is often significantly more tractable than the original problem and leads to approximate solutions that can be systematically improved. While the most basic form of perturbation is used in virtually every area of physics, the multi-scale perturbation theory that we apply in this chapter for the analysis of the quasistatic master equation (4.1) is somewhat less known. For the benefit of the reader, this section gives a pedagogical introduction to this technique with a focus on solving systems of first order differential equations that feature multiple time scales.

Before introducing multi-scale perturbation theory, we will briefly review standard perturbation theory with the aid of a simple example that can be exactly solved using other methods. Through this example we will uncover some of the pitfalls of the standard theory which subsequently will motivate the multi-scale approach. Consider the initial value problem

$$\frac{dx}{dt} = v \qquad \frac{dv}{dt} = -x - 2\varepsilon v \qquad x(0) = 0 \qquad v(0) = 1 \tag{4.2}$$

where $v(t)$ and $x(t)$ are real functions and $\varepsilon > 0$ is a small parameter. Furthermore

note that the exact solution for $x(t)$ is given by

$$x(t) = \frac{e^{-\varepsilon t}}{\sqrt{1-\varepsilon^2}} \sin(\sqrt{1-\varepsilon^2}t). \tag{4.3}$$

Physically one can think of equation (4.2) as describing the motion of a weakly damped harmonic oscillator of mass $m = 1$ and damping constant $\gamma = 2\varepsilon$ that is initially at the origin with unit velocity.

Approaching this problem from standard perturbation theory dictates that we expand the equation (4.2) in a power series of ε using $x(t) = \sum x^{(i)}(t)\varepsilon^i$ and $v(t) = \sum v^{(i)}(t)\varepsilon^i$ and apply the principle of dominant balance (i.e. matching terms according to their order in the small parameter ε) to obtain the hierarchy

$$\frac{dx^{(0)}}{dt} = v^{(0)} \qquad \frac{dv^{(0)}}{dt} = -x^{(0)} \qquad x^{(0)}(0) = 0 \qquad v^{(0)}(0) = 1 \tag{4.4}$$

$$\frac{dx^{(1)}}{dt} = v^{(1)} \qquad \frac{dv^{(1)}}{dt} = -x^{(1)} - 2v^{(0)} \qquad x^{(1)}(0) = 0 \qquad v^{(1)}(0) = 0 \tag{4.5}$$

$$\frac{dx^{(2)}}{dt} = v^{(2)} \qquad \frac{dv^{(2)}}{dt} = -x^{(2)} - 2v^{(1)} \qquad x^{(2)}(0) = 0 \qquad v^{(2)}(0) = 0 \tag{4.6}$$

$$\vdots \qquad \vdots \qquad \vdots \qquad \vdots.$$

The first order approximate solution $x^{[1]} = x^{(0)} + \varepsilon x^{(1)}$ and the corresponding leading order error term $\Delta^{[1]} = \varepsilon^2 x^{(2)}$ that results from solving equations (4.4), (4.5), and (4.6) are given by

$$x^{[1]}(t) = \sin(t) - \sin(t)\varepsilon t \tag{4.7}$$

$$\Delta^{[1]} = 1/2[\sin(t) - \cos(t)t + \sin(t)t^2]\varepsilon^2. \tag{4.8}$$

Here we have our first indication that standard perturbation theory has not produced a satisfactory result. The first order approximate solution (4.7) diverges in the long

time limit while the exact solution (4.3) approaches zero. Despite no explicit assumptions pertaining to the time interval over which we solve (4.2), our approximate solution is only valid when $|x^{[1]}| \ll |\Delta^{[1]}|$ which breaks down for $\varepsilon t \approx 1$. This issue occurs due to the presence of unbounded time dependent factors called secular terms and is common in problems where a system's dynamics includes mechanisms that influence the system at vastly different rates.

Multi-scale perturbation theory is an alternative approximation scheme that aims to systematically remove secular terms and extend the validity of solutions in the time domain. Mathematically the method is based on replacing functions of a single time variable governed by ordinary differential equations with functions of multiple variables (called timescales) and a corresponding system of partial differential equations. Unlike the single variable case, the multi-variable problem does not admit a unique solution which allows one to choose a solution without secular terms.

We now outline the muti-scale method by analyzing the problem (4.2) with two timescales. Consider new multi-variable functions $\tilde{x}(t,\tau)$ and $\tilde{v}(t,\tau)$ with the property that $\tilde{x}(t,\varepsilon t) = x(t)$ and $\tilde{v}(t,\varepsilon t) = v(t)$. Combining this condition with the single variable problem (4.2), one concludes that the partial differential equations

$$\frac{\partial \tilde{x}}{\partial t} = \tilde{v} - \varepsilon \frac{\partial \tilde{x}}{\partial \tau} \qquad \frac{\partial \tilde{v}}{\partial t} = -\tilde{x} - 2\varepsilon\tilde{v} - \varepsilon \frac{\partial \tilde{v}}{\partial \tau} \qquad \tilde{x}(0,0) = 0 \qquad \tilde{v}(0,0) = 1 \qquad (4.9)$$

must hold on the line $\tau = \varepsilon t$ in the t-τ plane. One of the main conceptual leaps of multi-scale perturbation theory is to now further demand that the multi-variable functions $\tilde{x}(t,\tau)$ and $\tilde{v}(t,\tau)$ satisfy equation (4.9) for all $t, \tau > 0$. In this new multi-variable problem, the initial conditions in (4.9) are no longer sufficient to fully specify a unique solution and it is exactly this freedom we will use to remove secular terms.

The next step in the multi-scale process is to perform standard perturbation theory

to multi-variable equation (4.9). To do so we replace $\tilde{x}(t,\tau)$ and $\tilde{v}(t,\tau)$ with their power series expansions in the small parameter ε and apply the principle of dominant balance. The resulting hierarchy of equations is given by

$$\frac{\partial \tilde{x}^{(0)}}{\partial t} = \tilde{v}^{(0)} \qquad \frac{\partial \tilde{v}^{(0)}}{\partial t} = -\tilde{x}^{(0)} \tag{4.10}$$

$$\frac{\partial \tilde{x}^{(1)}}{\partial t} = \tilde{v}^{(1)} - \frac{\partial \tilde{x}^{(0)}}{\partial \tau} \qquad \frac{\partial \tilde{v}^{(1)}}{\partial t} = -\tilde{x}^{(1)} - 2\tilde{v}^{(0)} - \frac{\partial \tilde{v}^{(0)}}{\partial \tau} \tag{4.11}$$

$$\frac{\partial \tilde{x}^{(2)}}{\partial t} = \tilde{v}^{(2)} - \frac{\partial \tilde{x}^{(1)}}{\partial \tau} \qquad \frac{\partial \tilde{v}^{(2)}}{\partial t} = -\tilde{x}^{(2)} - 2\tilde{v}^{(1)} - \frac{\partial \tilde{v}^{(1)}}{\partial \tau} \tag{4.12}$$

$$\vdots \qquad\qquad \vdots$$

where $\tilde{v}^{(0)}(0,0) = 1$ and all other initial conditions are zero. Integrating equations (4.10) and applying initial data, we obtain

$$\tilde{x}^{(0)}(t,\tau) = \tilde{v}^{(0)}(0,\tau)\sin(t) + \tilde{x}^{(0)}(0,\tau)\cos(t) \tag{4.13}$$

$$\tilde{v}^{(0)}(t,\tau) = \tilde{v}^{(0)}(0,\tau)\cos(t) - \tilde{x}^{(0)}(0,\tau)\sin(t). \tag{4.14}$$

Note that at this point the zeroth order solution is not fully specified as the τ dependence of $\tilde{x}^{(0)}(t,\tau)$ and $\tilde{v}^{(0)}(t,\tau)$ has not been determined. To complete the zeroth order calculation, we must examine the first order equations (4.11) and demand that secular terms of $\tilde{x}^{(1)}(t,\tau)$ and $\tilde{v}^{(1)}(t,\tau)$ vanish. Inserting expressions (4.13) and (4.14)

into (4.11) and solving the resulting equations yields

$$\tilde{x}^{(1)}(t,\tau) = [A(\tau)\sin(t) + F(\tau)\cos(t) + G(\tau)\sin(t)] - \underbrace{[A(\tau)\cos(t) + B(\tau)\sin(t)]t}_{s_1} \tag{4.15}$$

$$\tilde{v}^{(1)}(t,\tau) = [B(\tau)\sin(t) + J(\tau)\cos(t) + K(\tau)\sin(t)] + \underbrace{[A(\tau)\sin(t) - B(\tau)\cos(t)]t}_{s_2} \tag{4.16}$$

where $A = (1+\partial_\tau)\tilde{x}^{(0)}(0,\tau)$, $B = (1+\partial_\tau)\tilde{v}^{(0)}(0,\tau)$, $F = \tilde{x}^{(1)}(0,\tau)$, $G = \partial_t\tilde{x}^{(1)}(0,\tau)$, $J = \tilde{v}^{(1)}(0,\tau)$, and $G = \partial_t\tilde{v}^{(1)}(0,\tau)$. If we insist that the secular terms s_1 and s_2 vanish for all times, we conclude that $A(\tau) = 0$ and $B(\tau) = 0$ or equivalently

$$\frac{\partial\tilde{x}^{(0)}}{\partial\tau}(0,\tau) = -\tilde{x}^{(0)} \qquad \frac{\partial\tilde{v}^{(0)}}{\partial\tau}(0,\tau) = -\tilde{v}^{(0)}. \tag{4.17}$$

This implies that the zeroth order solutions decay exponentially with the slow time variable τ. Utilizing the initial condition $\tilde{x}(0,0) = 0$, we are left with the zeroth order approximation for the weakly damped oscillator's position

$$\tilde{x}^{[0]}(t,\varepsilon t) = e^{-\varepsilon t}\sin(t). \tag{4.18}$$

Unlike the results of standard perturbation theory which lead to divergent solutions, the multi-scale approach produces a result that decays to equilibrium in a similar fashion to the exact solution (4.3). Furthermore, it can be shown that the error in solution (4.18) remains of order ε for all times and does not break down when $\varepsilon t \approx 1$. Note that while this method produced a solution which tracks the exact solution for all times in this particular example, we generally only expect a two timescale approach give solutions valid until $\varepsilon^2 t = \varepsilon\tau \approx 1$. Generally solutions will have secular terms in

the τ variable which cannot be removed without introducing additional slower time scales.

There are two ways in which the solution (4.18) can be systematically improved. The first is to decrease the error of the approximation inside its time interval of validity through the addition of higher order corrections. For instance, in our example we could form a first order approximate solution $\tilde{x}^{[1]} = \tilde{x}^{(0)} + \varepsilon\tilde{x}^{(1)}$ once the τ dependence of $\tilde{x}^{(1)}$ in equation (4.15) is determined. Similar to the process for finding the slow time dependence of $\tilde{x}^{(0)}$, the τ dependence of the first order correction can be found by integrating (4.12) and demanding that the solution $\tilde{x}^{(2)}$ have no secular terms in the variable t. It is a general feature of multi-scale perturbation theory that the n^{th} order terms can only be fully determined after examining the secular terms of the $(n+1)^{th}$ and higher order terms.

A second way of improving a multi-scale solution is to extend its validity in the time domain. This is accomplished through the introduction of additional timescales. For instance in our example we could have used three timescales t,$\tau = \varepsilon t$, and $T = \varepsilon^2 t$. In this case we would eliminate secular terms in both the t and τ variables and find solutions that break down for $\varepsilon^3 t = \varepsilon T \approx 1$ rather than $\varepsilon^2 t = \varepsilon\tau \approx 1$. Notice that in this three time scale example it would generally be necessary to look at secular terms arising in the $(n+1)^{th}$ and $(n+2)^{th}$ expansion terms to fully determine the n^{th} terms. Had our example had three timescales, it would have been necessary to look at the second order equation to determine the T dependence of the zeroth order solution.

It must be pointed out that multi-scale perturbation theory cannot be regarded as a turn-crank method for finding approximations. While it is customary to use timescales t,εt, $\varepsilon^2 t$, ..., it is possible to introduce variables that are more complicated functions of t and ϵ. Additionally it is common to have both t and ε appear explicitly in a system's equations of motion. In this case, there can be ambiguity in how

these factors are written in terms of the timescales being considered. In slow driving problems, for instance, a Hamiltonian might depend on εt. In the case of three time scales t,$\tau = \varepsilon t$, $T = \varepsilon^2 t$ this could be written as either εt, τ, or T/ε. For these reasons it is often said that there is quite a bit of *art* to using multi-scale perturbation theory. That being said, it is best practice to choose timescales using physical intuition from the problem at hand. Generally it is also preferable to introduce timescales into the equation of motion in the simplest way possible before moving to more complicated schemes. With this understanding of the multi-scale method we now move to analyzing the quasi-static decohering master equation.

4.2 Multiscale Analysis of the Quasistatic Master Equation

In our multi-scale analysis of the quasi-static decohering master equation, we make the ansatz that the relavent timescales in our problem are t and $\tau = \varepsilon t$. The timescale t captures the fast evolution of the density operator over durations in which the super-operator $\mathcal{L}$ is essentially constant. Alternatively, the timescale τ parameterizes the small changes to the system that accumulate over long time intervals due to the slow driving of the master equation. Recasting the master equation (4.1) as a partial differential equation in the variables t and τ, we obtain

$$\frac{\partial \hat{\rho}}{\partial t} = \mathcal{L}(\tau)\hat{\rho} - \varepsilon \frac{\partial \hat{\rho}}{\partial \tau} \tag{4.19}$$

where now $\hat{\rho} = \hat{\rho}(t, \tau)$ and our initial condition is $\hat{\rho}(0, 0) = \hat{\Pi}_0(0)$. Throughout the analysis of equation (4.19), we will make use of the of the spectral decomposition of

the super-operator $\mathcal{L}$ which is given by

$$\mathcal{L} = \sum_{ij} \lambda_{ij} |i\rangle\langle j| \mathrm{Tr}[|j\rangle\langle i|(\cdot)] \tag{4.20}$$

$$\lambda_{ij} = -i(E_i - E_j)/\hbar - \gamma(1 - \delta_{ij}) \equiv i\omega_{ij} - \gamma(1 - \delta_{ij}). \tag{4.21}$$

Observe that we made the natural choice to replace the argument of $\mathcal{L}$ with the variable τ rather than leaving it in the form εt. Note that in this section we only will work with multi-variable functions and hence will not distinguish between the single variable function $\hat{\rho}(t)$ in equation (4.1) and the multi-variable function $\hat{\rho}(t, \tau)$ in equation (4.19). Expanding the density operator in the series $\hat{\rho}(t, \tau) = \hat{\rho}^{(0)}(t, \tau) + \hat{\rho}^{(1)}(t, \tau)\varepsilon + \hat{\rho}^{(2)}(t, \tau)\varepsilon^2 + \dots$ leads to the hierarchy of initial value problems

$$\frac{\partial \hat{\rho}^{(0)}}{\partial t} = \mathcal{L}(\tau)\hat{\rho}^{(0)} \qquad \hat{\rho}^{(0)}(0, 0) = \hat{\Pi}_0(0) \tag{4.22}$$

$$\frac{\partial \hat{\rho}^{(1)}}{\partial t} = \mathcal{L}(\tau)\hat{\rho}^{(1)} - \frac{\partial \hat{\rho}^{(0)}}{\partial \tau} \qquad \hat{\rho}^{(1)}(0, 0) = 0 \tag{4.23}$$

$$\frac{\partial \hat{\rho}^{(2)}}{\partial t} = \mathcal{L}(\tau)\hat{\rho}^{(2)} - \frac{\partial \hat{\rho}^{(1)}}{\partial \tau} \qquad \hat{\rho}^{(2)}(0, 0) = 0 \tag{4.24}$$

$$\vdots \qquad\qquad\qquad\qquad \vdots$$

Before moving onto the details of this analysis, it is useful to present some notation that greatly simplifies the calculation. For any super operator $\mathcal{O}$, we define

$$\widetilde{\mathcal{O}}(\cdot) = \sum_{ijkl} \frac{1 - \delta(\lambda_{ij} - \lambda_{kl})}{\lambda_{kl} - \lambda_{ij}} |i\rangle\langle j| \mathrm{Tr}[|j\rangle\langle i|\mathcal{O}|k\rangle\langle l| \mathrm{Tr}[|l\rangle\langle k|(\cdot)]] \tag{4.25}$$

$$\mathrm{Res}(\mathcal{O})(\cdot) = \sum_{ijkl} \delta(\lambda_{ij} - \lambda_{kl}) |i\rangle\langle j| \mathrm{Tr}[|j\rangle\langle i|\mathcal{O}|k\rangle\langle l| \mathrm{Tr}[|l\rangle\langle k|(\cdot)]] \tag{4.26}$$

$$\mathcal{O}^{-1}(\cdot) = \sum_{ij} \frac{\delta(\lambda_{ij})}{\lambda_{ij}} |i\rangle\langle j| \mathrm{Tr}[|j\rangle\langle i|(\cdot)] \tag{4.27}$$

where $\delta(0) = 1$ and vanishes elsewhere, λ_{ij} are the eigenvalues of $\mathcal{L}$ defined in (4.21), and Res stands for residual. Operationally definition (4.25) is calculated by first representing $\mathcal{O}$ eigenbasis of $\mathcal{L}$, deleting any element $\mathcal{O}_{ijkl}$ where $\lambda_{ij} - \lambda_{kl} = 0$, and finally dividing all remaining elements $\mathcal{O}_{ijkl}$ by the difference $\lambda_{ij} - \lambda_{kl}$. Likewise $\mathrm{Res}(\mathcal{O})$ comes from again representing $\mathcal{O}$ in the eignebasis of $\mathcal{L}$ but deleting all elements where $\lambda_{ij} - \lambda_{kl} \neq 0$. Finally $\mathcal{O}^{-1}$ is to be understood as a generalized inverse that agrees with the normal matrix inverse for invertable matrices but remains well defined for non-invertable matrices.

4.2.1 0^{th} Order Solution

Integration of equation (4.22) results in a preliminary 0^{th} order solution

$$\hat{\rho}^{(0)}(t,\tau) = e^{\mathcal{L}(\tau)t}\hat{\rho}^{(0)}(0,\tau). \tag{4.28}$$

Inserting (4.28) into equation (4.23) and integrating leads to a preliminary 1^{st} order term

$$\hat{\rho}^{(1)}(t,\tau) = e^{\mathcal{L}(\tau)t}[\hat{\rho}^{(1)}(0,\tau) - \underbrace{\int_0^t e^{-\mathcal{L}(\tau)s}\frac{\partial\hat{\rho}^{(0)}}{\partial\tau}(s,\tau)ds}_{\mathcal{I}^{(1)}}] \tag{4.29}$$

$$\mathcal{I}^{(1)} = [e^{-\mathcal{L}(\tau)t}\frac{\widetilde{\widetilde{d\mathcal{L}}}}{d\tau}e^{\mathcal{L}(\tau)t} - \frac{\widetilde{\widetilde{d\mathcal{L}}}}{d\tau} - \frac{\widetilde{d\mathcal{L}}}{d\tau}t + \mathrm{Res}(\frac{d\mathcal{L}}{d\tau})\frac{t^2}{2}]\hat{\rho}^{(0)}(0,\tau) + \frac{\partial\hat{\rho}^{(0)}}{\partial\tau}(0,\tau)t \tag{4.30}$$

where the super-operator tilde notation is defined in equation (4.25). The intermediate steps in the calculation of integral $\mathcal{I}^{(1)}$ are presented in section 4.5.2. Demanding

that the secular terms vanish in equation (4.29), we find the conditions

$$\text{Res}(\frac{d\mathcal{L}}{dt})\hat{\rho}^{(0)}(0,\tau) = 0 \tag{4.31}$$

$$\frac{\partial\hat{\rho}^{(0)}}{\partial\tau}(0,\tau) = \widetilde{\frac{d\mathcal{L}}{d\tau}}\hat{\rho}^{(0)}(0,\tau). \tag{4.32}$$

As shown in appendix 4.5.3, equations (4.31) and (4.32) determine the slow time scale dependence of $\hat{\rho}^{(0)}$ which in turn leads to the full 0^{th} order solution

$$\hat{\rho}^{(0)}(t,\tau) = \hat{\rho}^{(0)}(\tau) = \hat{\Pi}_0(\tau). \tag{4.33}$$

This confirms that a system prepared in its ground state and governed by equation (4.1) simply tracks its instantaneous ground state in the slow driving limit.

4.2.2 1^{st} Order Solution

Applying the 0^{th} order result (4.33) to the 1^{st} order preliminary term (4.29) gives the simplification

$$\begin{aligned}\hat{\rho}^{(1)}(t,\tau) =& e^{\mathcal{L}(\tau)t}\{\hat{\rho}^{(1)}(0,\tau) - \int_0^t e^{-\mathcal{L}(\tau)s}\frac{d\hat{\Pi}_0}{d\tau}ds\} \\ =& e^{\mathcal{L}(\tau)t}\{\hat{\rho}^{(1)}(0,\tau) - [(I - e^{-\mathcal{L}(\tau)t})\mathcal{L}^{-1}\frac{d\hat{\Pi}_0}{d\tau} + \cancelto{0}{(I - \mathcal{L}\mathcal{L}^{-1})\frac{d\hat{\Pi}_0}{d\tau}t}] \\ =& e^{\mathcal{L}(\tau)t}[\hat{\rho}^{(1)}(0,\tau) - \mathcal{L}^{-1}\frac{d\hat{\Pi}_0}{d\tau}] + \mathcal{L}^{-1}\frac{d\hat{\Pi}_0}{d\tau}\end{aligned} \tag{4.34}$$

which is the starting point for this section's calculation. The slow time dependence of (4.34) is determined by eliminating the secular terms of the second order term

$\hat{\rho}^{(2)}(t,\tau)$. Inserting (4.34) into (4.24) and integrating leads to

$$\hat{\rho}^{(2)}(t,\tau) = e^{\mathcal{L}(\tau)t}[\hat{\rho}^{(2)}(0,\tau) - \underbrace{\int_0^t e^{-\mathcal{L}(\tau)s}\frac{\partial\hat{\rho}^{(1)}}{\partial\tau}(s,\tau)ds}_{\mathcal{I}^{(2)}}] \tag{4.35}$$

$$\mathcal{I}^{(2)} = [e^{-\mathcal{L}(\tau)t}\frac{\widetilde{\widetilde{d\mathcal{L}}}}{d\tau}e^{\mathcal{L}(\tau)t} - \frac{\widetilde{\widetilde{d\mathcal{L}}}}{d\tau} - \frac{\widetilde{d\mathcal{L}}}{d\tau}t + \mathrm{Res}(\frac{d\mathcal{L}}{d\tau})\frac{t^2}{2}][\hat{\rho}^{(1)}(0,\tau) - \mathcal{L}^{-1}\frac{d\hat{\Pi}_0}{d\tau}] \tag{4.36}$$
$$+\frac{d}{d\tau}[\hat{\rho}^{(1)}(0,\tau) - \mathcal{L}^{-1}\frac{d\hat{\Pi}_0}{d\tau}]t + [(I - e^{-\mathcal{L}(\tau)t})\mathcal{L}^{-1} + (I - \mathcal{L}\mathcal{L}^{-1})t]\frac{d}{d\tau}[\mathcal{L}^{-1}\frac{d\hat{\Pi}_0}{d\tau}].$$

An outline of the calculation of integral $\mathcal{I}^{(2)}$ is given in appendix section 4.5.4. Demanding that the secular terms vanish in equation (4.35), we find the conditions

$$\mathrm{Res}(\frac{d\mathcal{L}}{d\tau})[\hat{\rho}^{(1)}(0,\tau) - \mathcal{L}^{-1}\frac{d\hat{\Pi}_0}{d\tau}] = 0 \tag{4.37}$$

$$\frac{d}{d\tau}[\hat{\rho}^{(1)}(0,\tau) - \mathcal{L}^{-1}\frac{d\hat{\Pi}_0}{d\tau}] = \frac{\widetilde{d\mathcal{L}}}{d\tau}[\hat{\rho}^{(1)}(0,\tau) - \mathcal{L}^{-1}\frac{d\hat{\Pi}_0}{d\tau}] \tag{4.38}$$
$$-(I - \mathcal{L}\mathcal{L}^{-1})m\frac{d}{d\tau}[\mathcal{L}^{-1}\frac{d\hat{\Pi}_0}{d\tau}].$$

The secular equations (4.37) and (4.38) are solved in appendix 4.5.5 which results in the first order term

$$\hat{\rho}^{(1)}(t,\tau) = \sum_i \kappa_i(\tau) + \mathcal{L}^{-1}\frac{d\hat{\Pi}_0}{d\tau} \tag{4.39}$$

$$\kappa_{i\neq 0}(\tau) = \int_0^\tau \frac{2\gamma(1-\delta_{i0})}{\omega_{i0}^2 + \gamma^2}|\langle i|\frac{d|0\rangle}{d\tau}|^2 ds \tag{4.40}$$

$$\kappa_0(\tau) = -\sum_{i\neq 0}\kappa_i. \tag{4.41}$$

In the instantaneous eigenbasis of the Hamiltonian, the first order term (4.39) takes the form

$$\hat{\rho}^{(1)}_{00}(t,\tau) = -\sum_i \int_0^\tau \frac{2\gamma(1-\delta_{i0})}{\omega_{i0}^2+\gamma^2} |\langle i| \frac{d|0\rangle}{d\tau}|^2 ds \tag{4.42}$$

$$\hat{\rho}^{(1)}_{ii,i\neq 0}(t,\tau) = \int_0^\tau \frac{2\gamma(1-\delta_{i0})}{\omega_{i0}^2+\gamma^2} |\langle i| \frac{d|0\rangle}{d\tau}|^2 ds \tag{4.43}$$

$$\hat{\rho}^{(1)}_{i0,i\neq 0}(t,\tau) = \frac{1}{i\omega_{i0}-\gamma} \langle i| \frac{d|0\rangle}{d\tau} \tag{4.44}$$

where $\hat{\rho}^{(1)}_{0i,i\neq 0}(t,\tau) = \hat{\rho}^{(1)}_{i0,i\neq 0}(t,\tau)^*$ and all other matrix elements vanish. Equations (4.42),(4.43), and (4.44) are the main result of this chapter and quantify the deviation of the density operator $\hat{\rho}(t)$ from the adiabatic trajectory $\hat{\Pi}_0(t)$.

4.3 Numerical Validation

In this section we validate results (4.42),(4.43), and (4.44) via a simple numerical example. In keeping close to the original motivations for this research, we consider a two state system driven according to protocol (2.28) which is used in the experimental setup found in Chapter 2 of this thesis. Specifically in equation (2.28) we will measure time in terms of the characteristic Hamiltonian timescale so that $\Omega_0 = 1$ and relate the duration of protocol to the slowness parameter via $T = 1/\varepsilon$. With these simplifications the Hamiltonian becomes

$$\hat{H}(t) = \frac{\hbar\Omega(t)}{2}\left[\hat{\sigma}_{\mathrm{x}}\cos\phi(t) + \hat{\sigma}_{\mathrm{y}}\sin\phi(t)\right] \tag{4.45}$$

$$\Omega(t) = \frac{\hbar}{2}\big(1-\frac{\varepsilon t}{2}\big) \quad ; \quad \phi(t) = \frac{\pi\varepsilon t}{2}. \tag{4.46}$$

The instantaneous ground and excited state of the Hamiltonian will be denoted by $|-(\varepsilon t)\rangle$ and $|+(\varepsilon t)\rangle$ respectively. This process can be interpreted as a spin interacting

with a magnetic field that starts at $t = 0$ in the x-dirction with strength $\hbar/2$ and ends at $t = 1/\varepsilon$ in the y-direction with strength $\hbar/4$ where both the field's angle and strength change at a uniform rate. The system evolves according to the quasi-static dephasing master equation (4.1) with decoherence rate γ and is initially in the ground state $\hat{\Pi}_-(0)$ of the Hamiltonian (4.45). Note that $\hbar$ plays no role in any of the following calculations as the contribution from the Hamiltonian exactly cancels the prefactor attached to the von Neumann term of the master equation.

In this setup, the first order expansion coefficients (4.43) and (4.44) reduce to

$$\begin{aligned} \rho_{++}^{(1)}(t) =& \int_0^{\epsilon t} 2\gamma \Big[\big(\frac{s-2}{2}\big)^2 + \gamma^2 \Big]^{-1} \frac{\pi^2}{16} ds \qquad (4.47) \\ =& \frac{\pi^2}{4} \Big[\operatorname{arccot}(\gamma) + \operatorname{arccot}\big(\frac{2\gamma}{\varepsilon t - 2}\big) \Big] \\ \rho_{+-}^{(1)} =& \frac{i\pi}{4} \Big[i\big(\frac{s-2}{2}\big) - \gamma \Big]^{-1}. \qquad (4.48) \end{aligned}$$

The first order approximate solutions for the density operator elements are given by $\rho_{++}^{[1]} = \varepsilon \rho_{++}^{(1)}$ and $\rho_{+-}^{[1]} = \varepsilon \rho_{+-}^{(1)}$ since $\rho_{++}^{(1)} = \rho_{+-}^{(1)} = 0$. The most important property that our approximate solution must faithfully replicate is the probability the driving protocol fails to end in the ground state at $t = T = 1/\varepsilon$. Particularly denoting the exact excited state population by ρ_{++}, we expect the error $\Delta_{++} = |\rho_{++} - \rho_{++}^{[1]}|$ to be of second order in ε. This is best checked by examining the logarithm of Δ_{++} as a function of the logarithm of $1/\varepsilon$ and verifying that the resulting slope is -2 in the limit of small ε. For $\gamma = .5$, figure 4.1 shows this is indeed the case for both Δ_{++} and $\Delta_{+-} = |\rho_{+-} - \rho_{+-}^{[1]}|$ using a numerical simulation of the exact solution.

To be complete, we also check that the approximate solutions (4.47) and (4.48) closely track the exact solutions when time and dephasing rate are varied. Figure 4.2 shows time traces of $\rho_{++}^{[1]}$ and $\rho_{+-}^{[1]}$ and the corresponding exact solutions ρ_{++} and ρ_{+-}

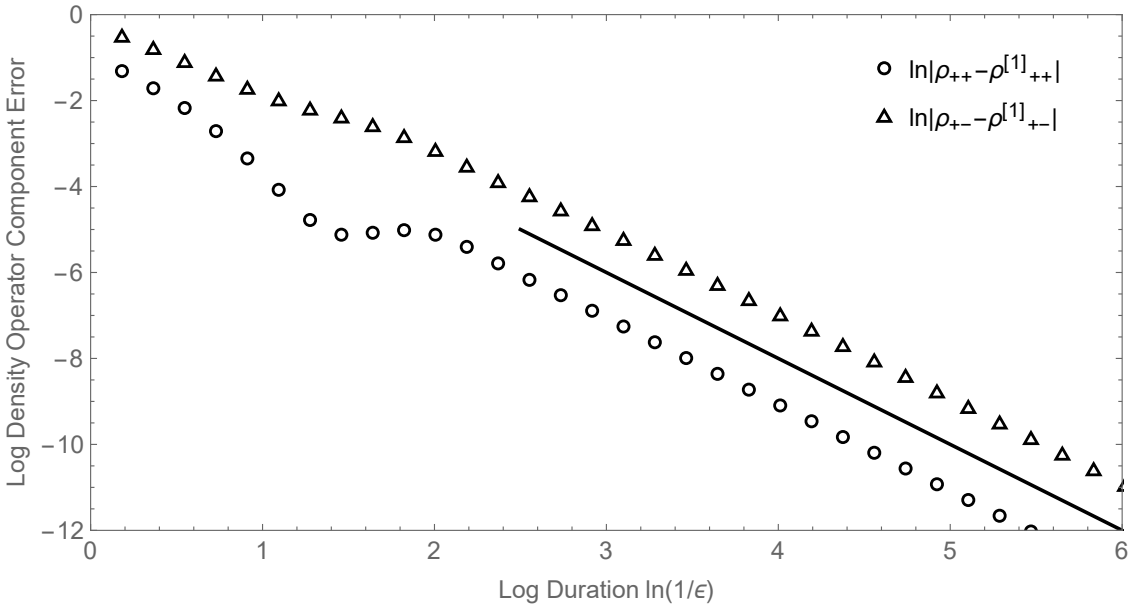

Figure 4.1: Log-Log Plot of protocol duration $1/\epsilon$ vs density operator component error. The dephasing rate is taken to be $\gamma = .5$ and the density operator components are evaluated at $t = 1/\epsilon$. The solid line corresponds to $y = -2x$ and has the same slope as the log component error in the slow driving limit.

obtained by numerical simulation for constant $\gamma = .5$ and $\varepsilon = .025$. Alternatively, figure 4.3 shows the γ dependence of $\rho^{[1]}_{++}$ and $\rho^{[1]}_{+-}$ and the corresponding exact solutions ρ_{++} and ρ_{+-} obtained by numerical simulation for constant $\varepsilon = .025$ and $t = 1/\varepsilon = 40$. In both cases, the approximate solutions closely resemble the exact solutions.

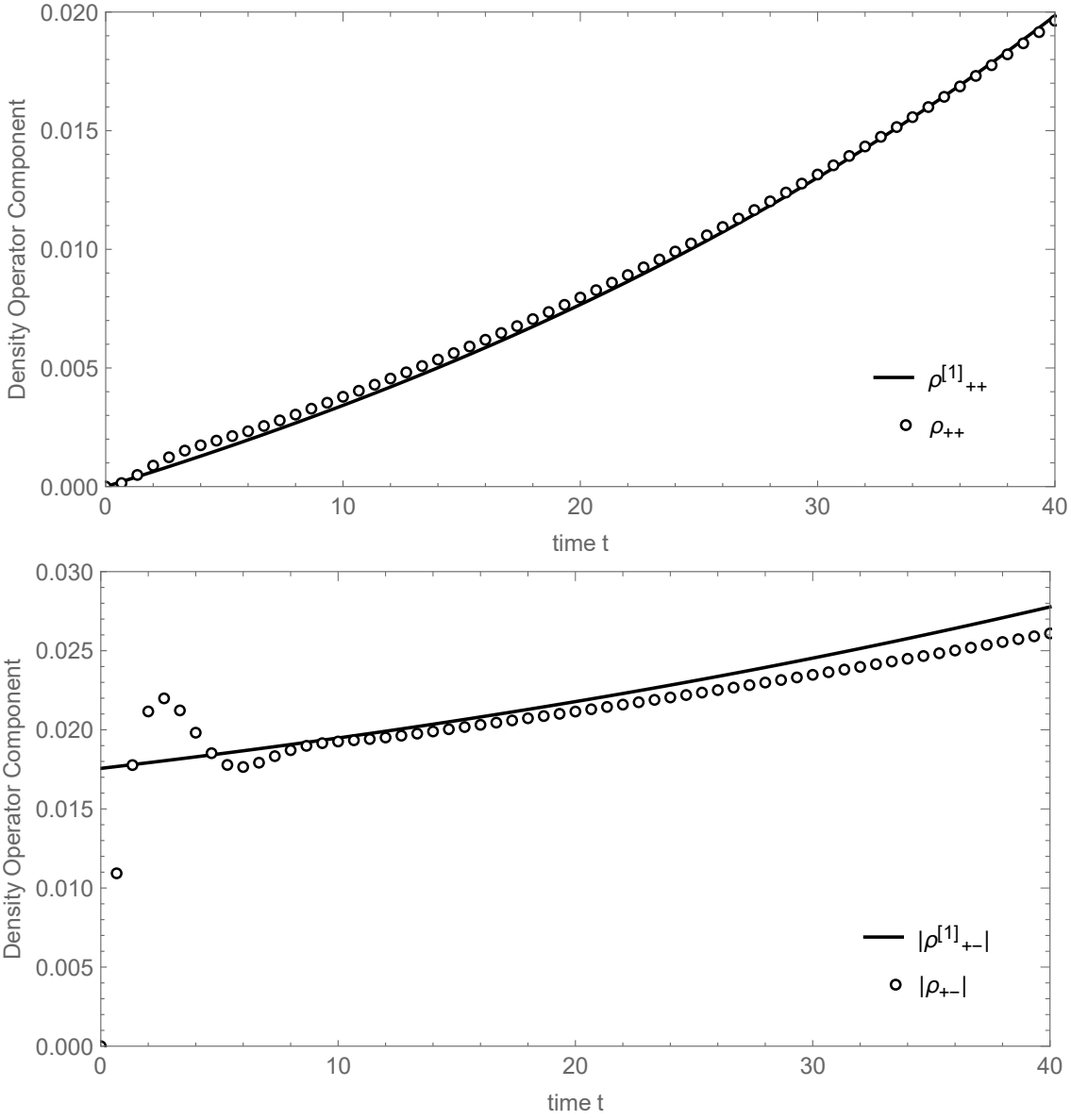

Figure 4.2: Plots of Approximate and Exact Density Operator Components as a Function of Time. In these plots the $\gamma = .5$ and $\varepsilon = .025$. Note that the density operator component $\rho^{[1]}_{+-}$ fails to track the exact solution for small times. This is due to the fact the boundary conditions of the first order coefficient $\rho^{(1)}$ can only be satisfied when the time dependence of the Hamiltonian is smoothly turned on at $t = 0$. Despite this, the solution is well approximated for most of the relevant time interval.

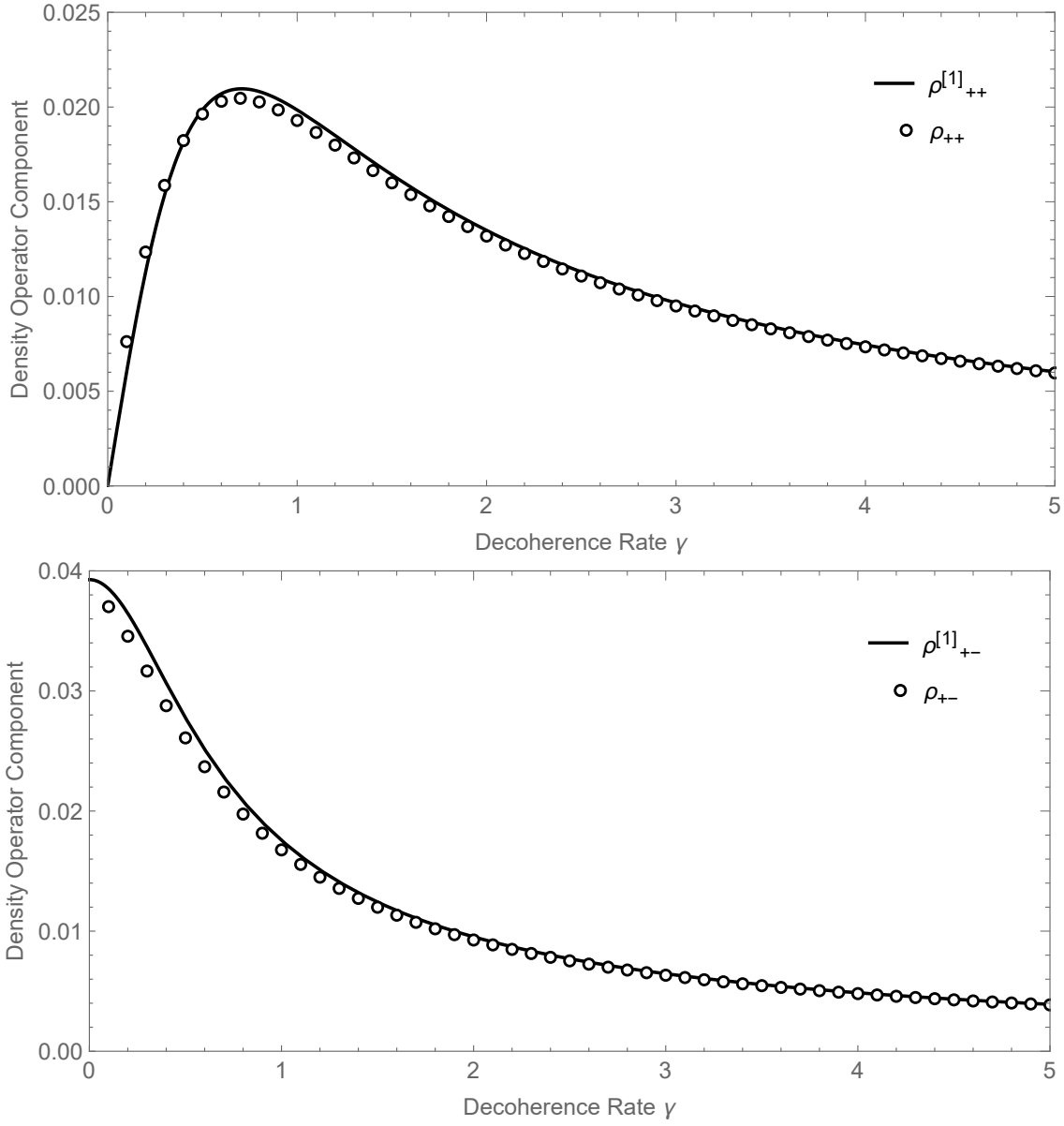

Figure 4.3: Plots of Approximate and Exact Density Operator Components as a Function of Dephasing Rate. In these plots $\varepsilon = .025$ and $t = 1/\varepsilon = 40$. The exact solution confirms that the dependence of the excited state population with γ is a Lorentzian function.

4.4 Results and Discussion

Recall that we examined adiabatic processes in the presence of decoherence to determine whether it is possible to further suppress energy transitions when compared to the standard case of purely Hamiltonian adiabatic driving. In this section we show that contrary to our hypothesis, decoherence always introduces additional level transitions in the slow driving limit.

For the sake of conversation, let us consider the case in which our system begins in the ground state of the Hamiltonian $\hat{H}(0)$ and our goal is to drive the system to the ground state of the final Hamiltonian $\hat{H(1)}$ corresponding to $t = 1/\varepsilon = T$. The failure probability that our system ends in a state other than the ground state is given by

$$\begin{aligned} P_{fail} =& 1 - P_{ground} \\ =& 1 - \rho_{00}(t) \\ =& 1 - [1 + \varepsilon\rho_{00}^{(1)}(t, \tau = 1) + \mathcal{O}(\varepsilon^2)] \\ =& \varepsilon\Big[\sum_{i\neq 0}\int_0^\tau \frac{2\gamma}{\omega_{i0}^2 + \gamma^2}|\langle i|\frac{d|0\rangle}{d\tau}|^2 ds\Big]\Big|_{\tau=1} + \mathcal{O}(\varepsilon^2). \end{aligned} \tag{4.49}$$

Note that multi-scale perturbation theory ensures that this approximation remains valid despite being evaluated for the large process duration $t = 1/\varepsilon$. Equation (4.49) shows that for any $\gamma > 0$ our failure probability is linear in the inverse process duration ε assuming we are in the slow driving regime. Alternatively in the case where $\gamma = 0$ and there is no decoherence, equation (4.49) predicts that the failure probability is of order ε^2. It follows that in the slow driving limit where ε is very small, the failure probability with decoherence is an order of magnitude larger than the failure probability without decoherence. For the example given in the validation

section (4.3) of this chapter this prediction can be tested by plotting the logarithm of failure probability vs the logarithm of duration.

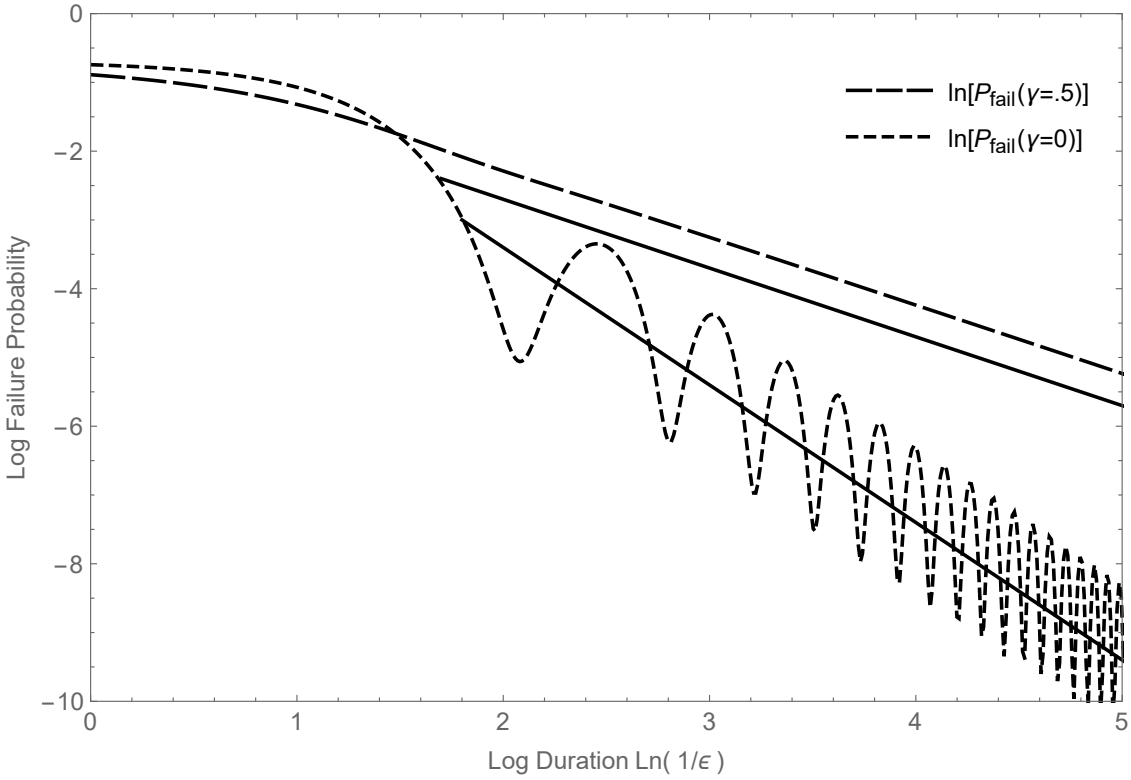

Figure 4.4: Log-log plot of protocol duration $1/\varepsilon$ vs numerical failure probabilities $P_{fail}(\gamma)$. The dephasing rate is taken to be $\gamma = .5$ and the density of the failure probabilities are evaluated at $t = 1/\epsilon$. The solid reference lines have slopes of -1 and -2. Note that for small ε, the decohering case $\gamma = .5$ has a failure probability that is linear in ε while in the Hamiltonian case $\gamma = 0$ the failure probability is quadratic in ε.

In conclusion, we believe that this analysis is good evidence that in the regime of slow driving and small to moderate decoherence, suppression of energy level transitions is best achieved using conventional methods rather than with a scheme including decoherence. This does not rule out the situation in which decoherence is the dominant term in the master equation. In Chapter 2 of this thesis, strong decoherence created by the addition of classical noise induced adiabatic evolution. In this chapter we studied small to moderate decoherence because it fits the paradigm of a system

weakly coupled to a bath. In the future it would be interesting to investigate if the strong decoherence regime could nonetheless be achieved through reservoir engineering. In that case, we expect that decoherence could aid in suppressing energy transitions in a way similar to the strong classical noise seen in Chapter 2.

4.5 Appendices

4.5.1 Formulas

In this appendix section we present a list of formulas used in other sections of this appendix. Consider a matrix $A(\tau)$ that changes with a parameter τ and a constant matrix B. The following are true

$$\frac{d}{d\tau}e^{A(\tau)} = \int_0^1 e^{A(\tau)\alpha}\frac{dA}{A\tau}e^{A(\tau)(1-\alpha)}d\alpha. \tag{4.50}$$

$$\int_0^t e^{-As}ds = (I - e^{-At})A^{-1} + (I - AA^{-1})t \tag{4.51}$$

$$\int_0^t e^{-As}Be^{As}ds = e^{-At}\widetilde{B}e^{At} - \widetilde{B} + \mathrm{Res}(B) \tag{4.52}$$

where definitions (1.36), (1.36), and (1.36) have been used.

4.5.2 Calculation of $\mathcal{I}^{(1)}$

In this appendix section we sketch the calculation of integral $\mathcal{I}^{(1)}$ which is defined in equation (4.29).

$$\begin{aligned}
\mathcal{I}^{(1)} &= \int_0^t e^{-\mathcal{L}(\tau)s}\{\frac{d}{d\tau}[e^{\mathcal{L}(\tau)s}]\hat{\rho}^{(0)}(0,\tau) + e^{\mathcal{L}(\tau)s}\frac{\partial\hat{\rho}^{(0)}}{\partial\tau}(0,\tau)\}ds \\
&= \{\int_0^t e^{-\mathcal{L}(\tau)s}\int_0^1 e^{\mathcal{L}(\tau)s\alpha}[\frac{d\mathcal{L}}{d\tau}s]e^{\mathcal{L}(\tau)s(1-\alpha)}d\alpha ds\}\hat{\rho}^{(0)}(0,\tau) + \frac{\partial\hat{\rho}^{(0)}}{\partial\tau}(0,\tau)t \\
&= \{\int_0^t\int_0^s e^{-\mathcal{L}(\tau)r}\frac{d\mathcal{L}}{d\tau}e^{\mathcal{L}(\tau)r}dr ds\}\hat{\rho}^{(0)}(0,\tau) + \frac{\partial\hat{\rho}^{(0)}}{\partial\tau}(0,\tau)t \\
&= \{\int_0^t [e^{-\mathcal{L}(\tau)s}\frac{\widetilde{d\mathcal{L}}}{d\tau}e^{\mathcal{L}(\tau)s} - \frac{\widetilde{d\mathcal{L}}}{d\tau} + \mathrm{Res}(\frac{d\mathcal{L}}{d\tau})s]ds\}\hat{\rho}^{(0)}(0,\tau) + \frac{\partial\hat{\rho}^{(0)}}{\partial\tau}(0,\tau)t \\
&= [e^{-\mathcal{L}(\tau)t}\frac{\widetilde{\widetilde{d\mathcal{L}}}}{d\tau}e^{\mathcal{L}(\tau)t} - \frac{\widetilde{\widetilde{d\mathcal{L}}}}{d\tau} - \frac{\widetilde{d\mathcal{L}}}{d\tau}t + \mathrm{Res}(\frac{d\mathcal{L}}{d\tau})\frac{t^2}{2}]\hat{\rho}^{(0)}(0,\tau) + \frac{\partial\hat{\rho}^{(0)}}{\partial\tau}(0,\tau)t
\end{aligned}$$

Note that the second line follows from the integral (4.50).

4.5.3 1^{st} Order Secular Conditions

In this appendix section we solve the first order secular conditions (4.31) and (4.32) to determine the function $\hat{\rho}^{(0)}(0,\tau)$. Examination of condition (4.31) gives

$$\begin{aligned}
\mathrm{Res}(\frac{d\mathcal{L}}{d\tau})\hat{\rho}^{(0)}(0,\tau) &= \sum_{ij}|i\rangle\langle j|\mathrm{Tr}[|j\rangle\langle i|\cancelto{\frac{d\lambda_{ij}}{d\tau}}{\frac{d\mathcal{L}}{d\tau}}|i\rangle\langle j|]\mathrm{Tr}[|j\rangle\langle i|\hat{\rho}^{(0)}(0,\tau)] \\
&\quad + \sum_{(i,j)\neq(j,k)}|i\rangle\langle j|\mathrm{Tr}[|j\rangle\langle i|\cancelto{0}{\frac{d\mathcal{L}}{d\tau}}|k\rangle\langle l|]\mathrm{Tr}[|l\rangle\langle k|\hat{\rho}^{(0)}(0,\tau)]\delta(\lambda_{ij}-\lambda_{kl}) \\
&= \sum_{ij}|i\rangle\langle j|\frac{d\lambda_{ij}}{d\tau}\langle i|\hat{\rho}^{(0)}(0,\tau)|j\rangle
\end{aligned}$$

Since $d\lambda_{ij}/d\tau$ generically vanishes only for $i=j$, one can conclude that (4.31) is satisfied only when $\hat{\rho}^{(0)}(0,\tau) = \sum_i \kappa_i(\tau)\hat{\Pi}_i(\tau)$ where κ is a constant. Using this

insight and the secular equation (4.32), we deduce

$$\sum_i \left(\frac{d\kappa_i}{d\tau}\hat{\Pi}_i + \kappa_i \frac{d\hat{\Pi}_i}{d\tau} - \kappa_i \frac{\widetilde{d\mathcal{L}}}{d\tau}\hat{\Pi}_i\right) = 0$$

$$\implies \sum_i \left(\frac{d\kappa_i}{d\tau}\underbrace{\mathrm{Tr}[\hat{\Pi}_j\hat{\Pi}_i]}_{\delta_{ij}} + \kappa_i \mathrm{Tr}[\hat{\Pi}_j \underbrace{\frac{d\hat{\Pi}_i}{d\tau}}_{0}] - \kappa_i \mathrm{Tr}[\hat{\Pi}_j \underbrace{\frac{\widetilde{d\mathcal{L}}}{d\tau}}_{0}\hat{\Pi}_i]\right) = 0$$

$$\implies \frac{d\kappa_i}{d\tau} = 0$$

Noting that our initial conditions dictate $\kappa_0(0) = 1$ and $\kappa_{i\neq 0}(0) = 0$, it follows that $\kappa_0(\tau) = 1$ and $\kappa_{i\neq 0}(\tau) = 0$ which implies $\hat{\rho}^{(0)}(0,\tau) = \hat{\Pi}_0(\tau)$.

4.5.4 Calculation of $\mathcal{I}^{(2)}$

In this appendix section we sketch the calculation of integral $\mathcal{I}^{(2)}$ which is defined in equation (4.35). Note that portions of this calculation are formally very similar to the calculation of $\mathcal{I}^{(1)}$ with $\hat{\rho}^{(0)}(0,\tau)$ replaced by $\hat{\rho}^{(1)}(0,\tau) - \mathcal{L}^{-1}d_\tau\hat{\Pi}_0$. Accordingly some intermediate steps are omitted. Inserting equation (4.34) into (4.35) we obtain

$$\begin{aligned}
\mathcal{I}^{(2)} &= \int_0^t e^{-\mathcal{L}(\tau)s}\frac{\partial}{\partial\tau}[e^{\mathcal{L}(\tau)s}(\hat{\rho}^{(1)}(0,\tau) - \mathcal{L}^{-1}\frac{d\hat{\Pi}_0}{d\tau}) + \mathcal{L}^{-1}\frac{d\hat{\Pi}_0}{d\tau}]ds \\
&= \int_0^t \{\frac{\partial}{\partial\tau}[e^{\mathcal{L}(\tau)s}][\hat{\rho}^{(1)}(0,\tau) - \mathcal{L}^{-1}\frac{d\hat{\Pi}_0}{d\tau}] + e^{\mathcal{L}(\tau)t}\frac{\partial}{\partial\tau}[\hat{\rho}^{(1)}(0,\tau) - \mathcal{L}^{-1}\frac{d\hat{\Pi}_0}{d\tau}] \\
&\quad + \frac{\partial}{\partial\tau}[\mathcal{L}^{-1}\frac{d\hat{\Pi}_0}{d\tau}]\}ds \\
&= [e^{-\mathcal{L}(\tau)t}\frac{\widetilde{\widetilde{d\mathcal{L}}}}{d\tau}e^{\mathcal{L}(\tau)t} - \frac{\widetilde{\widetilde{d\mathcal{L}}}}{d\tau} - \frac{\widetilde{d\mathcal{L}}}{d\tau}t + \mathrm{Res}(\frac{d\mathcal{L}}{d\tau})\frac{t^2}{2}][\hat{\rho}^{(1)}(0,\tau) - \mathcal{L}^{-1}\frac{d\hat{\Pi}_0}{d\tau}] \\
&\quad + \frac{d}{d\tau}[\hat{\rho}^{(1)}(0,\tau) - \mathcal{L}^{-1}\frac{d\hat{\Pi}_0}{d\tau}]t \\
&\quad + [(I - e^{-\mathcal{L}(\tau)t})\mathcal{L}^{-1} + (I - \mathcal{L}\mathcal{L}^{-1})t]\frac{d}{d\tau}[\mathcal{L}^{-1}\frac{d\hat{\Pi}_0}{d\tau}]
\end{aligned}$$

4.5.5 2^{nd} Order Secular Conditions

Following the same arguments made in appendix section 4.5.3 to solve equation (4.31), one can conclude that condition (4.37) leads to

$$\hat{\rho}^{(1)}(0,\tau) - \mathcal{L}^{-1}\frac{d\hat{\Pi}_0}{d\tau} = \sum_i \kappa(\tau)\hat{\Pi}_i(\tau)$$

where κ_i are scalar constants. Inserting this result into the secular condition (4.38) and tracing both sides according to $\mathrm{Tr}[\hat{\Pi}_i(\cdot)]$ gives

$$\begin{aligned}
\frac{d\kappa_i}{d\tau} =& -\mathrm{Tr}[\hat{\Pi}_i(I-\mathcal{L}^{-1}\mathcal{L})\frac{d}{d\tau}[\mathcal{L}^{-1}\frac{d\hat{\Pi}_0}{d\tau}]] \\
=& -\mathrm{Tr}[\hat{\Pi}_i\frac{d}{d\tau}[\mathcal{L}^{-1}\frac{d\hat{\Pi}_0}{d\tau}]] \\
=& -\frac{d}{d\tau}\mathrm{Tr}[\hat{\Pi}_i\mathcal{L}^{-1}\underbrace{\frac{d\hat{\Pi}_0}{d\tau}}_{\to 0}] + \mathrm{Tr}[\frac{d\hat{\Pi}_i}{d\tau}\mathcal{L}^{-1}\frac{d\hat{\Pi}_0}{d\tau}] \\
=&\mathrm{Tr}[(\frac{d|i\rangle}{d\tau}\langle i| + |i\rangle\frac{d\langle i|}{d\tau})\sum_{rs}\frac{1-\delta_{rs}}{\lambda_{rs}}|r\rangle\langle s|\mathrm{Tr}[|s\rangle\langle r|(\frac{d|0\rangle}{d\tau}\langle 0| + |0\rangle\frac{d\langle 0|}{d\tau})]] \\
=&\sum_{rs}\frac{1-\delta_{rs}}{\lambda_{rs}}(\langle s|\frac{d|i\rangle}{d\tau}\delta_{ir} + \delta_{is}\frac{d\langle i|}{d\tau}|r\rangle)(\langle r|\frac{d|0\rangle}{d\tau}\delta_{0s} + \delta_{0r}\frac{d\langle 0|}{d\tau}|s\rangle) \\
=&\frac{1-\delta_{i0}}{\lambda_{i0}}\langle 0|\frac{d|i\rangle}{d\tau}\langle i|\frac{d|0\rangle}{d\tau} + \delta_{i0}\sum_s\frac{1-\delta_{0s}}{\lambda_{0s}}\langle s|\frac{d|i\rangle}{d\tau}\frac{d\langle 0|}{d\tau}|s\rangle \\
&+ \delta_{i0}\sum_r\frac{1-\delta_{r0}}{\lambda_{r0}}\frac{d\langle i|}{d\tau}|r\rangle\langle r|\frac{d|0\rangle}{d\tau} + \frac{1-\delta_{0i}}{\lambda_{0i}}\frac{d\langle i|}{d\tau}|0\rangle\frac{d\langle 0|}{d\tau}|i\rangle \\
=& -(1-\delta_{i0})(\frac{1}{\lambda_{i0}}+\frac{1}{\lambda_{0i}})|\langle i|\frac{d|0\rangle}{d\tau}|^2 + \delta_{i0}\sum_j(1-\delta_{0j})(\frac{1}{\lambda_{0j}}+\frac{1}{\lambda_{j0}})|\langle j|\frac{d|0\rangle}{d\tau}|^2 \\
=&(1-\delta_{i0})\frac{2\gamma}{\omega_{i0}^2+\gamma^2}|\langle i|\frac{d|0\rangle}{d\tau}|^2 - \delta_{i0}\sum_j\frac{2\gamma(1-\delta_{0j})}{\omega_{j0}^2+\gamma^2}|\langle j|\frac{d|0\rangle}{d\tau}|^2
\end{aligned}$$

from which it follows

$$\kappa_{i\neq 0}(\tau) = \int_0^\tau \frac{2\gamma(1-\delta_{i0})}{\omega_{i0}^2+\gamma^2} |\langle i|\frac{d|0\rangle}{d\tau}|^2 ds$$
$$\kappa_0(\tau) = -\sum_{i\neq 0}\kappa_i.$$

Using the results of this appendix section, the first order correction (4.34) takes its final form

$$\begin{aligned}\hat{\rho}^{(1)}(t,\tau) =& e^{\mathcal{L}(\tau)t}[\mathcal{L}^{-1}\frac{d\hat{\Pi}_0}{d\tau} + \sum_i \kappa_i\hat{\Pi}_i] + (I - e^{\mathcal{L}(\tau)t})\mathcal{L}^{-1}\frac{d\hat{\Pi}_0}{d\tau} \\ =& \sum_i \kappa_i\hat{\Pi}_i + \mathcal{L}^{-1}\frac{d\hat{\Pi}_0}{d\tau}.\end{aligned}$$

In order to calculate the matrix elements (4.42),(4.43), and (4.44), it is useful to note

$$\begin{aligned}\mathcal{L}^{-1}\frac{d\hat{\Pi}_0}{d\tau} =& \sum_{ij}\frac{1-\delta_{ij}}{\lambda_{ij}}|i\rangle\langle j|\mathrm{Tr}[|j\rangle\langle i|(\frac{d|0\rangle}{d\tau}\langle 0| + |0\rangle\frac{d\langle 0|}{d\tau})] \\ =& \sum_{ij}\frac{1-\delta_{ij}}{\lambda_{ij}}|i\rangle\langle j|(\langle i|\frac{d|0\rangle}{d\tau}\delta_{j0} + \delta_{i0}\frac{d\langle 0|}{d\tau}|j\rangle) \\ =& \sum_i(1-\delta_{i0})(\frac{1}{\lambda_{i0}}\langle i|\frac{d|0\rangle}{d\tau}|i\rangle\langle 0| + \frac{1}{\lambda_{0i}}|0\rangle\langle i|\frac{d\langle 0|}{d\tau}|i\rangle).\end{aligned}$$

Chapter 5: Conclusions and New Directions

In this thesis we investigated a variety of topics in quantum thermodynamics and beyond.

Chapter 2 focused on the quantum nonequilibrium work relation in the presence of decoherence. There we argued in a heuristic way that heat plays no role in energy changes of a system that experiences decoherence but not dissipation. This heuristic approach was complimented by a Hamiltonian model that explicitly accounted for the bath and also showed the absence of heat. This allowed us to equate work with system energy change and thus build a work distribution using the two time energy measurement protocol. The resulting work distribution then was shown to satisfy a fluctuation theorem which was experimentally demonstrated using a system of trapped ions and decoherence simulated by classical noise.

Chapter 3 delved into the relationship between quantum work and coherence. Important results in quantum thermodynamics show that coherence is a resource that can always be used to extract additional work when compared to incoherent states. It has been suggested that this could be a true signature of quantum thermodynamics divergence from the thermodynamics of classical systems. We investigated this later assertion in the framework of classical Hamiltonian dynamics and canonical quantization. We found that classical phase space distributions have a quantity analogous to coherence that we called non-uniformity. We showed that like coherence, non-uniformity allows for additional work extraction when compared to the correspond-

ing uniform state. Going further, we developed the idea of energy equivalent sets which allowed a more quantitative comparison of quantum coherence with classical non-uniformity. Importantly in the classical limit of small $\hbar$, we found that the work extracted from non-uniformity and coherence agreed– at least in the case of energy equivalent sets. We concluded that while coherence does offer an advantage when quantum systems are compared to discrete state classical systems, coherence does not offer a wholesale advantage when quantum Hamiltonian systems are compared to their classical Hamiltonian counterparts.

Finally Chapter 4 took inspiration from the experimental portion of Chapter 2 and asked if decoherence could assist in suppressing transitons in an adiabatic (quasistatic) process. In addressing this question, we developed an approximate solution for the a decohering master equation in the slow driving limit using multi-scale perturbation theory. These solutions were tested against a simulation of the experimental protocol from Chapter 2 and found to accurately track the numerical solutions. Our core finding was that in the regime of slow driving and moderate decoherence, the standard adiabatic scheme always leads to less transitions than the corresponding scheme with decoherence.

Based on the results of this thesis and insights from my advisor, collaborators, and the broader community, I see numerous possible directions of future research in quantum thermodynamics. As some final food for thought, I outline two such problems as a conclusion to this thesis.

In chapter 3 of this thesis, we saw that the nonequilibirum second law could be saturated in both the quantum and classical setting using protocols (3.7) and (3.20). While these protocols are acceptable at the purely theoretical level, they leave much to be desired in terms of actual experimental implementation. These protocols generally require control of a Hamiltonian that is a complicated function

of both position and momentum which cannot be carried out in the context of an experimentally controlled potential. I believe that investigating the intersection of thermodynamics and restricted control could be a fruitful direction of future research. For instance assume a system with base Hamiltonian $\hat{H}$ is driven from a state $\hat{\rho}_0$ to a state $\hat{\rho}_\tau$. The nonequilibrium second law states that $\langle \mathcal{W} \rangle \geq \Delta \mathcal{F}$, which is the best bound one can find assuming an arbitrary driving protocol. Would it be possible to obtain a stronger bound for the work invested if one restricted the protocol to only manipulations of a position dependent potential? For research along this direction see [16, 77, 86].

Another issue that we touched on briefly in both chapters 2 and 3, is the debate surrounding quantum work. Quantum work has been approached from the perspective of ensemble averages [4], the two time energy measurement scheme [74, 95, 130], path integrals [122], quantum histories [92], Bohmian trajectories [113], and quantum resource theory [52] to name just a few. Understanding the resulting zoo of often inconsistent work definitions has become of important topic in the field of quantum thermodynamics. One property that many of these approaches have in common is that the effects of the external control system are incorporated into the setup via a time dependent Hamiltonian. We believe that aspects of quantum work could be clarified by explicitly modeling the control field as a Hamiltonian system. In this approach work can be defined as the energy change of the auxiliary control system. One approach to obtaining such a model could be to append an auxiliary system to the system of interest and considering the limit in which the auxiliary system's mass goes to infinity. An alternate method could be to append an auxiliary system with a Hamiltonian proportional to its momentum coordinate that couples to the system of interest through its position. Such a model's Hamiltonian, sometimes called a

quantum clock [88], is written as

$$\hat{H} = \hat{H}^{sys}(\hat{X}/V) + \hat{P}V \tag{5.1}$$

where V is a constant with dimensions of velocity and $\hat{X}$ and $\hat{P}$ correspond respectively to the control field's position and momentum operators. Here the reduced dynamics of the system will be identical to the non-autonomous case with Hamiltonian $\hat{H}^{sys}(t)$ provided the control field starts in the the position eignestate $|x = 0\rangle$. It is the opinion of the author that this autonomous approach would show that the uncertainty relation $\Delta X \Delta P \geq \hbar/2$ applied to the control field contributes to the difficulty of defining quantum work.

Bibliography

[1] J. Åberg. Catalytic coherence. *Physical Review Letters*, 113(15):1–6, 2014.

[2] T. Albash and D. A. Lidar. Adiabatic quantum computation. *Rev. Mod. Phys.*, 90:015002, Jan 2018.

[3] T. Albash, D. A. Lidar, M. Marvian, and P. Zanardi. Fluctuation theorems for quantum processes. *Phys. Rev. E*, 88:032146, 2013.

[4] R. Alicki. On the detailed balance condition for non-hamiltonian systems. *Rep. Math. Phys.*, 10(2):249–258, 1976.

[5] R. Alicki. The quantum open system as a model of the heat engine. *Journal of Physics A: Mathematical and General*, 12(5):L103–L107, may 1979.

[6] A. E. Allahverdyan and Th. M. Nieuwenhuizen. Fluctuations of work from quantum subensembles: The case against quantum work-fluctuation theorems. *Phys. Rev. E*, 71:066102, Jun 2005.

[7] S. An, D. Lv, A. del Campo, and K. Kim. Shortcuts to adiabaticity by counterdiabatic driving in trapped-ion transport. *Nature Comm.*, 7(12999), 2009.

[8] S. An, J. Zhang, M. Um, D. Lv, Y. Lu, J. Zhang, Z. Yin, H. T. Quan, and K. Kim. Experimental test of the quantum Jarzynski equality with a trapped-ion system. *Nature Phys.*, 11:193 – 199, 2015.

[9] Y. B. Band. Open quantum system stochastic dynamics with and without the rwa. *Journal of Physics B: Atomic, Molecular and Optical Physics*, 48(4):045401, 2015.

[10] S.M. Barnett and D.T. Pegg. On the hermitian optical phase operator. *Journal of Modern Optics*, 36(1):7–19, 1989.

[11] T. B. Batalhão, A. M. Souza, L. Mazzola, R. Auccaise, R. S. Sarthour, I. S. Oliveira, J. Goold, G. De Chiara, M. Paternostro, and R. M. Serra. Experimental reconstruction of work distribution and study of fluctuation relations in a closed quantum system. *Phys. Rev. Lett.*, 113:140601, 2014.

[12] T. Baumgratz, M. Cramer, and M. B. Plenio. Quantifying coherence. *Physical Review Letters*, 113(14):1–5, 2014.

[13] M. V. Berry. Transitionless quantum driving. *J. Phys. A: Math. and Theor.*, 42(36):365303, 2009.

[14] F. Binder, L. A. Correa, C. Gogolin, J. Anders, and G. Adesso. *Thermodynamics in the Quantum Regime*. Springer, Berlin, 20.

[15] V. Blickle, T. Speck, L. Helden, U. Seifert, and C. Bechinger. Thermodynamics of a colloidal particle in a time-dependent nonharmonic potential. *Phys. Rev. Lett.*, 96:070603, 2006.

[16] A. B. Boyd, D. Mandal, and J. P. Crutchfield. Thermodynamics of modularity: Structural costs beyond the landauer bound. *Phys. Rev. X*, 8:031036, Aug 2018.

[17] F. G.S.L. Brandão, M. Horodecki, J. Oppenheim, J. M. Renes, and R. W. Spekkens. Resource theory of quantum states out of thermal equilibrium. *Physical Review Letters*, 111(25):1–5, 2013.

[18] H. B. Callen. *Thermodynamics and an Introduction to Thermostatistics*. John Wiley Sons, New York, 1985.

[19] M. Campisi, P. Hänggi, and P. Talkner. Colloquium: Quantum fluctuation relations: Foundations and applications. *Rev. Mod. Phys.*, 83:771, 2011.

[20] M. Campisi, J. Pekola, and R. Fazio. Feedback-controlled heat transport in quantum devices: theory and solid-state experimental proposal. *New Journal of Physics*, 19(5):053027, 2017.

[21] M. Campisi, P. Talkner, and P. Hänggi. Fluctuation theorem for arbitrary open quantum systems. *Phys. Rev. Lett.*, 102:210401, 2009.

[22] M. Campisi, P. Talkner, and P. Hänggi. Fluctuation theorems for continuously monitored quantum fluxes. *Phys. Rev. Lett.*, 105:140601, 2010.

[23] M. Campisi, P. Talkner, and P. Hänggi. Influence of measurements on the statistics of work performed on a quantum system. *Phys. Rev. E*, 83:041114, 2011.

[24] M. Campisi, P. Talkner, and P. Hänggi. Quantum Bochkov-Kuzovlev work fluctuation theorems. *Philos. Trans. R. Soc. A*, 369:291, 2011.

[25] W. B. Case. Wigner functions and weyl transforms for pedestrians. *American Journal of Physics*, 76(10):937–946, 2008.

[26] A. Chenu, M. Beau, J. Cao, and A. del Campo. Quantum simulation of generic many-body open system dynamics using classical noise. *Phys. Rev. Lett.*, 118:140403, 2017.

[27] R. Chetrite and K. Mallick. Quantum fluctuation relations for the Lindblad master equation. *J. Stat. Phys.*, 148:480, 2012.

[28] C. Chipot and A. Pohorille. *Free Energy Calculations*. Springer, Berlin, 2007.

[29] D. Collin, F. Ritort, C. Jarzynski, S. B. Smith, I. Tinoco Jr., and C. Bustamante. Verification of the crooks fluctuation theorem and recovery of RNA folding free energies. *Nature*, 437:231–234, 2005.

[30] G. E. Crooks. Quantum operation time reversal. *Phys. Rev. A*, 77:034101, 2008.

[31] J. Dalibard, Y. Castin, and K. Mølmer. Wave-function approach to dissipative processes in quantum optics. *Phys. Rev. Lett.*, 68:580, 1992.

[32] S. Deffner and E. Lutz. Nonequilibrium entropy production for open quantum systems. *Phys. Rev. Lett.*, 107:140404, 2011.

[33] S. Deffner, J. P. Paz, and W. H. Zurek. Quantum work and the thermodynamic cost of quantum measurements. *Phys. Rev. E*, 94:010103(R), 2016.

[34] C. Dellago and G. Hummer. Computing equilibrium free energies using non-equilibrium molecular dynamics. *Entropy*, 16(1):41–61, 2014.

[35] M. Demirplak and S. A. Rice. Adiabatic population transfer with control fields. *J. Phys. Chem. A*, 107(46):9937–9945, 2003.

[36] M. Demirplak and S. A. Rice. Adiabatic population transfer with control fields. *The Journal of Physical Chemistry A*, 107(46):9937–9945, 2003.

[37] M. Demirplak and S. A. Rice. Assisted adiabatic passage revisited. *The Journal of Physical Chemistry B*, 109(14):6838–6844, 2005. PMID: 16851769.

[38] M. Demirplak and S. A. Rice. On the consistency, extremal, and global properties of counterdiabatic fields. *The Journal of Chemical Physics*, 129(15):154111, 2008.

[39] C. Van den Broeck and M. Esposito. Ensemble and trajectory thermodynamics: A brief introduction. *Physica A: Statistical Mechanics and its Applications*, 418:6 – 16, 2015. Proceedings of the 13th International Summer School on Fundamental Problems in Statistical Physics.

[40] V. V. Dodonov. nonclassical states in quantum optics: a squeezed review of the first 75 years. *Journal of Optics B: Quantum and Semiclassical Optics*, 4(1):R1–R33, jan 2002.

[41] R. Dorner, S.R. Clark, L. Heaney, R. Fazio, J. Goold, and V. Vedral. Extracting quantum work statistics and fluctuation theorems by single-qubit interferometry. *Phys. Rev. Lett.*, 110:230601, 2013.

[42] F. Douarche, S. Ciliberto, A. Petrosyan, and I. Rabbiosi. An experimental test of the Jarzynski equality in a mechanical experiment. *Europhys. Lett.*, 70:593–599, 2005.

[43] A. Elgart and G. A. Hagedorn. A note on the switching adiabatic theorem. *Journal of Mathematical Physics*, 53(10):102202, 2012.

[44] C. Elouard, A. Auffeves, and M. Clusel. Stochastic thermodynamics in the quantum regime. arXiv:1507.00312v1, 2015.

[45] C. Elouard, N. K. Bernardes, A. R. R. Carvalho, M. F. Santos, and A. AuffÃšves. Probing quantum fluctuation theorems in engineered reservoirs. *New Journal of Physics*, 19(10):103011, 2017.

[46] C. Elouard, D. A. Herrera-Martí, M. Clusel, and A. Auffèves. The role of quantum measurement in stochastic thermodynamics. *Nature Quantum Information*, 3:9, 2017.

[47] M. Esposito, U. Harbola, and S. Mukamel. Nonequilibrium fluctuations, fluctuation theorems, and counting statistics in quantum systems. *Rev. Mod. Phys.*, 81:1665, 2009.

[48] M. Esposito and S. Mukamel. Fluctuation theorems for quantum master equations. *Phys. Rev. E*, 73:046129, 2006.

[49] M. Esposito and C. Van Den Broeck. Second law and Landauer principle far from equilibrium. *Epl*, 95(4), 2011.

[50] J. Goold, M. Paternostro, and K. Modi. Nonequilibrium quantum landauer principle. *Phys. Rev. Lett.*, 114:060602, 2015.

[51] V. Gorini, A. Frigerio, M. Verri, A. Kossakowski, and E.C.G. Sudarshan. Properties of quantum Markovian master equations. *Rep. Math. Phys.*, 13(2):149–173, 1978.

[52] G. Gour, M. P. Müller, V. Narasimhachar, R. W. Spekkens, and N. Y. Halpern. The resource theory of informational nonequilibrium in thermodynamics. *Physics Reports*, 583:1 – 58, 2015. The resource theory of informational nonequilibrium in thermodynamics.

[53] P. Hänggi and P. Talkner. The other QFT. *Nat. Phys.*, 11:108–110, 2015.

[54] N. C. Harris, Y. Song, and C. Kiang. Experimental free energy surface reconstruction from single-molecule force spectroscopy using Jarzynski's equality. *Phys. Rev. Lett.*, 99:068101, 2007.

[55] H.-H. Hasegawa, J. Ishikawa, K. Takara, and D.J. Driebe. Generalization of the second law for a nonequilibrium initial state. *Physics Letters A*, 374(8):1001 – 1004, 2010.

[56] F. W. J. Hekking and J. P. Pekola. Quantum jump approach for work and dissipation in a two-level system. *Phys. Rev. Lett.*, 111:093602, 2013.

[57] M. Hillery, R.F. O'Connell, M.O. Scully, and E.P. Wigner. Distribution functions in physics: Fundamentals. *Physics Reports*, 106(3):121 – 167, 1984.

[58] M. Horodecki and J. Oppenheim. Fundamental limitations for quantum and nanoscale thermodynamics. *Nature Communications*, 4(May):1–6, 2013.

[59] J. M. Horowitz. Quantum-trajectory approach to the stochastic thermodynamics of a forced harmonic oscillator. *Phys. Rev. E*, 85:031110, 2012.

[60] J. M. Horowitz and J. M. R. Parrondo. Entropy production along nonequilibrium quantum jump trajectories. *New J. Phys.*, 15:085028, 2013.

[61] G. Huber, F. Schmidt-Kaler, S. Deffner, and E. Lutz. Employing trapped cold ions to verify the quantum Jarzynski equality. *Phys. Rev. Lett.*, 101:070403, 2008.

[62] C. Jarzynski. Equilibrium free-energy differences from nonequilibrium measurements: A master-equation approach. *Phys. Rev. E*, 56:5018–5035, Nov 1997.

[63] C. Jarzynski. Nonequilibrium equality for free energy differences. , 78(14):2690 – 2693, 1997.

[64] C. Jarzynski. Nonequilibrium work relations: foundations and applications. *European Physical Journal B*, 64(3-4):331–340, 2008.

[65] C. Jarzynski. Equalities and inequalities: irreversibility and the second law of thermodynamics at the nanoscale. *Annu. Rev. Cond. Matt. Phys.*, 2:329 – 351, 2011.

[66] I. Junier, A. Mossa, M. Manosas, and F. Ritort. Recovery of free energy branches in single molecule experiments. *Phys. Rev. Lett.*, 102:070602, 2009.

[67] D. Kafri and S. Deffner. Holevo's bound from a general quantum fluctuation theorem. *Phys. Rev. A*, 86:044302, 2012.

[68] P. Kammerlander and J. Anders. Coherence and measurement in quantum thermodynamics. *Sci. Reports*, 6:22174, 2016.

[69] J. G. Kirkwood. Statistical mechanics of fluid mixtures. *The Journal of Chemical Physics*, 3(5):300–313, 1935.

[70] J. Klatzow, J. N. Becker, P. M. Ledingham, C. Weinzetl, K. T. Kaczmarek, D. J. Saunders, J. Nunn, I. A. Walmsley, R. Uzdin, and E. Poem. Experimental demonstration of quantum effects in the operation of microscopic heat engines. *Phys. Rev. Lett.*, 122:110601, Mar 2019.

[71] D. H. Kobe. Canonical transformation to energy and "tempus" in classical mechanics. *American Journal of Physics*, 61(11):1031–1037, 1993.

[72] K. Korzekwa, M. Lostaglio, J. Oppenheim, and D. Jennings. The extraction of work from quantum coherence. *New Journal of Physics*, 18(2):023045, feb 2016.

[73] A. Kossakowski, A. Frigerio, V. Gorini, and M. Verri. Quantum detailed balance and the KMS condition. *Comm. Math. Phys.*, 57(2):97–110, 1977.

[74] J. Kurchan. A quantum fluctuation theorem. arXiv:cond-mat/0007360v2, 2000.

[75] L. D. Landau and E. M. Lifshitz. *Statistical Physics 3rd Ed.* Elsevier, Amsterdam, 1980.

[76] B. Leggio, A. Napoli, A. Messina, and H.-P. Breuer. Entropy production and information fluctuations along quantum trajectories. *Phys. Rev. A*, 89:042111, 2013.

[77] J. Lekscha, H. Wilming, J. Eisert, and R. Gallego. Quantum thermodynamics with local control. *Phys. Rev. E*, 97:022142, Feb 2018.

[78] A. Levy, E. Torrontegui, and R. Kosloff. Action-noise-assisted quantum control. *Phys. Rev. A*, 96, 2017.

[79] Gö. Lindblad. Completely positive maps and entropy inequalities. *Communications in Mathematical Physics*, 40(2):147–151, Jun 1975.

[80] J. Liphardt, S. Dumont, S. B. Smith, I. Tinoco Jr., and C. Bustamante. Equilibrium information from nonequilibrium measurements in an experimental test of Jarzynski's equality. *Science*, 296:1832–1835, 2002.

[81] F. Liu. Derivation of quantum work equalities using a quantum Feynman-Kac formula. *Phys. Rev. E*, 86:010103, 2012.

[82] F. Liu. Calculating work in adiabatic two-level quantum Markovian master equation: A characteristic function method. *Phys. Rev. E*, 90:032121, 2014.

[83] F. Liu. Equivalence of two Bochkov-Kuzovlev equalities in quantum two-level systems. *Phys. Rev. E*, 89:042122, 2014.

[84] F. Liu. Calculating work in weakly driven quantum master equations: Backward and forward equations. *Phys. Rev. E*, 93:012127, 2016.

[85] F. N. Loreti and A. B. Balantekin. Neutrino oscillations in noisy media. *Phys. Rev. D*, 50:4762–4770, 1994.

[86] M. Lostaglio, Á. M. Alhambra, and C. Perry. Elementary Thermal Operations. *Quantum*, 2:52, February 2018.

[87] M. Lostaglio, D. Jennings, and T. Rudolph. Description of quantum coherence in thermodynamic processes requires constraints beyond free energy. *Nature Communications*, (6):6383, Jan 2015.

[88] A. S. L. Malabarba, A. J. Short, and P. Kammerlander. Clock-driven quantum thermal engines. *New Journal of Physics*, 17(4):045027, apr 2015.

[89] G. Manzano, J. M. Horowitz, and Juan M. R. Parrondo. Nonequilibrium potential and fluctuation theorems for quantum maps. *Phys. Rev. E*, 92:032129, 2015.

[90] L. Mazzola, G. De Chiara, and M. Paternostro. Measuring the characteristic function of the work distribution. *Phys. Rev. Lett.*, 110:230602, 2013.

[91] R. Medeiros de Araújo, T. Häffner, R. Bernardi, D. S. Tasca, M. P. J. Lavery, M. J. Padgett, A. Kanaan, L. C. Céleri, and P. H. Souto Ribeiro. Experimental study of quantum thermodynamics using optical vortices. *ArXiv e-prints*, May 2017.

[92] H. Miller and J. Anders. Time-reversal symmetric work distributions for closed quantum dynamics in the histories framework. *New Journal of Physics*, 19(6):062001, jun 2017.

[93] B. Misra and E. C. G. Sudarshan. The zeno's paradox in quantum theory. *Journal of Mathematical Physics*, 18(4):756–763, 1977.

[94] M. T. Mitchison, M. P. Woods, J. Prior, and M. Huber. Coherence-assisted single-shot cooling by quantum absorption refrigerators. *New Journal of Physics*, 17(11):115013, nov 2015.

[95] S. Mukamel. Quantum extension of the Jarzynski relation: Analogy with stochastic dephasing. *Phys. Rev. Lett.*, 90:170604, May 2003.

[96] M. Naghiloo, A. D. Tan, P. M. Harrington, J. J. Alonso, E. Lutz, A. Romito, and K. W. Murc. Thermodynamics along individual trajectories of a quantum bit. arXiv:1703.05885v2, 2017.

[97] M. Naghiloo, D. Tan, P. M. Harrington, J. J. Alonso, E. Lutz, A. Romito, and K. W. Murch. Thermodynamics along individual trajectories of a quantum bit. *ArXiv e-prints*, March 2017.

[98] M. A. Nielsen and I. L. Chuang. *Quantum Computation and Quantum Information*. Cambridge University Press, Cambridge, 2000.

[99] S. Olmschenk, K. C. Younge, D. L. Moehring, D. N. Matsukevich, P. Maunz, and C. Monroe. Manipulation and detection of a trapped yb^+ hyperfine qubit. *Phys. Rev. A*, 76:052314, Nov 2007.

[100] S. Pascazio. All you ever wanted to know about the quantum zeno effect in 70 minutes. *Open Systems & Information Dynamics*, 21(01n02):1440007, 2014.

[101] J. P. Pekola, Y. Masuyama, Y. Nakamura, J. Bergli, and Y. M. Galperin. Dephasing and dissipation in qubit thermodynamics. *Phys. Rev. E*, 91:062109, 2015.

[102] F. Petruccione and H. P. Breuer. *The theory of open quantum systems*. Oxford University Press, London, 2002.

[103] S. Pigeon, L. Fusco, A. Xuereb, G. De Chiara, and M. Paternostro. Thermodynamics of trajectories and local fluctuation theorems for harmonic quantum networks. *New J. Phys.*, 18:013009, 2016.

[104] A. Pohorille, C. Jarzynski, and C. Chipot. Good practices in free-energy calculations. *J. Chem. Phys. B*, 114:10235, 2010.

[105] W. Pusz and S. L. Woronowicz. Passive states and kms states for general quantum systems. *Comm. Math. Phys.*, 58(3):273–290, 1978.

[106] A. E. Rastegin. Non-equilibrium equalities with unital quantum channels. *J. Stat. Mech.: Theor. Exp.*, page P06016, 2013.

[107] A. E. Rastegin and K. Życzkowski. Jarzynski equality for quantum stochastic maps. *Phys. Rev. E*, 89:012127, 2014.

[108] G. Rigolin, G. Ortiz, and V. H. Ponce. Beyond the quantum adiabatic approximation: Adiabatic perturbation theory. *Phys. Rev. A*, 78:052508, Nov 2008.

[109] W. De Roeck and C. Maes. Quantum version of free-energy-irreversible-work relations. *Phys. Rev. E*, 69:026115, 2004.

[110] A.J. Roncaglia, F. Cerisola, and J. P. Paz. Work measurement as a generalized quantum measurement. *Phys. Rev. Lett.*, 113:250601, 2014.

[111] J. Roßnagel, O. Abah, F. Schmidt-Kaler, K. Singer, and E. Lutz. Nanoscale heat engine beyond the carnot limit. *Phys. Rev. Lett.*, 112:030602, Jan 2014.

[112] O.-P. Saira, Y. Yoon, T. Tanttu, M. Möttönen, D.V. Averin, and J.P. Pekola. Test of the Jarzynski and Crooks fluctuation relations in an electronic system. *Phys. Rev. Lett.*, 109:180601, 2012.

[113] R. Sampaio, S. Suomela, T. Ala-Nissila, J. Anders, and T. G. Philbin. Quantum work in the bohmian framework. *Phys. Rev. A*, 97:012131, Jan 2018.

[114] M. O. Scully, M. S. Zubairy, G. S. Agarwal, and H. Walther. Extracting work from a single heat bath via vanishing quantum coherence. *Science*, 299(5608):862–864, 2003.

[115] U. Seifert. Stochastic thermodynamics, fluctuation theorems and molecular machines. *Reports on Progress in Physics*, 75(12):126001, nov 2012.

[116] E.M. Sevick, R. Prabhakar, S. R. Williams, and D. J. Searles. Fluctuation theorems. *Annual Review of Physical Chemistry*, 59(1):603–633, 2008. PMID: 18393680.

[117] E. A. Shank, C. Cecconi, J. W. Dill, S. Marqusee, and C. Bustamante. The folding cooperativity of a protein is controlled by its chain topology. *Nature*, 465:637, 2010.

[118] M. Silaev, T. T. Heikkilä, and P. Virtanen. Lindblad-equation approach for the full counting statistics of work and heat in driven quantum systems. *Phys. Rev. E*, 90:022103, 2014.

[119] P. Skrzypczyk, A. J. Short, and S. Popescu. Work extraction and thermodynamics for individual quantum systems. *Nature Communications*, 5(May):1–8, 2014.

[120] A. Smith, Y. Lu, S. An, X. Zhang, J. Zhang, Z. Gong, H. T. Quan, C. Jarzynski, and K. Kim. Verification of the quantum nonequilibrium work relation in the presence of decoherence. *New Journal of Physics*, 20(1):013008, jan 2018.

[121] A. Soare, H. Ball, D. Hayes, X. Zhen, M. C. Jarratt, J. Sastrawan, H. Uys, and M. J. Biercuk. Experimental bath engineering for quantitative studies of quantum control. *Phys. Rev. A*, 89:042329, 2014.

[122] P. Solinas and S. Gasparinetti. Full distribution of work done on a quantum system for arbitrary initial states. *Phys. Rev. E*, 92:042150, 2015.

[123] P. Solinas, H. J. D. Miller, and J. Anders. Measurement-dependent corrections to work distributions arising from quantum coherences. *Phys. Rev. A*, 96:052115, Nov 2017.

[124] H. Spohn and J. L. Lebowitz. *Advances in Chemical Physics: For Ilya Prigogine, Volume 38*, chapter Irreversible Thermodynamics for Quantum Systems Weakly Coupled to Thermal Reservoirs, pages 109–142. John Wiley and Sons, Inc., Hoboken, NJ, USA, 1978.

[125] P. Strasberg, G. Schaller, T. Brandes, and M. Esposito. Quantum and information thermodynamics: A unifying framework based on repeated interactions. *Phys. Rev. X*, 7:021003, Apr 2017.

[126] K. Takara, H. H. Hasegawa, and D. J. Driebe. Generalization of the second law for a transition between nonequilibrium states. *Physics Letters A*, 375(2):88–92, Dec 2010.

[127] P. Talkner, M. Campisi, and P. Hänggi. Fluctuation theorems in driven open quantum systems. *J. Stat. Mech.: Theor. Exp.*, 2009(02):P02025, 2009.

[128] P. Talkner, E. Lutz, and P. Hänggi. Fluctuation theorems: Work is not an observable. *Phys. Rec. E*, 75:050102(R), 2007.

[129] P. Talkner, P.and Hänggi. Aspects of quantum work. *Phys. Rev. E*, 93:022131, 2016.

[130] H. Tasaki. Jarzynski relations for quantum systems and some applications. arXiv:cond-mat/0009244, 2000.

[131] E. Torrontegui, S. Ibáñez, S. Martínez-Garaot, M. Modugno, A. del Campo, D. Guéry-Odelin, A. Ruschhaupt, X. Chen, and J. G. Muga. Chapter 2 - shortcuts to adiabaticity. In E. Arimondo, P. R. Berman, and C. C. Lin, editors, *Advances in Atomic, Molecular, and Optical Physics*, volume 62 of *Advances In Atomic, Molecular, and Optical Physics*, pages 117 – 169. Academic Press, 2013.

[132] A. Uhlmann. Relative entropy and the wigner-yanase-dyson-lieb concavity in an interpolation theory. *Communications in Mathematical Physics*, 54(1):21–32, Feb 1977.

[133] R. Uzdin, A. Levy, and R. Kosloff. Equivalence of quantum heat machines, and quantum-thermodynamic signatures. *Phys. Rev. X*, 5:031044, Sep 2015.

[134] J. A. Vaccaro, S. Croke, and S. M. Barnett. Is coherence catalytic? *Journal of Physics A: Mathematical and Theoretical*, 51(41):414008, sep 2018.

[135] N. G. Van Kampen. *Stochastic Processes in Physics and Chemisty*. Elsevier, Amsterdam, 2007.

[136] S. Vinjanampathy and J. Anders. Quantum thermodynamics. *Contemporary Physics*, 57(4):545–579, 2016.

[137] A. Wehrl. General properties of entropy. *Rev. Mod. Phys.*, 50:221–260, Apr 1978.

[138] H. M. Wiseman and G. J. Milburn. Interpretation of quantum jump and diffusion processes illustrated on the Bloch sphere. *Phys. Rev. A*, 47:1652, 1993.

[139] H. M. Wiseman and G. J. Milburn. *Quantum Measurement and Control*. Cambridge University Press, Cambridge, 2010.

[140] S Yukawa. A quantum analogue of the Jarzynski equality. *J. Phys. Soc. Jap.*, 69:2367, 2000.

[141] X. Zhang, M. Um, J. Zhang, S. An, Y. Wang, D. Deng, C. Shen, L. Duan, and K. Kim. State-independent experimental tests of quantum contextuality in a three dimensional system. *Phys. Rev. Lett.*, 110:070401, 2013.

[142] W. Zurek. Decoherence and the transition from quantum to classical–revisited. *Los Alamos Science*, 27:2–25, 2002.

[143] R. W. Zwanzig. High temperature equation of state by a perturbation method. i. nonpolar gases. *The Journal of Chemical Physics*, 22(8):1420–1426, 1954.